NASA CR-122366

FINAL REPORT
FOR
TRACKING SYSTEM STUDY

August 1969

Contract No.: NAS 5-9756-138

Goddard Space Flight Center

Contracting Officer: R.R. Dapice
Technical Monitor: A.J. Rolinski

(ACCESSION NUMBER) 32 (PAGES) N-122366 (NASA CR OR TMX OR AD NUMBER)
(THRU) 63 (CODE) 08 (CATEGORY)
FACILITY FORM 602

Prepared by:

Wolf Research and Development Corporation
6801 Kenilworth Avenue
Riverdale, Maryland

Contributors:

A.R. Dennis
D. Tabak
L.D. Gifford
H.M. Mednick
J. Buchert

Technical Coordinator and Report Editor:

D. Tabak

Reproduced by
NATIONAL TECHNICAL
INFORMATION SERVICE
U S Department of Commerce
Springfield VA 22151

for

Goddard Space Flight Center
Greenbelt, Maryland

(NASA-CR-122366) TRACKING SYSTEM STUDY A.R. Dennis, et al (Wolf Research and Development Corp.) Aug. 1969 192 p CSCL 09B
N72-19239
Unclas
G3/08 20582

CONTENTS

CONTENTS (Cont.)

1. Introduction

The purpose of this project was to generate a digital computer program which mathematically describes an optimal estimator-controller technique as applied to the control of antenna tracking systems used by NASA. Simulation studies utilizing this program were to be conducted using the IBM 360/91 computer.

Previous work performed by Stanford Research Institute (SRI) for NASA, ERC, Cambridge, Mass., served as a starting point in this project. The program written by SRI was not addressed to a real-life tracking system and it assumed the system to be linear. In this project, the optimal estimator-controller program was adopted for the 30 ft and 40 ft NASA MSFN and STADAN antenna tracking systems. Simulations including the nonlinearities were performed and algorithms for direct synthesis of the control signal, taking into account the nonlinearities, were proposed. The results of this study are summarized in this report.

The basic ideas of applying optimal estimator-controller techniques to antenna tracking systems are discussed in Chapter 2. A survey of existing tracking methods is given along with shortcomings and inherent errors. It is explained how these errors can be considerably reduced if optimal estimation and control are used.

The modified programs generated in this project are described in Chapter 3, and the simulation results are summarized in Chapter 4. The new algorithms for direct synthesis and stabilization of the systems including nonlinearities, are presented in Chapter 5. Conclusions are given in Chapter 6.

The report includes four Appendices. Basic notions of optimal recursive estimation are presented in Appendix A, while the optimal control policy used in this project is outlined in Appendix B. Appendix C constitutes a detailed documentation of the optimal estimation-control program RATS generated in this project. Various reference angle coordinate representations are given in Appendix D.

2. The Application of Optimal-Control Theory to Space Vehicle Tracking

2.1 Introduction

The basic reason for considering the application of optimum stochastic control to a tracking antenna system is the possibility of achieving some measure of dynamically minimized pointing error. Thus the object is to realize optimum pointing estimates in real time as opposed to their determination through post-flight analysis. Such critical real-time tracking support may be necessary during manned flight missions where, for example, extremely accurate coverage of a rendevous and docking maneuver is required. Also, for systems exhibiting very narrow beam widths (such as laser ranging devices), precise pointing may be necessary to maintain lock-on.

In general, the design of an optimal controller begins with a precise definition of both input signal and plant dynamics. In stochastic applications, the state must be estimated from measurements made at various points within the combined systems. Once these estimates are obtained, they become input to a control law, the purpose of which is to minimize some (average) measure of (in this case) antenna pointing error.

A detailed discussion of the mathematical theory of optimum control is beyond the scope of this report; however, a great body of literature exists on this subject for reference, and a few pertinent sources are listed in Section 2.6. The next section (2.2) contains a brief, general description of the theory as applied to the sys-

tem studied under this contract, while in Section 2.3, the tracking system itself is discussed. In Section 2.4 major errors inherent in the overall dynamical system are discussed, and in Section 2.5 an example is given of how certain errors are formulated mathematically in the estimator/controller model.*

* This inclusion of this formulation in the simulation program was beyond the scope of this effort, and is included mainly to indicate one direction for future work.

2.2 The Optimization Problem

Figure 2.1 is a simplified block diagram of the tracking problem considered in this study. The "input signal" is described by means of a set of non-linear differential equations which define the trajectory of the space vehicle. The instanteneous trajectory state is then transformed into a set of "observables" to which the tracking system responds (for example, a typical set of observables is comprised of two orthogonal pointing angles with respect to an antenna datum, plus measurements of range and/or range-rate).

In this study, the observables which drive the antenna system are angluar offsets from the "mechanical" boresight (which is, in this simple model, assumed to correspond to the RF-boresight). This displacement is sensed in a set of error detectors which generate appropriate electronic signals which in turn drive the antenna system back into a null error situation.

The optimization problem is to find a controller which, given appropriate knowledge of the state of the entire system, will maintain a minimum average value of squared pointing error 'ε'.

In general, however, although the input signal dynamics may be known fairly well, the "first order" stochastic problem requires that the initial conditions be estimated from the measurements themselves. In addition, other components of the composite state vector may not be known a priori, so that they must also be estimated. Thus, the more general "stochastic optimum" control problem requires consideration of a method for state estimation.*

---

* See References 2 and 4 for a more detailed, mathematical discussion of the stochastic optimum control problem.

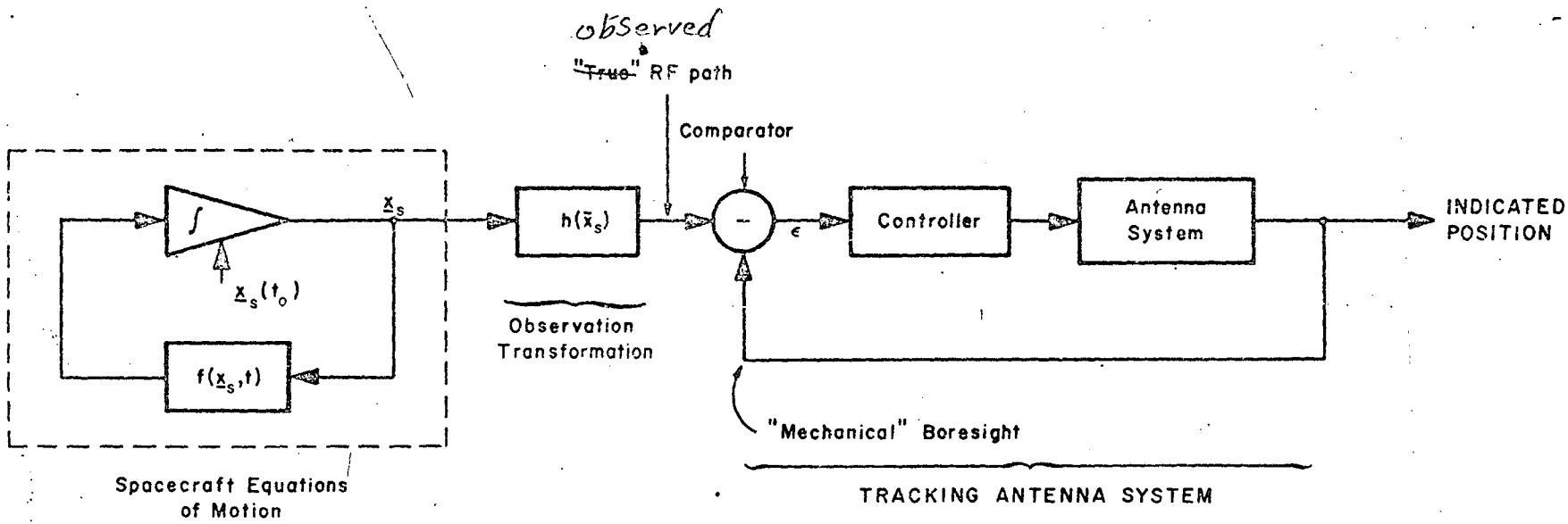

Fig. 2.1
The Space Vehicle Tracking Problem
Simplified Block Diagram

Although a detailed discussion of these added uncertainities is beyond the scope of this effort, some examples are given in Section 2.4 as an aid for future study. First, however, a more complete description of how the present-day tracking systems operate is presented to set the basis for the simulations described in Chapter 4. There are two basic modes of operation: "autotrack" and "program". A detailed description of the observables (i.e., "X and Y angles") is included in Appendix D.

2.3 Antenna System Operating Modes

2.3.1 The "Autotrack Mode" of Operation

The "Autotrack Mode" constitutes a closed loop automatic control operation of the antenna tracking system. It is most widely used in actual tracking operations. A block diagram is sketched in Figure 2.2.

In this case, the difference between the RF or Boresight axis of the antenna and the actual line of sight to the satellite is measured, and the reading constitutes the error signal in the feedback loop. The control action tries to minimize this error. Although there is a certain amount of feedback involved in this operation, the information fed back to the control system is still incomplete. For instance, no information concerning the actual and predicted trajectory of the satellite is being transmitted. With respect to the trajectory information, the autotrack system could be regarded as an "open loop" system, although, technically it does have a closed loop.

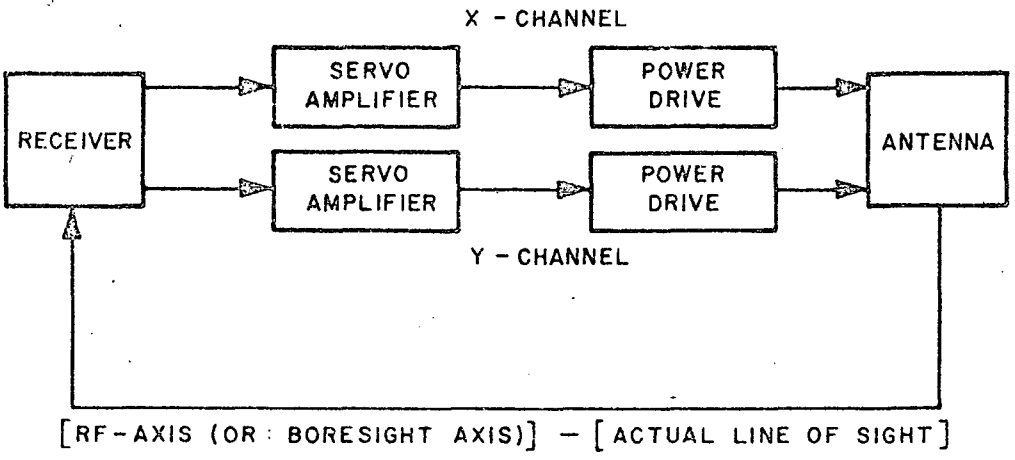

Fig. 2.2 Autotrack Mode Operation

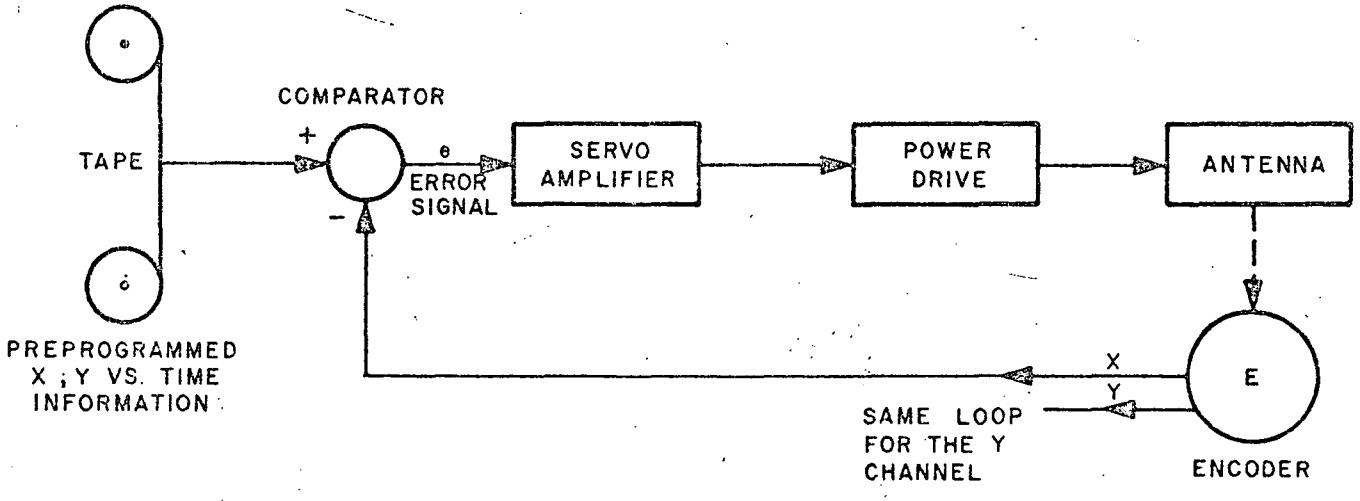

Fig. 2.3 Program Mode Operation

2.3.2 The Program Mode of Operation

The basic principle of this Program Mode operation of an antenna tracking system is illustrated in Figure 2.3. The trajectory of the satellite as well as the precise location of the tracking station are assumed known. Using this information one may pre-calculate the values of the X, Y angles as functions of time for the whole tracking period. This information is stored on tape and fed to the comparator at the output of which appears the error signal. This error signal drives the antenna in the direction of minimizing this error.

The main disadvantage of this method is the fact that the whole control action is accomplished without any knowledge of the actual position of the satellite. It may happen that the satellite's trajectory may become displaced for some reason, and in this mode, the tracking system may not "know" anything about it. Although there is a closed loop in the block diagram, this mode of operation is basically open-loop from the control systems standpoint, since there is no feedback signal which represents the actually controlled entity. In this mode of operation it is easy to wind up with a situation where the satellite is at one place and the antenna is pointing to another.

2.4 Examples of Errors in the "Autotrack" System

The autotrack system is plagued by a set of errors inherent in the system's operation. Some possible errors can be introduced as schematically sketched in Figure 2.4. For the sake of simplicity, only, one channel is shown in the figure.

The typical errors existing at various stages of the operation of the autotrack system are the following:

1. e_1 - ray path errors, which may include

   (a) Error due to refraction of transmitted signal paths in the atmosphere.

   (b) Errors resulting from imprecise knowledge of station location.

   (c) Timing errors. (Station relative to orbit)

2. e_2 - errors resulting from receiver noise, for instance: polarization shift error.

3. e_3 - dynamic errors of the feedback control system, which may include

   (a) Servo dynamic errors of the control system, (acceleration error, velocity error)

   (b) Wind gust errors, (zenith structure shift, direction effect)

   (c) Mechanical misalignments, (deflection coefficient, deflection angular effect, tilt, axis lack of orthogonality)

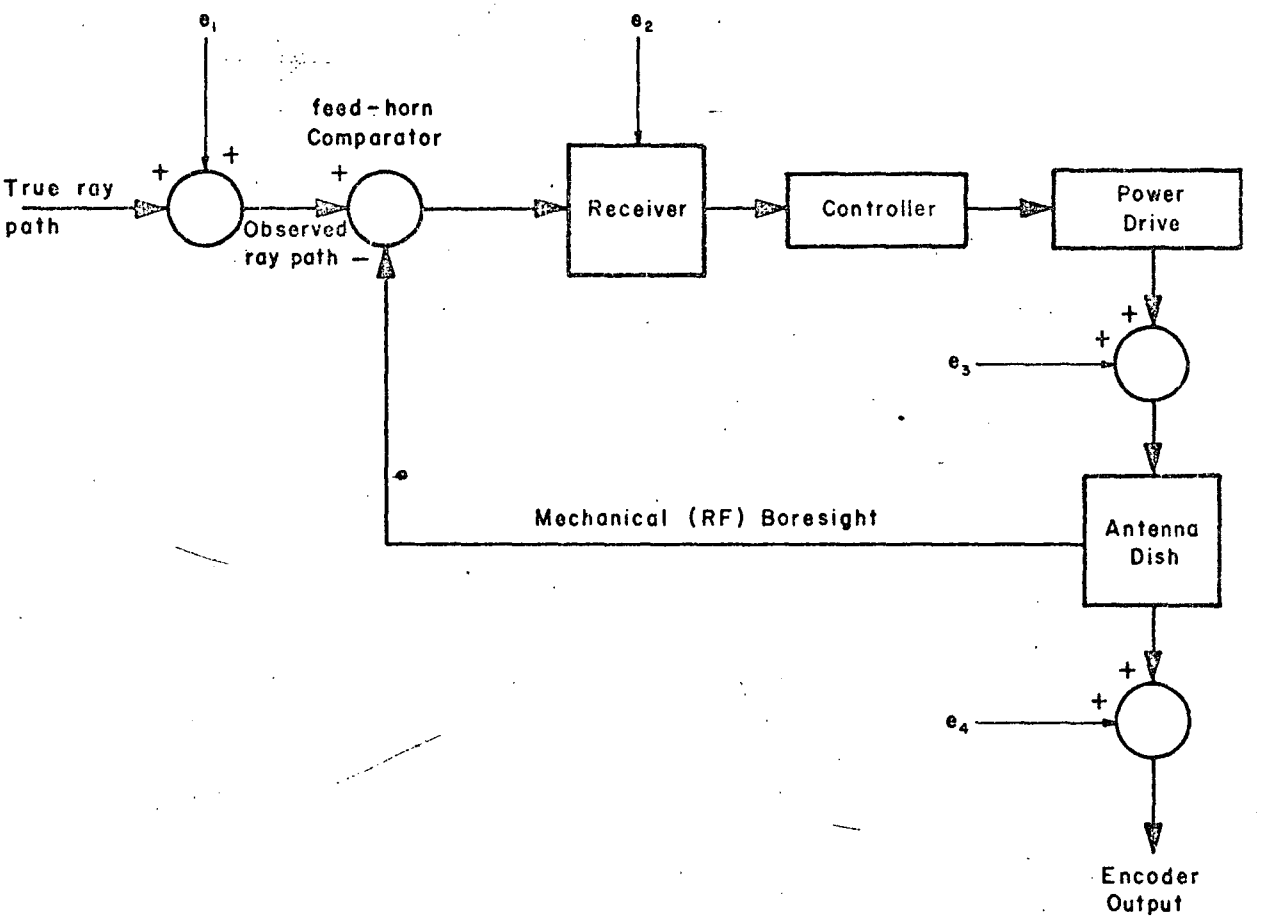

Fig. 2.4 An Example of Errors in the Autotrack System

4. e_4 - RF axis tracking errors. [1]
(encoder and axis bias, encoder hysteresis)

In the usual autotrack system very little can be done to alleviate the effect of these errors. On the other hand, as indicated in the next section, by using the optimal estimator/controller idea, one may compute an optimal estimate of these errors and hence account for their presence in the design of the controller.

2.5 Estimation of Errors

By formulating the problem within the framework of the optimum stochastic control, it is possible to consider these errors and, in some cases, to either remove their effects from the state variables used by the optimum controller or include them in the actual controller design.

The basic notion behind successful application of this idea is the notion of observability, that is, whether or not, given all measurements up to and including a given time 't', the desired error sources are observable in the sense that meaningful estimates of their values can be obtained from these measurements. Also, the degree of observability is important inasmuch as those errors that can be estimated with smaller amounts of data will tend to yield more optimum overall results as far as fixed interval real time optimum control is concerned. This question is, however, a complicated one in general and will not be discussed further here*;

* Some research into the area of orbital state trajectory, estimation in the presence of unknown dynamic equation and measurement errors has been carried out by A. Dennis[5]. Application of the techniques developed should simplify the general controller estimation problem and will be examined in future work.

rather, an example will be given of how a typical error source might be contained within the estimator formulation.

To be specific, for the case of one quarter of the prescribed bandwidth for the system under study, [3, Chapter 12], the transfer function of the plant is:

$$\frac{X(s)}{U(s)} = \frac{.125}{s(.5s+1)} \tag{2-1}$$

where

X(s) = s-transform of the X angle.

U(s) = s-transform of the forcing functions.

The treatment will be confined to the X-channel only, since the treatment of the Y-channel would be identical.

Introducing the following state variables:

$$x_1(t) = X(t)$$

$$x_2(t) = \dot{x}_1(t)$$

one obtains the following state equations:

$$\dot{x}_1 = x_2$$

$$\dot{x}_2 = -2x_2 + .25u \tag{2-2}$$

or

$$\dot{\underline{x}} = A\underline{x} + \underline{b}u \tag{2-3}$$

where

$$\underline{x} = \begin{bmatrix} x_1 \\ \\ x_2 \end{bmatrix} \quad ; \quad A = \begin{bmatrix} 0 & 1 \\ \\ 0 & -2 \end{bmatrix} \quad ; \quad \underline{b} = \begin{bmatrix} 0 \\ \\ .25 \end{bmatrix}$$

In practice, the state variables of the system are not directly observable. Moreover, as pointed out in Section 2.2, they are corrupted by a set of errors. The errors could be represented as additional state variables of the system. The way it is done, will be illustrated by a specific example.

One should start in this case from the state transition equation obtained from the state Eq. (2-2). This would actually be the closed-form solution of these equations:

$$\underline{x}(t_k) = e^{A(t_k - t_{k-1})}\, \underline{x}(t_{k-1}) + \int_{t_{k-1}}^{t_k} e^{A(t_k - \tau)} \underline{b}u(\tau)\, d\tau \tag{2-4}$$

In this case:

$$e^{At} = \begin{bmatrix} 1 & \frac{1}{2}(1-e^{-2t}) \\ 0 & e^{-2t} \end{bmatrix} \tag{2-5}$$

So, Eq. (2-4) becomes:

$$\underline{x}(t_k) = \begin{bmatrix} 1 & \frac{1}{2}[1-e^{-2(t_k-t_{k-1})}] \\ 0 & e^{-2(t_k-t_{k-1})} \end{bmatrix} \underline{x}(t_{k-1}) +$$

$$+ \int_{t_{k-1}}^{t_k} \begin{bmatrix} .125\ [1-e^{-2(t_k-\tau)}] \\ .25\ e^{-2(t_k-\tau)} \end{bmatrix} u d\tau \tag{2-6}$$

Or:

$$\underline{x}(t_k) \begin{bmatrix} 1 & \frac{1}{2}\ [1-e^{-2(t_k-t_{k-1})}] \\ 0 & e^{-2(t_k-t_{K-1})} \end{bmatrix} \underline{x}(t_{k-1}) +$$

$$+ \begin{bmatrix} .125[t_k-t_{k-1} + \frac{1}{2}(1-e^{-2(t_k-t_{k-1})})] \\ .125(e^{-2(t_k-t_{k-1})}-1) \end{bmatrix} u(t_{k-1})$$

$$= \Phi\ (k,k-1)\ \underline{x}\ (t_{k-1}) + \underline{\Gamma}\ (k,k-1)\ u\ (t_{k-1}) \qquad (2\text{-}7)$$

This expression is similar to the one in Eq. (A-1), in Appendix A. The same expression could be written for the Y-Channel.

The errors to be considered, as an example, are the bias and the tilt errors. They are expressed as follows:[1]

Bias Error at $t = t_k$; $E_1 = B_k$, a constant

Tilt error at $t = t_k$; $E_2 = T_k\ tgY sinX$

The tilt error consists of a fixed coefficient T_k, but the measured result depends on X and Y.

Both B_k and T_k are unknown a priori and are to be estimated by the optimal estimation process. They are represented as additional state variables. The original state vector is augmented as follows, to form a new state vector:

$$\underline{X}_k = \begin{bmatrix} \underline{x}(t_k) \\ \hline B_k \\ T_k \end{bmatrix} = \begin{bmatrix} x_1(t_k) \\ x_2(t_k) \\ B_k \\ T_k \end{bmatrix} \qquad (2\text{-}8)$$

Since B_k and T_k are assumed time invariant, the augmented state transition equation will be:

$$\underline{X}_k = \begin{bmatrix} \Phi(k,k-1) & 0 \\ 0 & I_2 \end{bmatrix} \underline{X}_{k-1} + \begin{bmatrix} \underline{\Gamma}(k,k-1) \\ 0 \end{bmatrix} u_{k-1} \qquad (2\text{-}9)$$

where

$$u_{k-1} = u(t_{k-1})$$

$$I_2 = \begin{bmatrix} 1 & 0 \\ 0 & 1 \end{bmatrix}$$

or:

$$\underline{X}_k = \Phi_1(k,k-1)\ \underline{X}_{k-1} + \underline{\Gamma}_1(k_1k-1)\ u_{k-1} \qquad (2\text{-}10)$$

where the definition of Φ_1 and $\underline{\Gamma}_1$ is obvious from Eq. (2-9).

For the sake of simplicity, assume that there is no extra noise on the state equation, of the antenna, i.e.,

$$\underline{w}_k = \underline{0} \qquad (2\text{-}11)$$

(see Eq. (A-1) in Appendix A)

Now one has to formulate the measurement equations. Considering the X-channel only, it will be assumed that the following entities are measurable:

1. $X - X_s$

2. ρ_s

3. X

where

X_s = predicted line of sight of the satellite for the X-angle.

ρ_s = range from tracking station to the satellite.

Forgetting for the moment the errors, the measurement equations will have the following form:

$$\underline{\beta}_k = H_1(k)\ \underline{\chi}_k + \underline{v}_k \qquad (2\text{-}12)$$

$\underline{\chi}_k$ = overall state vector, (including satellite and antenna). Same as Eq. (A-2), with all symbols defined identically.

In this case, n=8, m=3, so, H will be a 3x8 matrix, (n=8, since there are 6 state variables for the satellite equations and 2 for the X-channel of the antenna).

Let the overall state vector be defined as follows:

$$\underline{Y} = \begin{bmatrix} z_1 \\ z_2 \\ z_3 \\ \dot{z}_1 \\ \dot{z}_2 \\ \dot{z}_3 \\ x_1 \\ x_2 \end{bmatrix}$$

Cartesian coordinates of the satellite in tracking station centered system. z_1 - zenith, z_2 - east, z_3 - north

Cartesian velocity components of the satellite.

Details concerning the satellite and measurements equations may be found in references[2,4].

The overall augmented state vector will be:

$$Y_k = \begin{bmatrix} \underline{Y} \\ B_k \\ T_k \end{bmatrix}.$$

And the overall augmented state transition equations will be of the form

$$Y_k = \Phi_2(k,k-1)\, Y_{k-1} + \Gamma_2\,(k,k-1)\, u_{k-1} + \underline{w}_{k-1} \qquad (2\text{-}13)$$

where Φ_2 and Γ_2 may be worked out as was clear before.

The linearized measurement matrix $H_1(k)$ in Eq. (2-12) may be expressed as follows:

$$H_1(k) = \begin{bmatrix} -\frac{\partial X_s}{\partial z_1} & -\frac{\partial X_s}{\partial z_2} & -\frac{\partial X_s}{\partial z_3} & 0 & 0 & 0 & 1 & 0 \\ \frac{\partial \rho_s}{\partial z_1} & \frac{\partial \rho_s}{\partial z_2} & \frac{\partial \rho_s}{\partial z_3} & 0 & 0 & 0 & 0 & 0 \\ 0 & 0 & 0 & 0 & 0 & 0 & 1 & 0 \end{bmatrix} \qquad (2\text{-}14)$$

It was shown in [4]:

$$\frac{\partial X_s}{\partial z_1} = -\frac{z_2}{z_1^2+z_2^2}$$

$$\frac{\partial X_s}{\partial z_2} = \frac{z_1}{z_1^2+z_2^2} \qquad (2\text{-}15)$$

$$\frac{\partial X_s}{\partial z_3} = 0$$

$$\frac{\partial \rho_s}{\partial z_i} = \frac{z_i}{\sqrt{z_1^2+z_2^2+z_3^2}} \; ; \; i=1, 2, 3 \qquad (2\text{-}16)$$

Taking into account the errors, the augmented linearized measurement matrix will take the following form:

$$H(k) = \left[\begin{array}{c|cc} & \frac{\partial E_1}{\partial B_k} & \frac{\partial E_2}{\partial T_k} \\ H_1(k) & & \\ & \frac{\partial {}^0E_1}{\partial B_k} & \frac{\partial {}^0E_2}{\partial T_k} \end{array}\right] = \left[\begin{array}{c|cc} & 1 & tgYsinX \\ H_1(k) & 0 & 0 \\ & 1 & tgYsinX \end{array}\right]$$

Applying the optimal estimation techniques to this system, as described in Appendix A, one finds an optimal estimate of the overall state vector, at any time $t = t_k$, $\hat{Y}_k$. This optimal estimate includes also the estimates of the errors $\hat{B}_k$, $\hat{T}_k$. The overall estimated state vector $\hat{Y}_k$, is then applied as an input to the optimal controller. (See Appendix B) The optimal controller produces a control signal which takes into account the whole state vector $\hat{Y}_k$, including all the errors and which extremizes the performance index. In this case, it would be minimizing the pointing error.

2.5.1 Discussion

The above simple example, as noted earlier, is presented only to indicate the usefulness of the formalism of optimum stochastic control in handling realistic measurement error sources. In the real world, although some modifications to the basic structures may be necessary[5], the overall effectiveness of these ideas can be retained. This topic is not discussed further in this report, although it is recommended that realistic systems be examined from this viewpoint in future work.

2.6 References

1. Apollo Unified S-Band, Engineering Report, Collins Radio Co., 523-0560613-001D3M, 15 April 1968, Contract NAS 5-9035.

2. J. Peschon, et al., "Research on the Design of Adaptive Control Systems," Final Report, Vol. 2, Stanford Research Institute, Menlo Park, California, September 1966.

3. Design Analysis - Unified S-Band System for Apollo Network, Engineering Report, Collins Radio Co., 523-0556527-001D3M, 28 October 1964, Contract NAS 5-9035.

4. R.M. Dressler, E.C. Fraser, "Optical Communication and Tracking Systems," Final Report, Stanford Research Institute, Menlo Park, California, October 1967.

5. Dennis, A.R., "Functional Updating and Adaptive Noise Variance Estimation in Recursive-Type Trajectory Estimators," presented at the NASA/GSFC Special Project Branch Astrodynamics Conference, May 1967.

3. Estimation and Control Simulation Programs

3.1 Introduction

Two programs served as a basis for the present simulation studies:

(a) ORBTRACK, [1,2].

This program simulates the autotrack and the optimal estimator-controller modes of operation, of an optical tracking system for an interplanetary mission. The basic theory underlying the program is described in reference [1], along with some simulation results. The program documentation is given in Reference [2]. This includes a gross flowchart and subroutine and symbols vocabulary. The program was originally implemented on an IBM 7094 system.

(b) RADIO ANTENNA, [3]. This program simulates the optimal estimator-controller mode of operation of an ~~imaginary~~ hypothetical radar tracking antenna, for a satellite around the earth trajectory mission. The tracking works on an elevation-azimuth reference basis. Only the elevation channel was originally available in the program. The theory relevant to the program was described in reference [3], Chapter 7. No program documentation was available. The program itself was not debugged to the end and was not in a working condition. The program was originally written for the IBM 7094.

Both programs, with the exception of a few subroutines in Assembly Language, were written in FORTRAN IV.

In the current project, both programs were adopted on the IBM 360/91 systems. Both programs were equipped with optional graphical display facilities. The modified ORBTRACK program was renamed: ATRK30, and the RADIO ANTENNA program: RATS. Both ATRK30 and RATS are written in FORTRAN IV, without any subroutines in Assembly Language. The following basic changes were made in the programs:

ATRK30

(1) Adoption of the IBM 360/91 system.

(2) Replacement of Assembly Language subroutines with library subroutines called in FORTRAN IV.

(3) Addition of optional graphical display of various functions as a function of time.

(4) Transformation into the X-Y angle reference system.

(5) Replacement of the original optical tracking system by a model of the GSFC 30 Ft. tracking antenna.

(6) Inclusion of options to perform simulations with nonlinearities in the loop.

RATS

(1)-(4) Same as in ATRK30.

(5) Replacement of the original imaginary antenna tracking system by a model of the GSFC 40 Ft. tracking antenna.

(6) Inclusion of an additional angle channel into the program. (Only one channel was originally available).

(7) Convergence in the state transition matrix calculation was achieved. (There was a divergence in the original program). Convergence was achieved by implementing a new method.

(8) The previous matrix inversion routine, which gave unacceptable results, was replaced by an improved routine. Moreover, the total number of inversions to be performed, was reduced.

(9) The input was modified to read directly the system matrix A (See Eq. (2-3)) of the state equations.

(10) Generation of program documentation. More details will be given further in the chapter. Details concerning simulation runs performed, will be given in Chapter 4.

3.2 The ATRK30 Program

As mentioned before, the ATRK30 program is basically the same as the ORBTRACK. The main difference is in the plant configuration. It so appears, that both plants may be represented by the following transfer function:

$$G(s) = \frac{K}{s(s+a)} \qquad (3-$$

The interchange between them is accomplished by changing the values of K, a, which are functions of input data.

$$K = \frac{1}{J}$$

$$a = \frac{f}{J}$$

J = moment of inertia of the system
f = friction coefficient of the system

} Input data of the program.

It should be noted that Eq. (1) is a very simplified representation of the antenna power system. However, it is the one used in the original report concerning the 30 Ft. antenna, [4].

The actual transfer function used in the simulation was:

$$G(s) = \frac{.25}{S(s+2)} \tag{3-2}$$

This is the case of 1/4 of the total available bandwidth, as specified in [4], Chapter 12.

There is a difference in the controller structure in autotrack mode. In the ORBTRACK program, for the optical tracking system, the controller has the form:

$$C(s) = K_1 + K_2 s + \frac{K_3}{s} \tag{3-3}$$

This is the well known parallel combination of an amplifier, differentiator and integrator. In the 30 Ft. antenna system, the controller has the form: [4]

$$C(s) = \frac{a_1 s+1}{s(b_1 s+1)} \tag{3-4}$$

In this particular case of 1/4 BW: $a_1 = 12.5$; $b_1 = 1.5$.

3.3 The RATS Program

The basic theory underlying this program was described in Reference [7]. This program underwent, however, considerable changes in this project. No previous programming documentation was available, so this documentation will be given in this report. A gross flow-chart of the program is shown in Figure 3.1. A glossary of programming notation is given in Appendix C. A list of the program's subroutines with a short description of the function of each as well as a list of all input data is also given in Appendix C.

Description of the Program

The program is started by setting some initial parameters which include the angular rate of rotation of the earth, Ω, earth's radius, R_e, and the earth gravitational constant, μ_e.

In subroutine TRAK1 the basic input data are read in. (See Appendix C for a detailed list). The radius vector components from tracking station to the satellite are calculated and the input data are printed out. The initial direction angles X, Y are calculated in TZERO. (See Appendix D for basic formulas on calculating X, Y.)

Subroutine FPHI reads in the data for the state equations of the antenna, i.e., matrix A and vector $\underline{b}$ from Eq. (2-3). This arrangement makes the program flexible enough to be applied to various types of tracking antennas, just by changing some input variables. The state transition matrices of the system are computed. (See Eq. (25) of [3].)

Figure 3.1. RATS Flow Chart

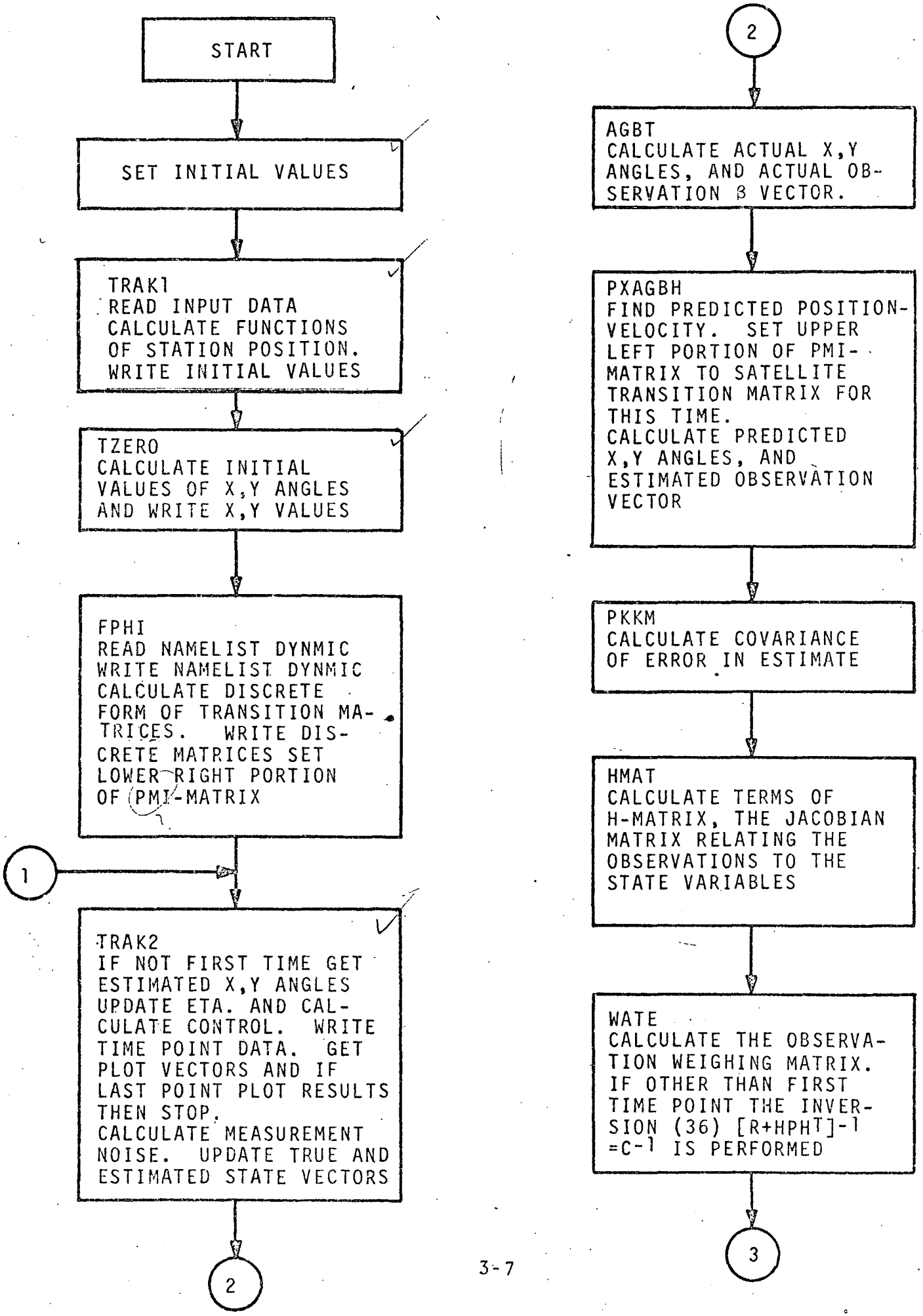

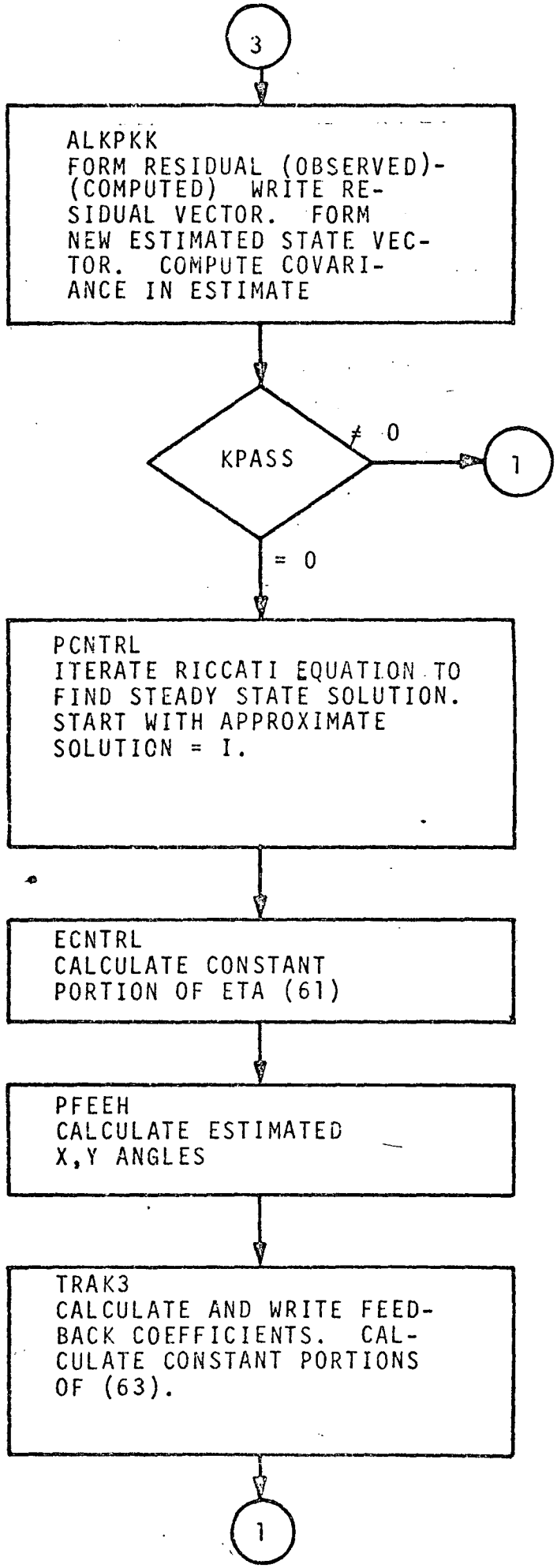

NOTE: Numbers in ( ) refer to formulas in reference [3], ch. 7

In subroutine TRAK2 the estimated X and Y angles are used to update the variable of (Eq. (61) of [3]) and to compute the optimal control, (Eq. (63) of [3]). Satellite position is updated to current time. The predicted antenna state is calculated (Eq. (32) of [3]), and the new overall state vector is calculated, (Eq. (42) of [3]). The measurement noise vector is also calculated in this subroutine, using a pseudo-random number generator.

The actual X, Y angles of the antenna and the actual measurement vector β, (Eq. (27) of [3]), are calculated by subroutine AGBT.

Subroutine PXAGBH, called by AGBT, (which in turn is called by TRAK2), calculates the predicted satellite state vector x_e (Eq. (32) of [3]), the predicted X, Y angles and the measurement vector $\hat{\beta}$, (Eq. (34) of [3]).

Subroutine PKKM, called by PXAGBH, calculates the covariance of the error in the prediction, P(k/k-1), from Eq. (33) of [3]. The measurement matrix H(k), (Eq. (31) of [3]), is calculated by the subroutine HMAT, called by PKKM. (See also Appendix B of [3]). The observation weighting matrix, W(k), (Eq. (36) of [3]), is calculated by the subroutine WATE, called by HMAT. The new estimated state vector, (Eq. (35) of [3]) and the new covariance of the error, P(k/k), (Eq. (37) of [3]), are computed by the subroutine ALKPKK, called by WATE.

Since the steady state solution of the Riccati equation is used, the Riccati equation has to be solved only once. A special index KPASS is set to zero initially. A test for (KPASS = 0?) is made at the end of the ALKPKK subroutine. If KPASS = 0, i.e., the program is in its first iteration, subroutine PCNTRL is called. Otherwise, the program goes back to TRAK2.

Subroutine PCNTRL solves the Riccati equation, (Eq. (50) in [3]), by an iterative procedure, starting with an initial unit matrix. The iteration results with the matrix P_2, (Eq. (52) in [3]). Subroutine ECNTRL is called to compute η and ψ, (Eqs. (61), (62) in [3]), which are needed in the computation of the optimal control. Subroutine ECNTRL calls subroutine PFEEH to compute the estimated X, Y angles. PFEEH calls TRAK3, where the constant portions of Eq. (63) in [3] are calculated. Equation (63) is later used in the calculation of the optimal control. At the end of subroutine TRAK3, KPASS is set to a value of 341 and the program is routed to TRAK2.

The Antenna System

A model of the 40 Ft. GSFC antenna system was chosen. A block diagram is given in Fig. 3.2, (For X channel; Y channel is identical).

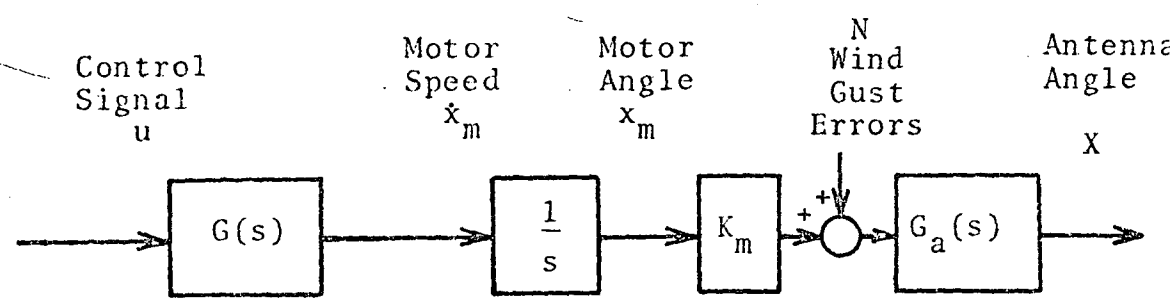

Figure 3.2

Antenna System Block Diagram

The data for the antenna were taken from unpublished notes by Philco-Ford Corporation.

The transfer function for the tachometer loop is given by:

$$\frac{\dot{X}_m(s)}{U(s)} = \frac{8.33(.0475s+1)}{.00505s^2 + .108s+1}$$

$$= \frac{78.2s^{-1} + 1650s^{-2}}{1+21.4s^{-1} + 198s^{-2}} \qquad (3\text{-}5)$$

or:

$$\dot{X}_m(s) = (-21.4s^{-1}-198s^{-2})\,\dot{X}_m(s) + (78.2s^{-1}+1650s^{-2})U(s) \qquad (3\text{-}6)$$

The relation between the antenna angle X and the motor angle X_m is given by the following differential equation: (Eq. (13) of [3]).

$$J\ddot{X}(t) + f\dot{X}(t) + N^2K\left(X-\frac{1}{N}X_m\right) = n(t) \qquad (3\text{-}7)$$

where

J = moment of inertia of the antenna = 1.95×10^6 in lb-sec^2

f = friction coefficient = .1 in lb/rad/sec

N = gear ratio from motor to antenna = 763

K = spring coefficient = 1.53×10^9 in lb/rad

$n(t)$ = wind gust disturbance

The differential equation for the wind gust disturbance is: (Eq. (14) of [3]):

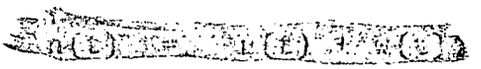

(3-

where $w(t)$ is assumed to be white noise.

Taking into account the data, Equation (3-7), becomes in Laplace transform:

$$X(s)\ (1+785s^{-2}) = 1.03s^{-2}\ X_m(s)$$

$$+ .507 \times 10^{-6}\ s^{-2}\ n(s) \qquad (3\text{-}9$$

and the Laplace transform of Eq. (3-8) is:

$$n(s) = -s^{-1} n(s) + s^{-1} W(s) \tag{3-10}$$

Combining equations (3-6), (3-9), (3-10), one obtains a signal flow graph of the whole antenna system shown in Figure 3.3. The assignment of the state variables is shown in the same figure.

The system state equations are readily written out from Figure 3.3:

$$\begin{aligned}
\dot{x}_1 &= x_2 \\
\dot{x}_2 &= -785x_1 + 1.03x_3 + .507\times10^{-6}x_6 \\
\dot{x}_3 &= x_4 \\
\dot{x}_4 &= -21.4x_4 + x_5 + 78.2u \\
\dot{x}_5 &= -198x_4 + 1650u \\
\dot{x}_6 &= -x_6 + w
\end{aligned} \tag{3-11}$$

or in matrix vector form:

$$\dot{\underline{x}} = F\underline{x} + D\underline{u} + G\underline{w} \tag{3-12}$$

(See Eqs. (17) (21) of [3])

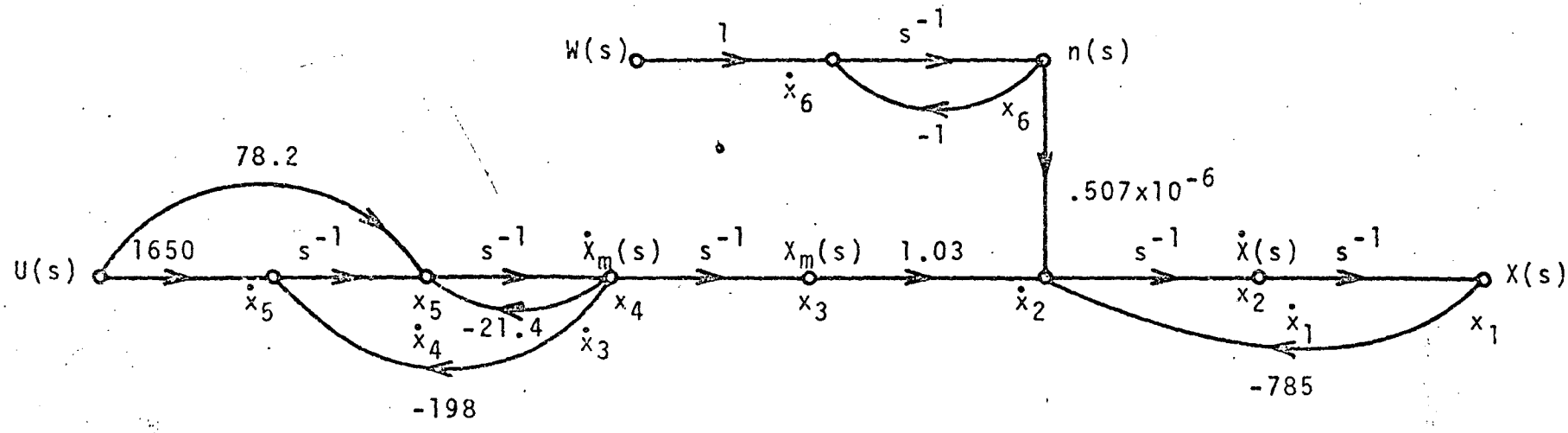

Figure 3.3 Signal Flow Diagram of the X-channel of the 40 foot Antenna Tracking System.

where:

$$F = \begin{bmatrix} 0 & 1 & 0 & 0 & 0 & 0 \\ -785 & 0 & 1.03 & 0 & 0 & .507\text{x}10^{-6} \\ 0 & 0 & 0 & 1 & 0 & 0 \\ 0 & 0 & 0 & -21.4 & 1 & 0 \\ 0 & 0 & 0 & -198 & 0 & 0 \\ 0 & 0 & 0 & 0 & 0 & -1 \end{bmatrix}$$

$$\underline{D} = \begin{bmatrix} 0 \\ 0 \\ 0 \\ 78.2 \\ 1650 \\ 0 \end{bmatrix} \qquad G = \begin{bmatrix} 0 \\ 0 \\ 0 \\ 0 \\ 0 \\ 1 \end{bmatrix}$$

The same set of state equations applies to channel y as well.

The matrices F, D are read in as input data; they are the ones which characterize the specific antenna control system. If it is desired to implement a different antenna, or tracking system, it is only necessary to change the F, D matrices, which are read in as array FP, DPHI by the NAMELIST/DYNMIC/ in subroutine FPHI. After reading in the antenna system data, the program proceeds as described in reference [3], and in this section.

Note that the wind gust distrubance appears as one of the state variables in this model. It is one of the errors mentioned in section 2.2. In this course of the solution, the wind gust state variable will be estimated by the optimal estimator, and the optimal controller will provide a control signal, minimizing the pointing error and taking into account also the wind gust error, among other data. This cannot be accomplished in the autotrack mode and it illustrates the potential usefulness of an optimal estimator controller technique.

Particular Problems Encountered in RATS Development

In the following, some of the problems encountered during the development of the RATS program are described.

(1) Computation of the State Transition Matrix - A Taylor series expansion is made to obtain the state transition matrix EXP[FΔt], (Eq. (20) of [3]). The programmed computation in the original program did not converge. The previously used convergence criterion was changed to the following one:

$$|\text{trace } \Phi_{n+1} - \text{trace } \Phi_n| < 10^{-6} \ ?$$

where

Φ_n = Taylor expansion including n terms

Φ_{n+1} = Taylor expansion including n+1 terms

This revised criterion produced acceptable values. As a further check EXP[FΔt] for a 6x6 matrix was calculated by taking the exact inverse Laplace transform of $(sI-F)^{-1}$. The results of the two methods agreed to an acceptable degree of accuracy.

(2) Matrix Inversion Calculation - The matrix inversion routine, used in the previous version of the program was found to produce unacceptable results. The routine was replaced, and an additional routine incorporated, using an iterative method of calculation of calculating the inverse. In addition, the calculation of the weighting matrix used in the Kalman filter was modified to calculate the required inverse by a short iterative scheme, not involving an actual inversion.

Referring to Eq. (36) in [3], it is required to calculate

$$B^{-1} = [R + HPH^T]^{-1}$$

at each time point. The short inversion proceeds as follows:

Let $B^{-1}(n+1) = B^{-1}(n)[2I-B(n+1)B^{-1}(n)]$ be the desired inverse at the next time point. The method saves considerable time and in the cases run yielded good results.

RATS COMPUTER SPACE ALLOTMENT

For a two-channel antenna control system with 6 state variables per channel, the computer space allotment in the IBM 360/91 is as follows:

1. With the plotting capabilities with 200 points per graph:

   $38A80_{16}$ Bytes
   or: $232,064_{10}$ Bytes
   or: $58,016_{10}$ Words (single precision)

2. Without the plotting capabilities, approximately

   $10D00_{16}$ Bytes
   or: $68,864_{10}$ Bytes
   or: $17,216_{10}$ Words (single precision)

The computing time is less than 2 minutes for 200 points. There is no significant difference in computing time if the plotting option is used. In real time 200 point represent:

200*0.05=10 seconds

REFERENCES

1. R.M. Dressler, E.C. Fraser, "Optical Communication and Tracking Systems," Final Report, Stanford Research Institute, Menlo-Park, California, October 1967.

2. M.A. Kisner, "Earth-Based Terminal of the Optical Communication and Tracking System," Programmer's Manual, Stanford Research Institute, Menlo-Park, California, October 1967.

3. J. Peschon, R.M. Dressler, L. Meier, R.E. Larson, E.C. Fraser, O.J. Tveit, "Research on the Design of Adaptive Control Systems," Final Report, Vol. 2, Chapter 7, Stanford Research Institute, Menlo-Park, California, September 1966. (Reproduced in Appendix E for the reader's convenience.)

4. Design Analysis - Unified S-Band System for Apollo Network, Engineering Report, Collins Radio Company, 523-0556527-001D3M, 28 October 1964, Contract NAS 5-9035.

4. Simulation Results

4.1 ORBTRACK Testing

In order to test the original SRI ORBTRACK program, after it has been adapted to the IBM 360/91 system, several simulation runs were performed. The same data as in some of the original SRI runs were used and the results compared to the ones reported in reference [1].

A Mars mission case was chosen. The details concerning the input data are given on pp. 57-61 of reference [1]. For the purpose of comparison, the cases illustrated in Figure 10(a), (b) and Figure 16(a), (b) of reference [1], were run on the 360/91 system. The results of these runs are reported in Figure 4.1, (a) - (f). These figures show the time functions of the antenna angle errors. The ordinate is in units of radians, scaled by a factor of 10^{-6}. The abscissa is scaled in units of sampling, K. For these runs the sampling period was $\Delta t = .25$ sec. The runs were performed for a total of $K = 400$, i.e., $t = K*\Delta t = 400*.25 = 100$ seconds. The graphs in Figure 4.1 illustrate the additional graphical capability that was added to the program. The angles are in the elevation-azimuth reference frame. (In the new ATRK30 version it was converted to the X, Y angles).

Figure 4.1(a) shows the error between the estimated (by the optimal estimator) and the true (predicted from trajectory data) ϕ angle. Figure 4.1(b) shows the same for the Θ angle. Figure 4.1(c) shows the error between the actual antenna position, for the ϕ channel, and the true ϕ angle. Figure 4.1(d) shows the same for the Θ angle. The errors between the actual antenna positions

for the ϕ and Θ channels, in Autotrack mode, and the true ϕ and Θ angles, are shown in Figure 4.1(e) and (f), respectively. As mentioned in Chapter 3 and in reference [1], the system actually considered was an optical tracking system. However the plant equations happen to be of the same form as these for the 30 foot tracking antenna model. The difference is in the parameters only and in the controller in Autotrack mode. As one may see, the general form of the curves, as well as the range of values, correspond to the previous results. [1]

4.2 Simulation with Nonlinearities. (ORBTRACK)

It is well known that the actual antenna control system is nonlinear. Four types of nonlinearities, considered in this study, are shown in Figure 4.2 (a) - (d). The abscissa is the control signal, u, at the input of the nonlinearity, while u_N is the control signal at its output.

All practical servo amplifiers saturate for signals with large amplitudes. This property is reflected in the nonlinearity in Figure 4.2(a). The antenna has a finite resolution for changes in attitude angles. If there is a change around the zero angle, there exists a dead zone, shown in Figure 4.2(b). Due to limited resolution there also exists a quantizing nonlinearity in the loop, as the one shown in Figure 4.2(d). In the 40 foot antenna the hydraulic power drive contains quadratic nonlinearities of the type shown in Figure 4.2(c).

by optimal estimator

ESTIMATOR-CONTROLLER

$(\phi)_{EST} - (\phi)_T$

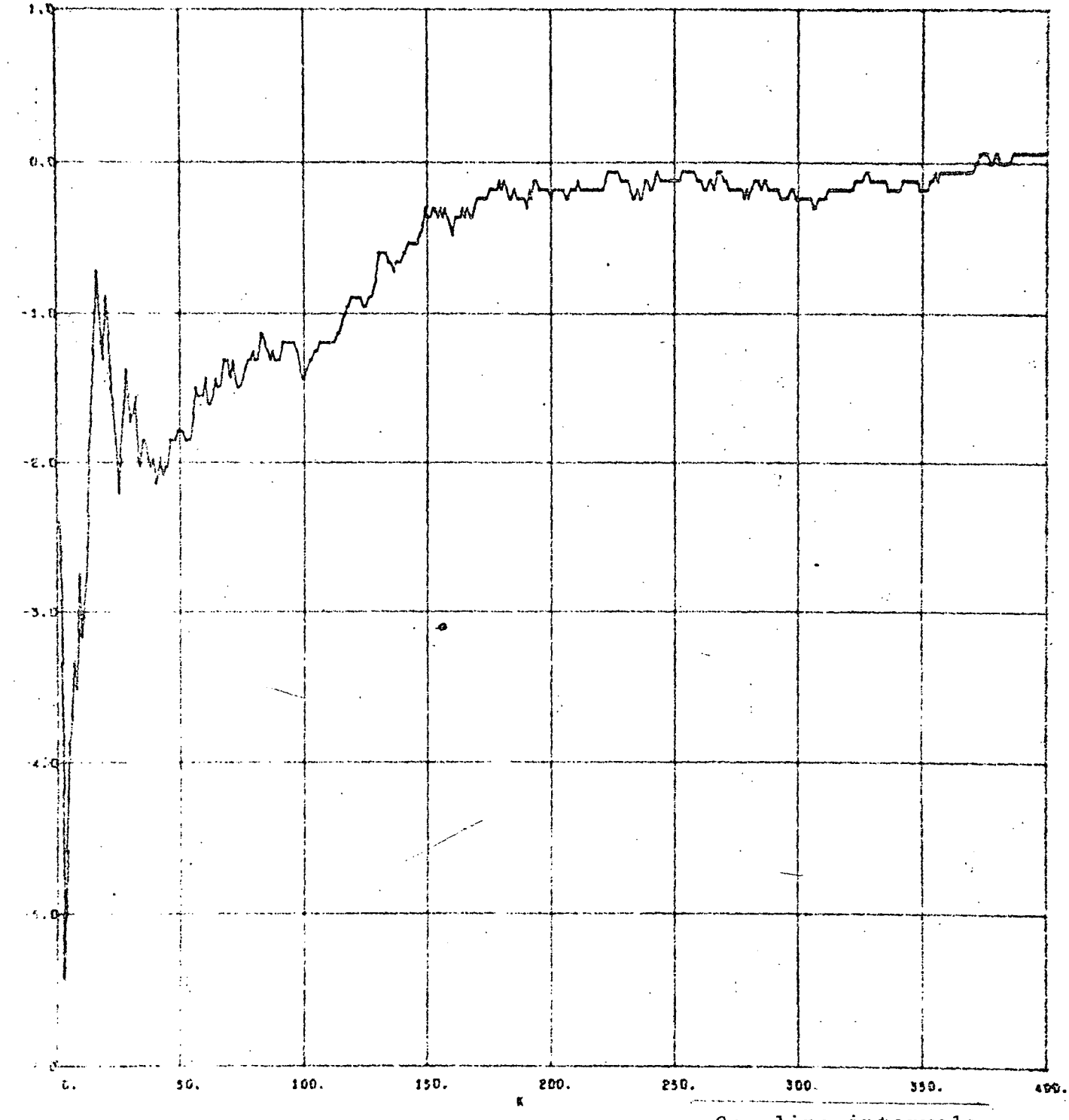

Sampling intervals
$\Delta t = .25$ sec.

Figure 4.1-(a)

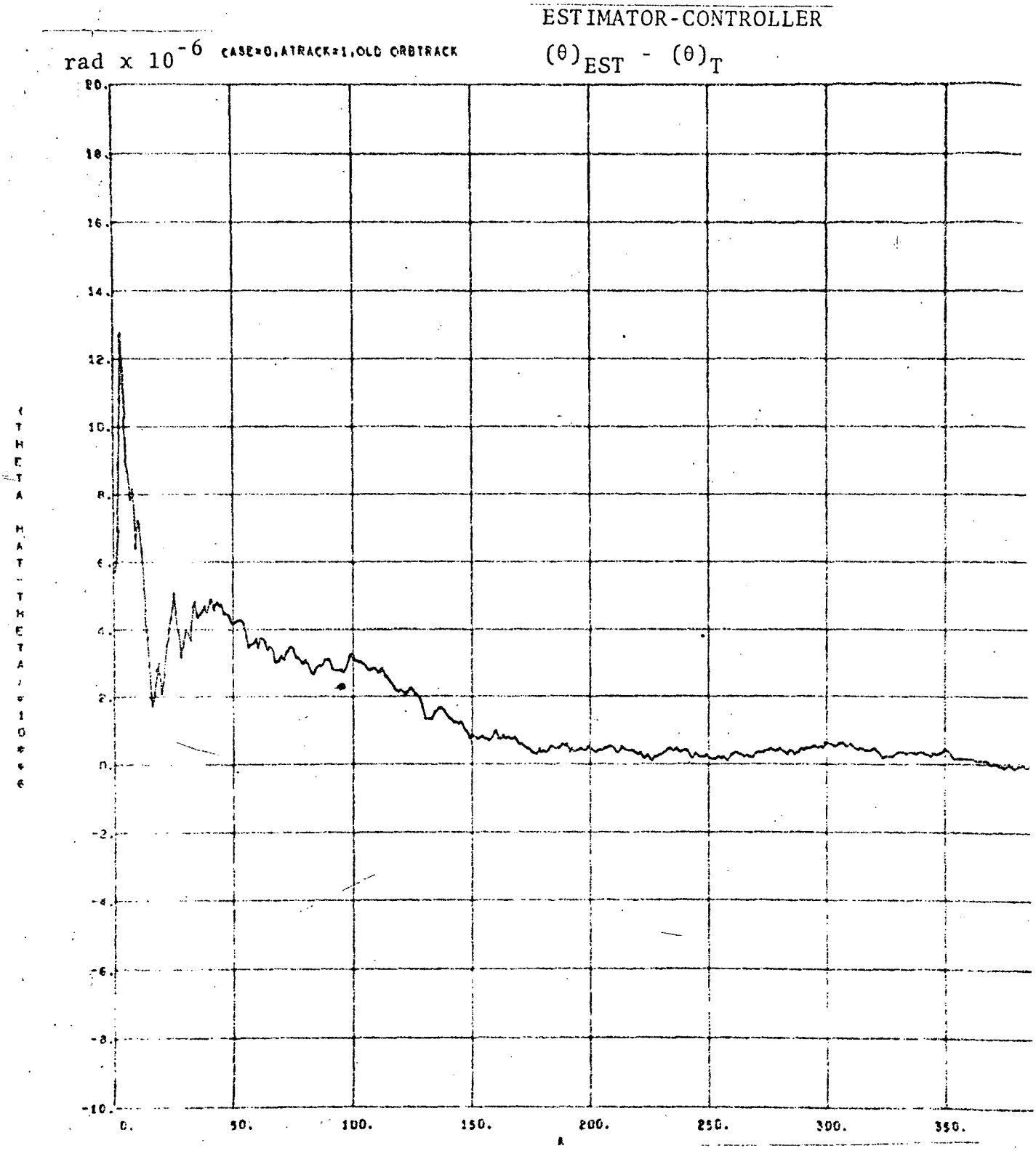

Sampling intervals
$\Delta t = .25$ sec.

Figure 4.1(b)

ESTIMATOR-CONTROLLER

$(\phi)_{ANT} - (\phi)_T$

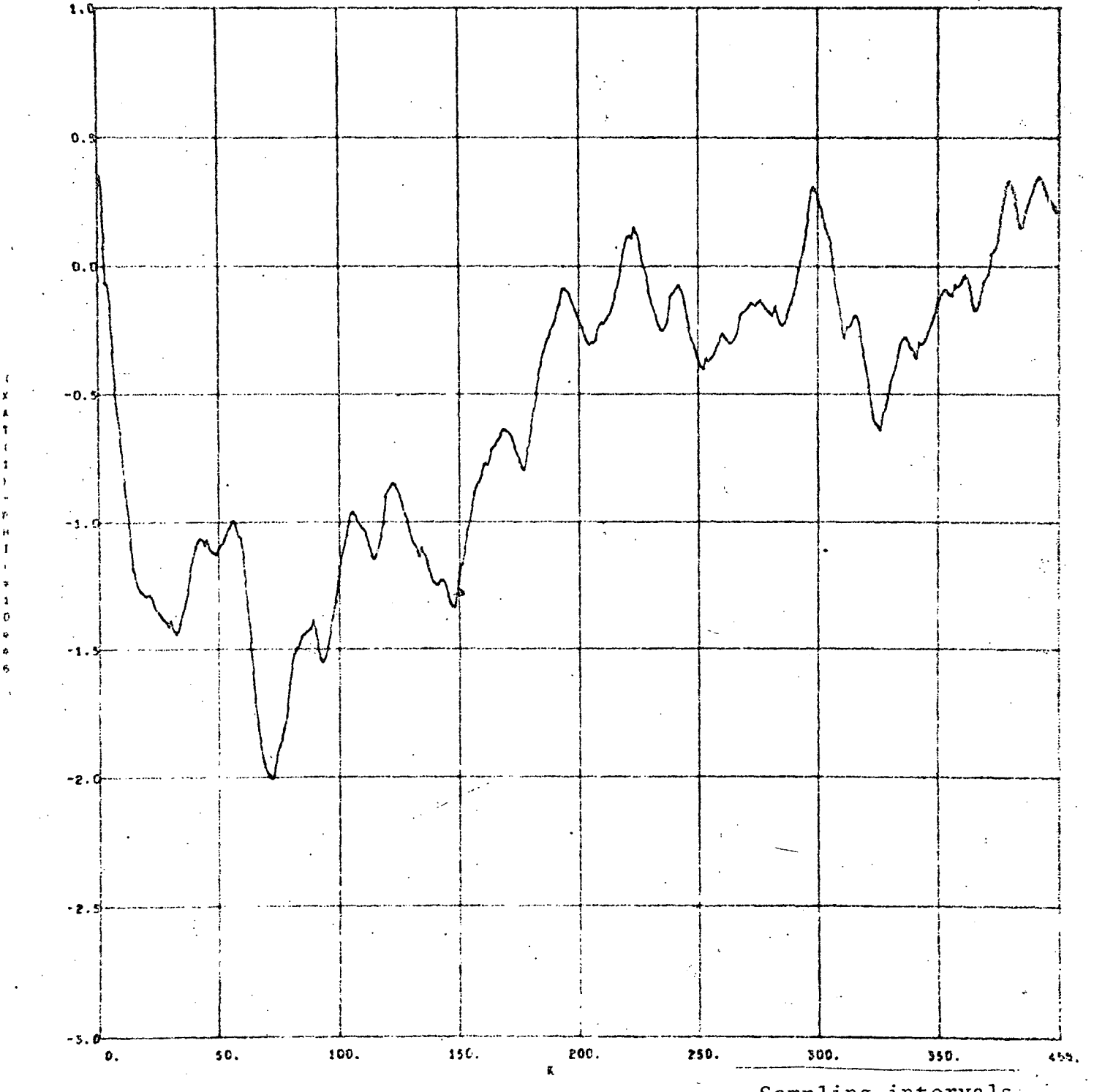

Sampling intervals
$\Delta t = .25$ sec.

Figure 4.1(c)

ESTIMATOR-CONTROLLER

$(\theta)_{ANT} - (\theta)_T$

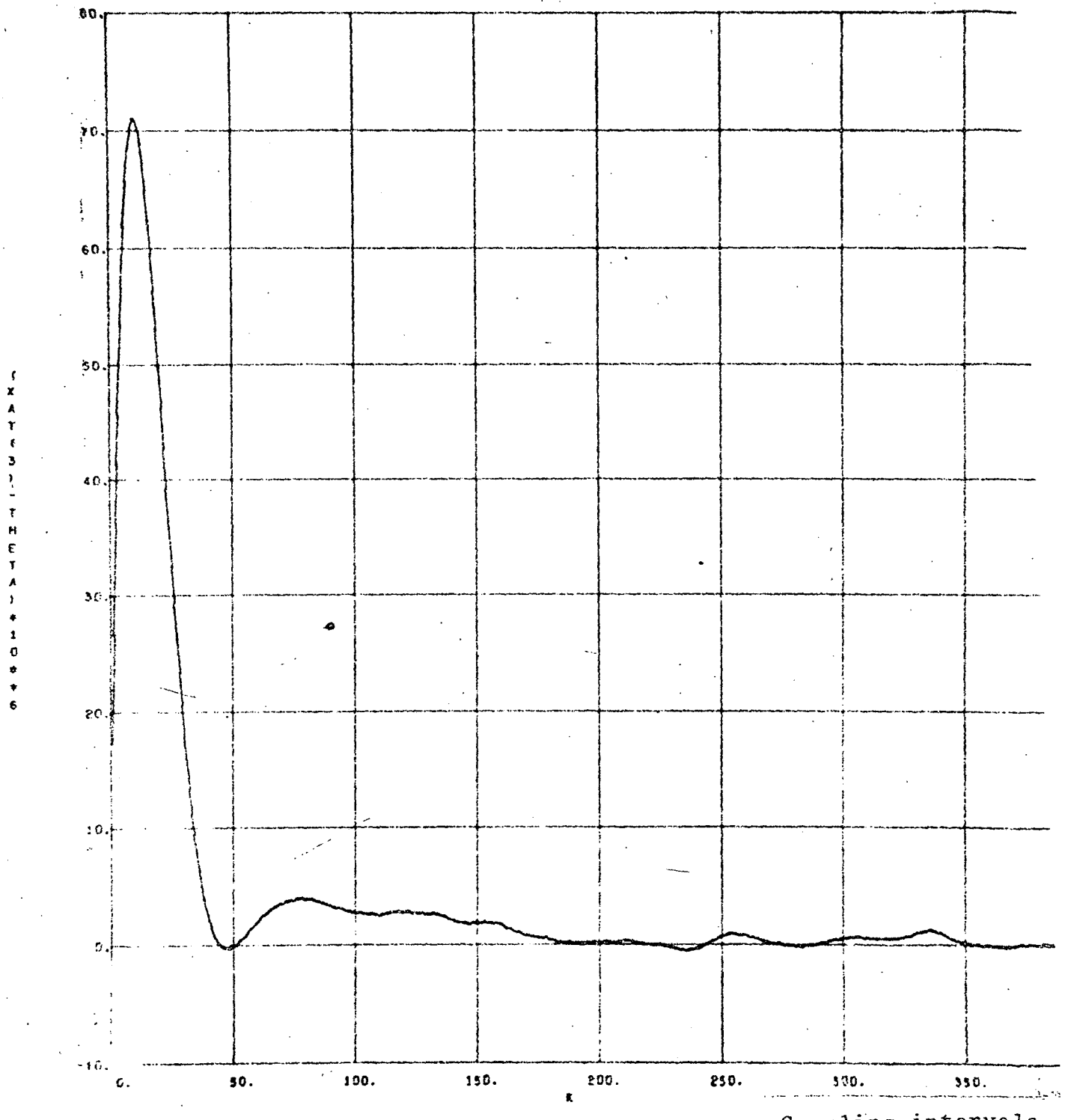

Sampling intervals

$\Delta t = .25$ sec.

Figure 4.1(d)

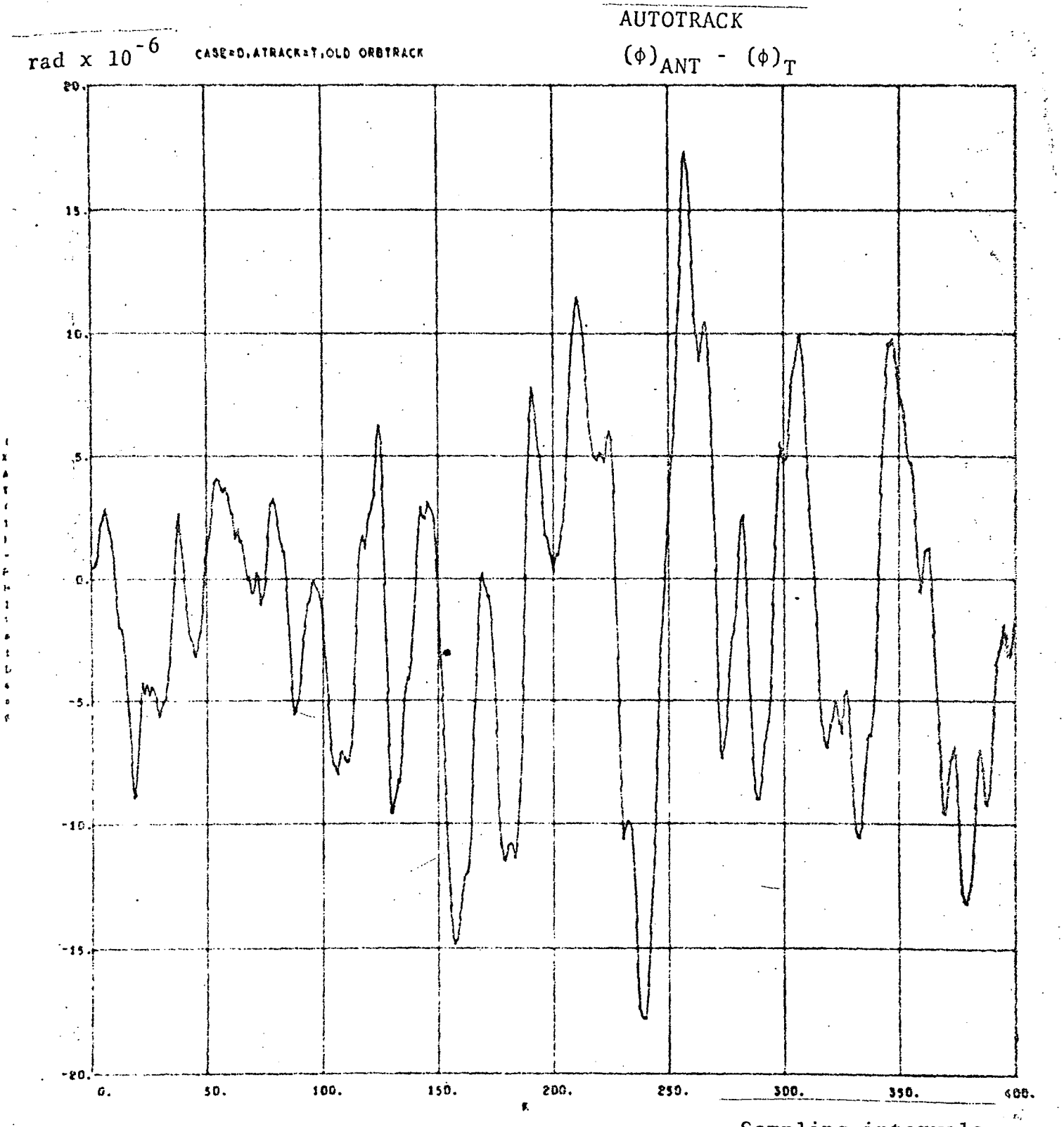

Sampling intervals
Δt = .25 sec.

Figure 4.1(e)

AUTOTRACK

$(\theta)_{ANT} - (\theta)_T$

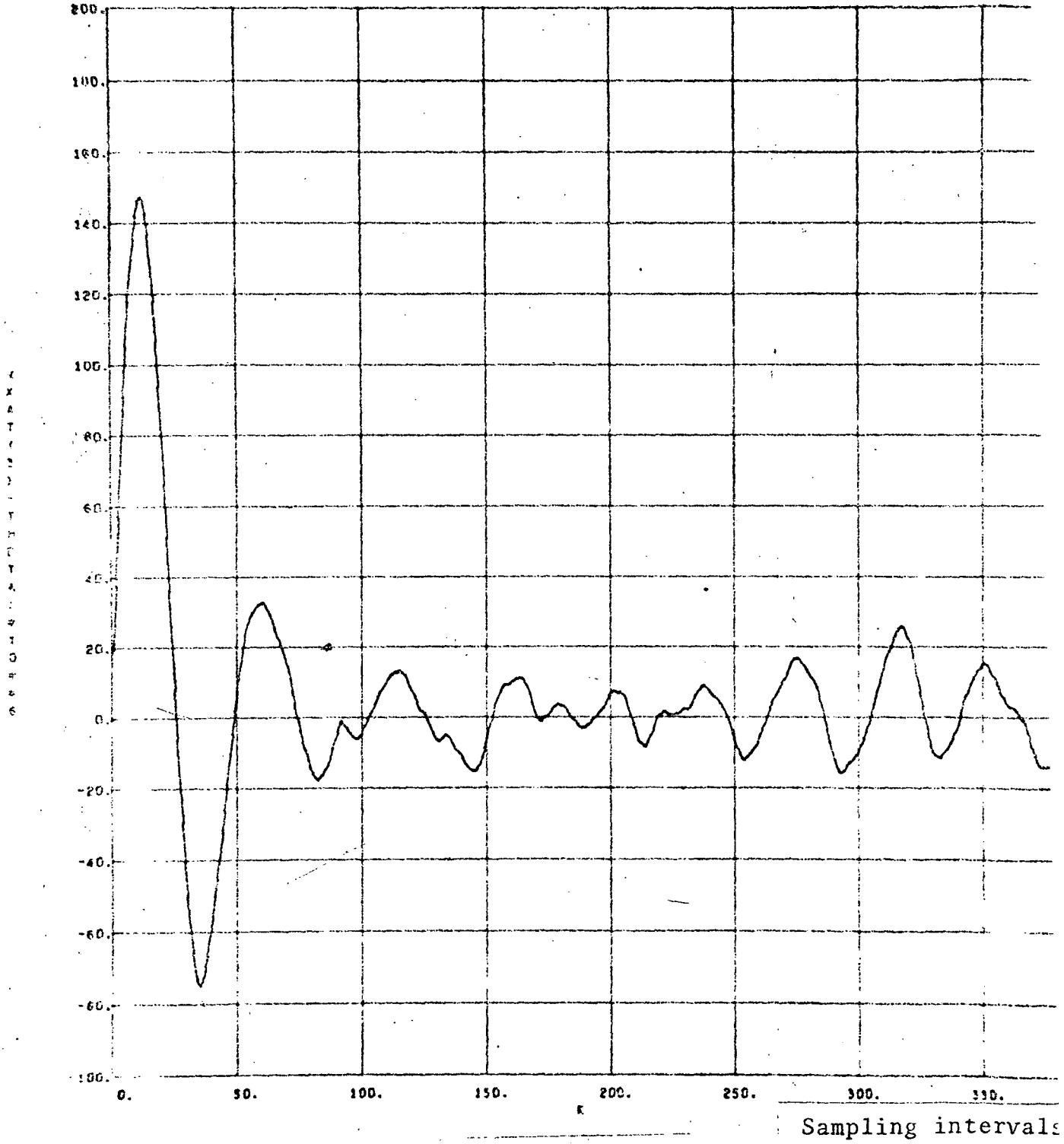

Sampling intervals
Δt = .25 sec.

Figure 4.1(f)

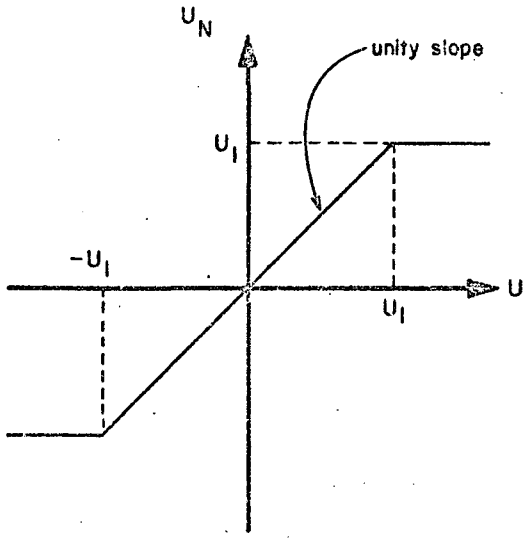

(A) SATURATION

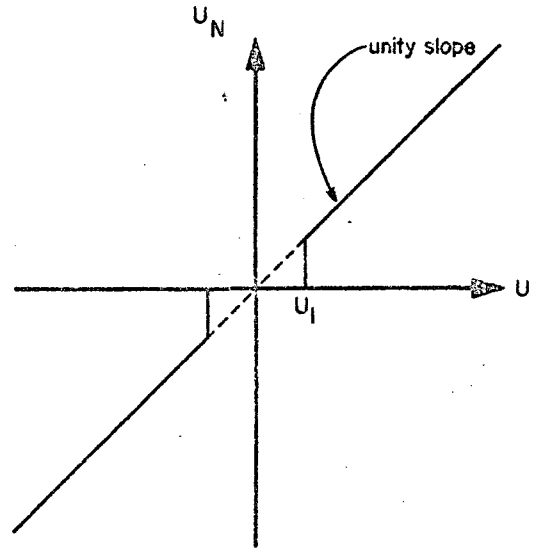

(B) DEAD ZONE

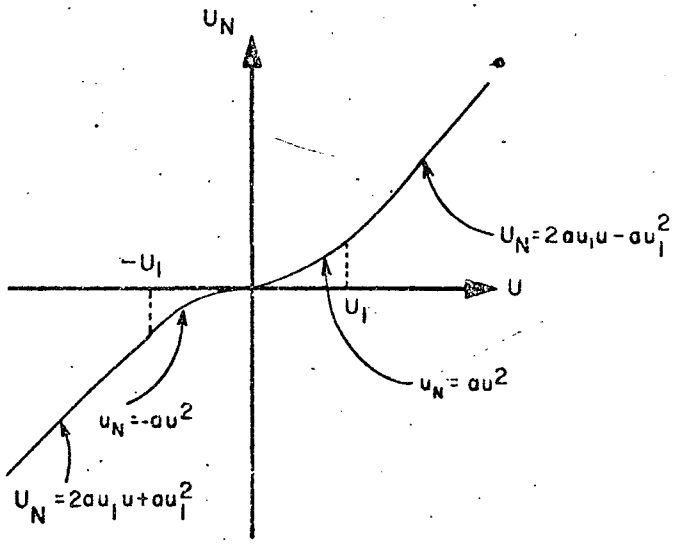

(C) QUADRATIC FORM

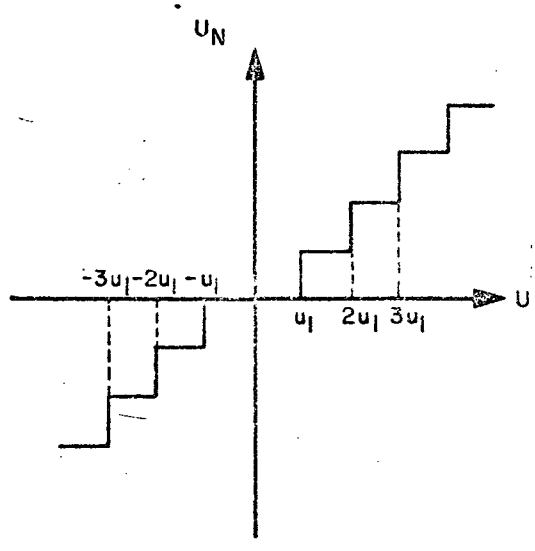

(D) QUANTIZER

FIGURE 4.2 NONLINEARITIES OF THE ANTENNA CONTROL SYSTEM

In the simulations that were performed, a nonlinearity was applied in the forward path of the control signal. In other words, as soon as the control signal u was calculated by the regular procedure, (assuming the whole system is linear), a new control signal u_N was calculated, depending what nonlinearity was assumed, according to Figure 4.2. The simulation indicates the behavior of a system with a nonlinearity in which the control signal is calculated assuming that the system is linear. The simulations were carried out using the plant available in the ORBTRACK program. However, as mentioned before, that plant has the same general form as the 30 foot antenna control system. All basic data were the same as the ones used in the simulation shown in Figure 4.1. All the simulations with the nonlinearities were performed in the optimal estimator-controller mode.

The saturation nonlinearity, shown in Figure 4.2(a), was tried first with a very low threshold value of $u_1 = .002$. The results of this are shown in Figure 4.3(a), (b). As one may see, the system is highly unstable, which should have been expected for such a low value of u_1.

By increasing the value of u_1 to $u_1 = 1.$, the ϕ channel was stabilized, as may be seen from Figure 4.4(a). Channel Θ still remains unstable as shown in Figure 4.4(b). This channel is stabilized by choosing $u_1 = 30.$, however it still has a relatively high overshoot, (Figure 4.5(b)). The behavior of the ϕ channel is basically the same as for $u_1 = 1.$ as shown in Figure 4.5(a).

Another aspect of the optimal control process involved was investigated, namely, the influence of the values of the weighting coefficients of the control signals in the performance index, b_ϕ and b_Θ. The same runs, shown in

(unstable)

Saturation Nonlinearity

$u_1 = .002$

$b_\phi = 10^{-10}$

$b_\theta = 10^{-11}$

rad x 10^{-6} $(\phi)_{ANT} - (\phi)_T$

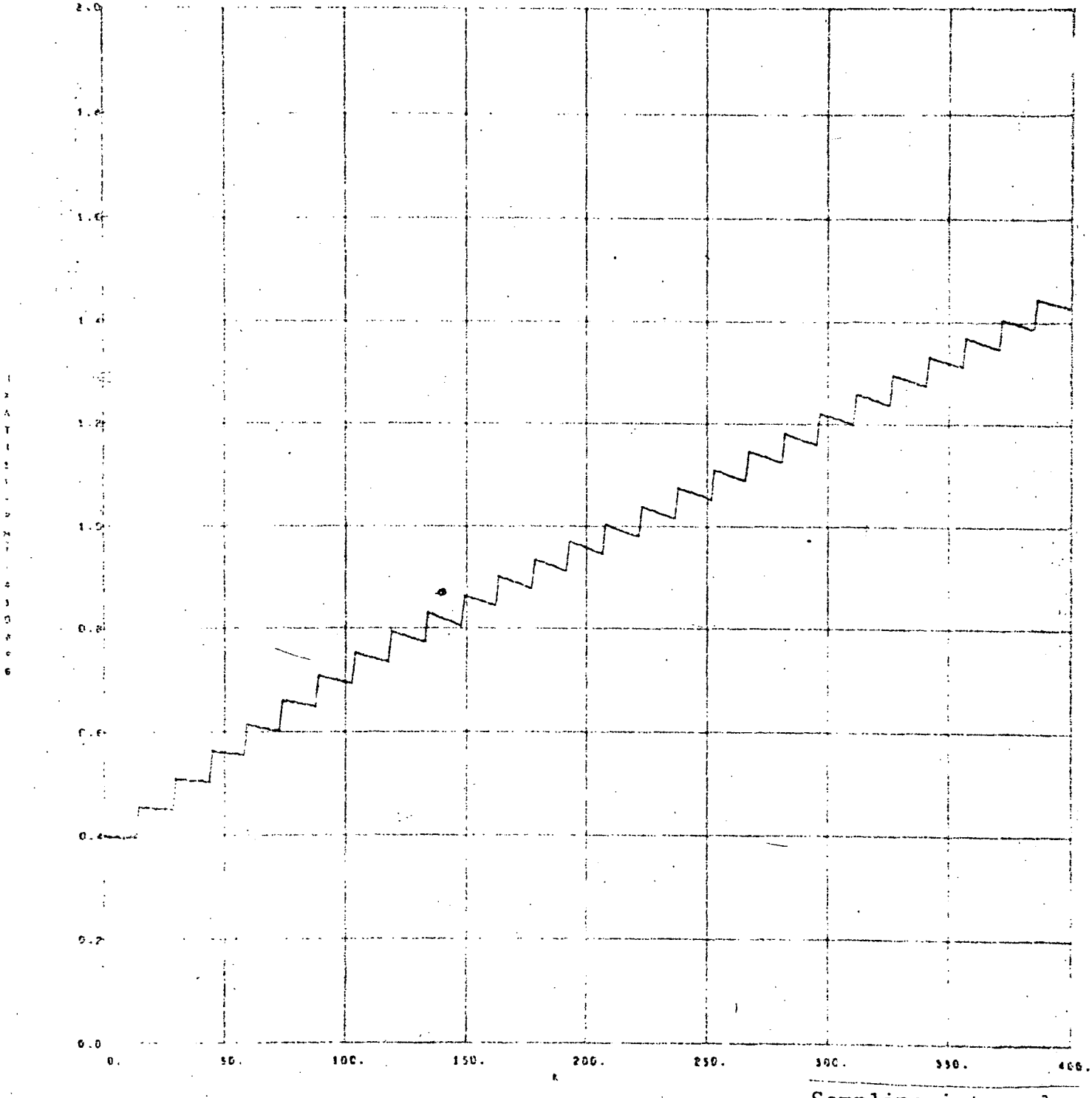

Sampling intervals
$\Delta t = .25$ sec.

Figure 4.3(a)

(unstable)

Saturation Nonlinearity

$u_1 = .002$ $b_\phi = 10$

$b_\theta = 10$

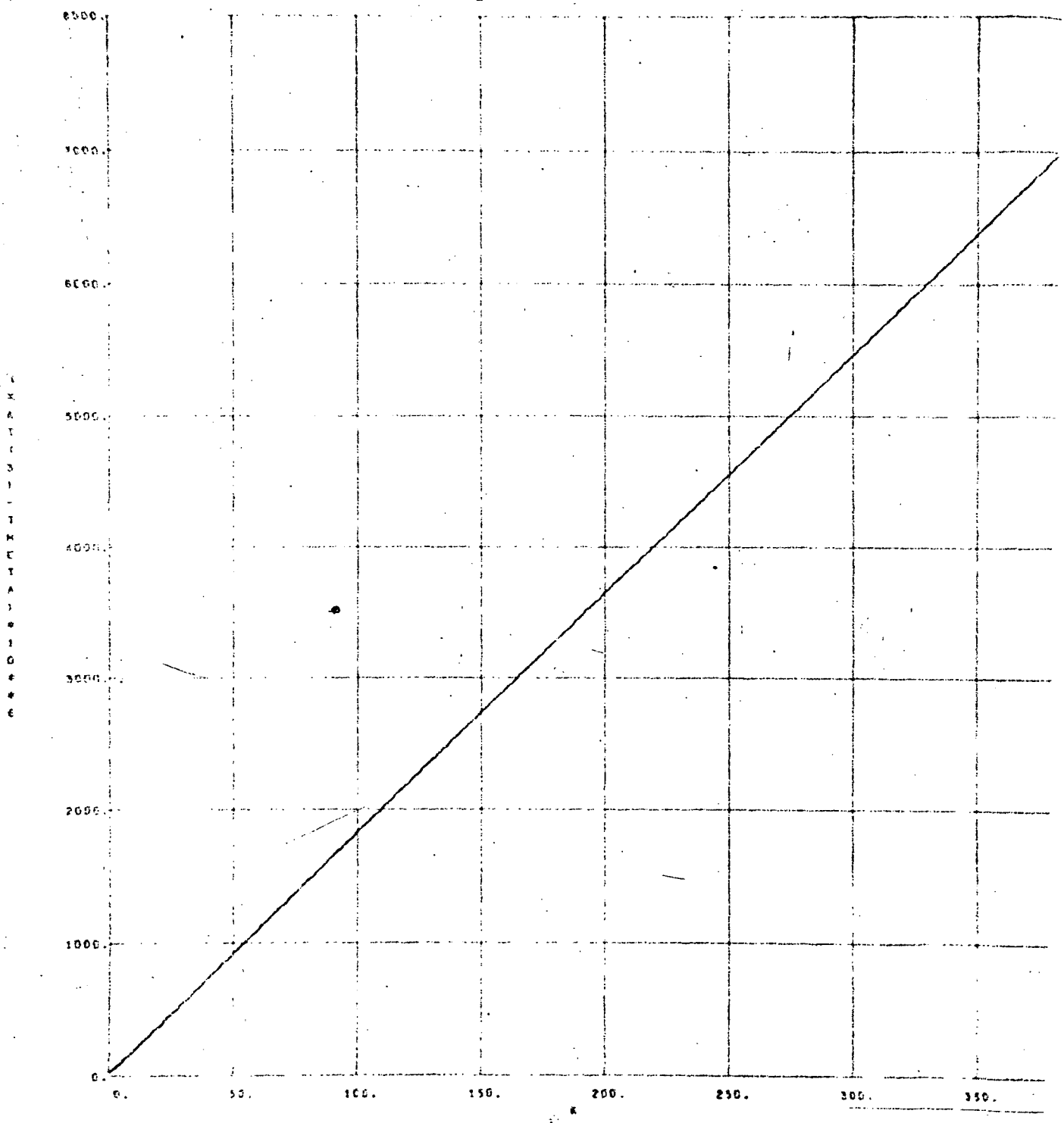

Figure 4.3(b)

Sampling inte

$\Delta t = .25$ sec.

(stable)

Saturation Nonlincarity

$u_1 = 1.$

$b_\phi = 10^{-9}$

rad x 10^{-6}

$(\phi)_{ANT} - (\phi)_T$

$b_\theta = 10^{-10}$

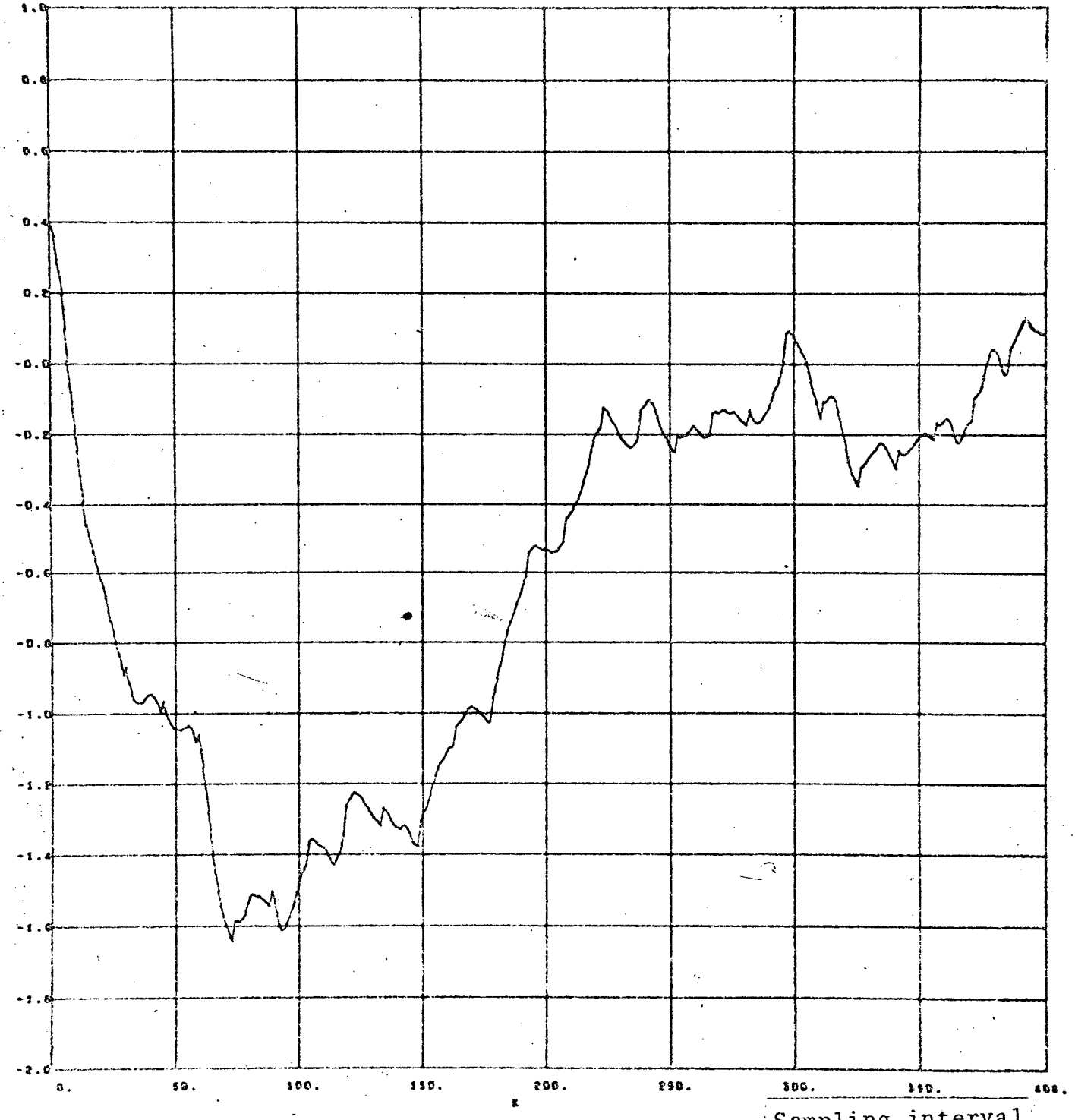

Figure 4.4(a)

Sampling interval

$\Delta t = .25$ sec.

(unstable)

Saturation Nonlinearity

$u_1 = 1.$ $b_\phi = 10^{-9}$

rad x 10^{-6} $(\theta)_{ANT} - (\theta)_T$ $b_\theta = 10^{-1}$

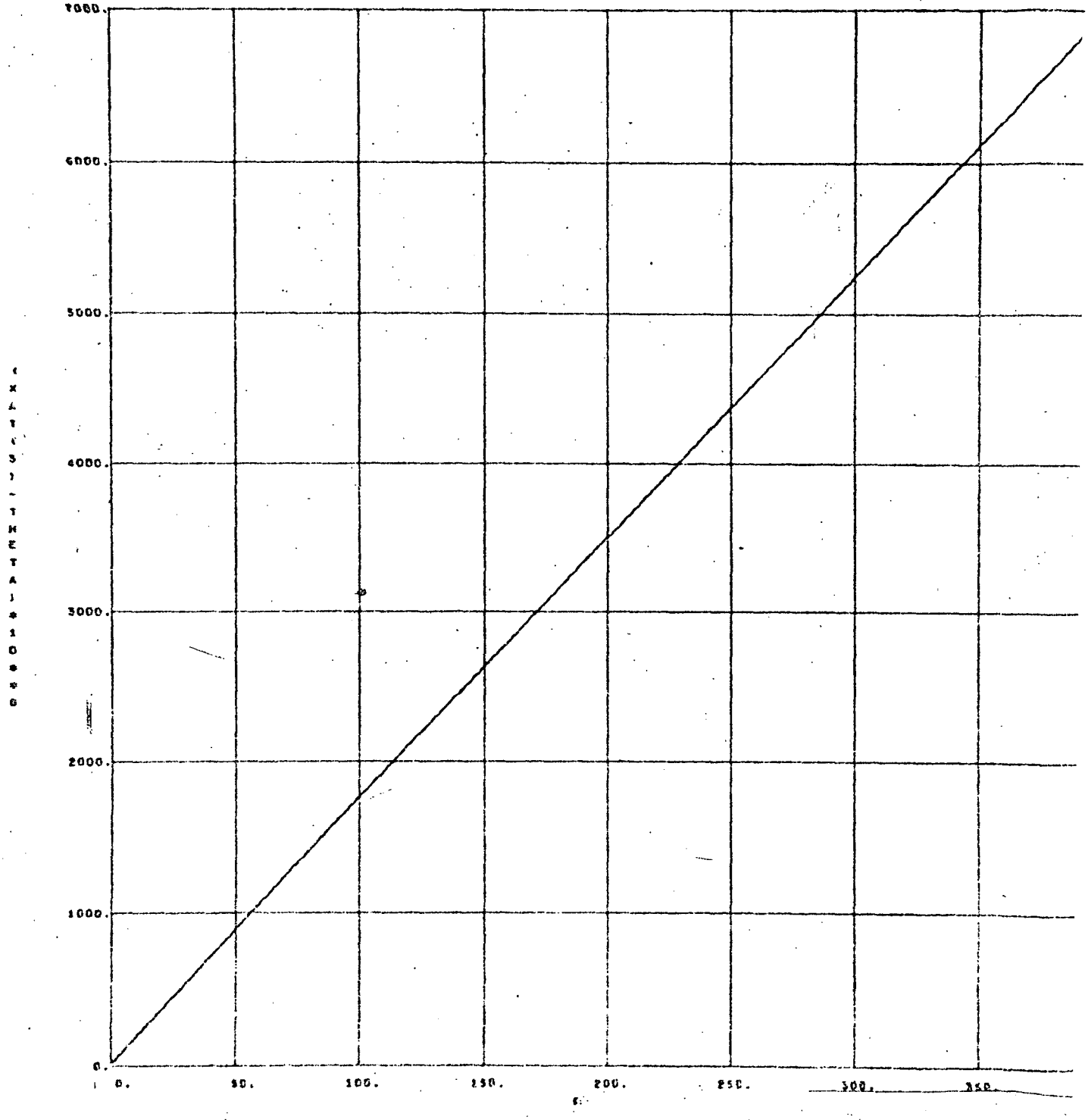

Figure 4.4(b)

Sampling interval
$\Delta t = .25$ sec.

2

(Stable)

Saturation Nonlinearity

$u_1 = 30.$

$b_\phi = 10^{-9}$

$b_\theta = 10^{-10}$

rad x 10^{-6}

$(\phi)_{ANT} - (\phi)_T$

Figure 4.5(a)

Sampling intervals

$\Delta t = .25$ sec.

(Stable)

Saturation Nonlinearity

$u_1 = 30.$

$b_\phi = 10^{-1}$

$b_\theta \quad 10^{-1}$

rad x 10^{-6}

$(\theta)_{ANT} - (\theta)_T$

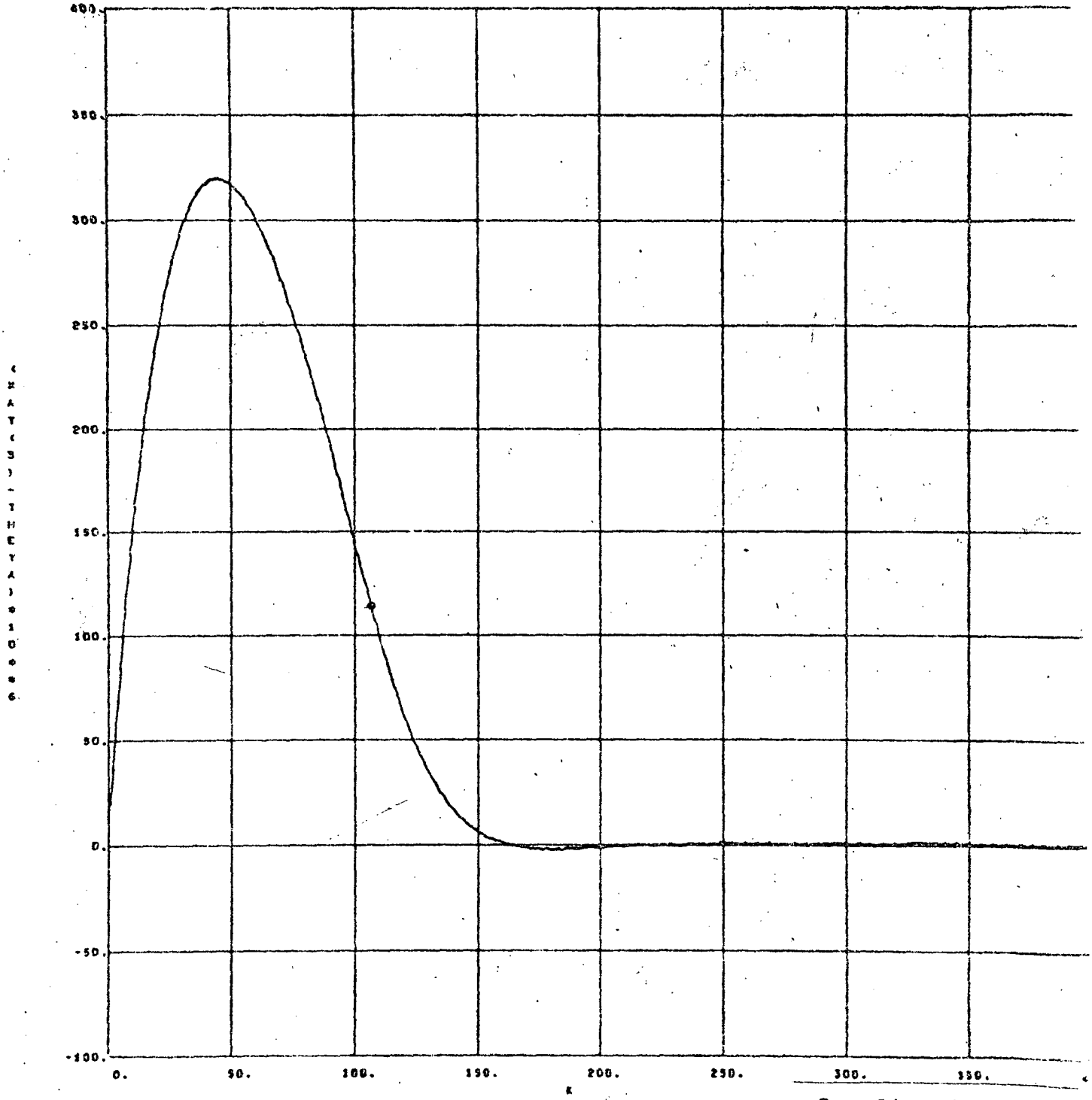

Sampling intervals

$\Delta t = .25$ sec.

Figure 4.5(b)

(stable)

Saturation Nonlinearity

$u_1 = 1.$

$b_\phi = 10^{-11}$

$b_\theta = 10^{-12}$

rad x 10^{-6}, $(\phi) - (\phi)_T$

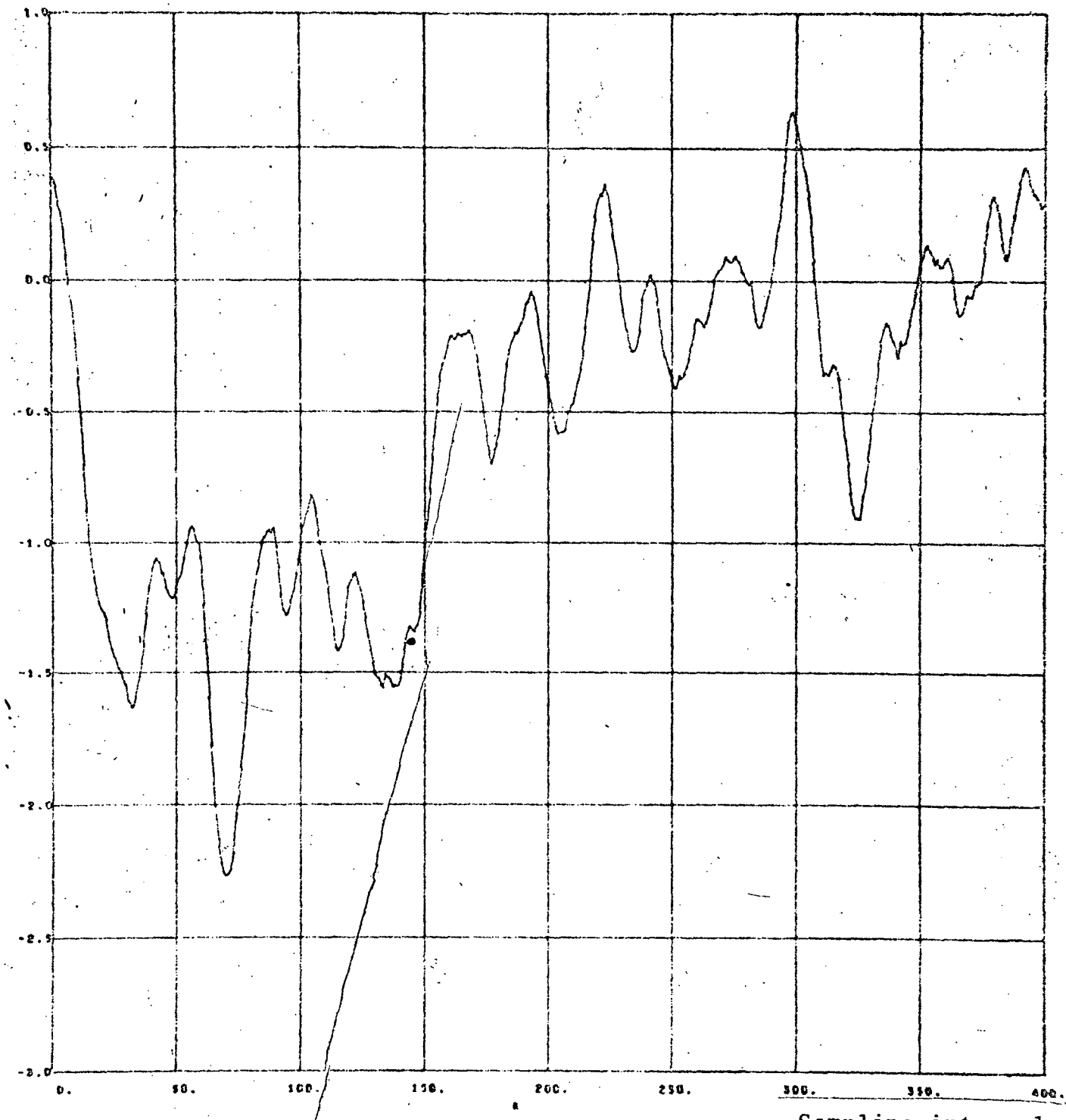

Sampling intervals

$\Delta t = .25$ sec.

Figure 4.6(a)

(unstable)

Saturation Nonlinearity

$u_1 = 1.$

gain c

b_ϕ = 1

b_θ = 1

rad x 10^{-6} $(\theta)_{ANT} - (\theta)_T$

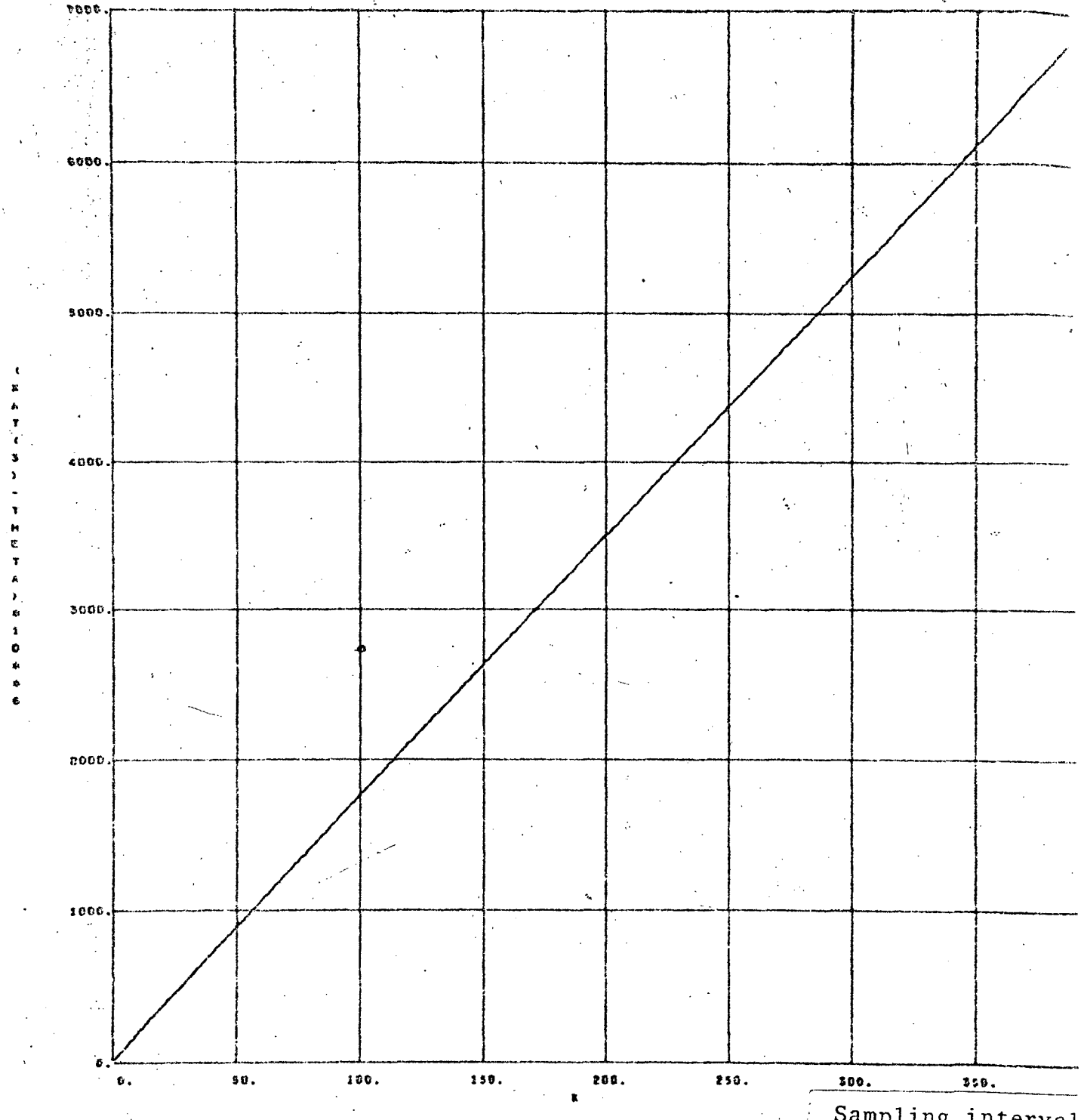

Figure 4.6(b)

Sampling interval

Δt = .25 sec.

(stable)

gain change

Saturation Nonlinearity

$b_\phi = 10^{-11}$

$u_1 = 30.$

rad x 10^{-6} $(\phi)_{ANT} - (\phi)_T$

$b_\theta = 10^{-12}$

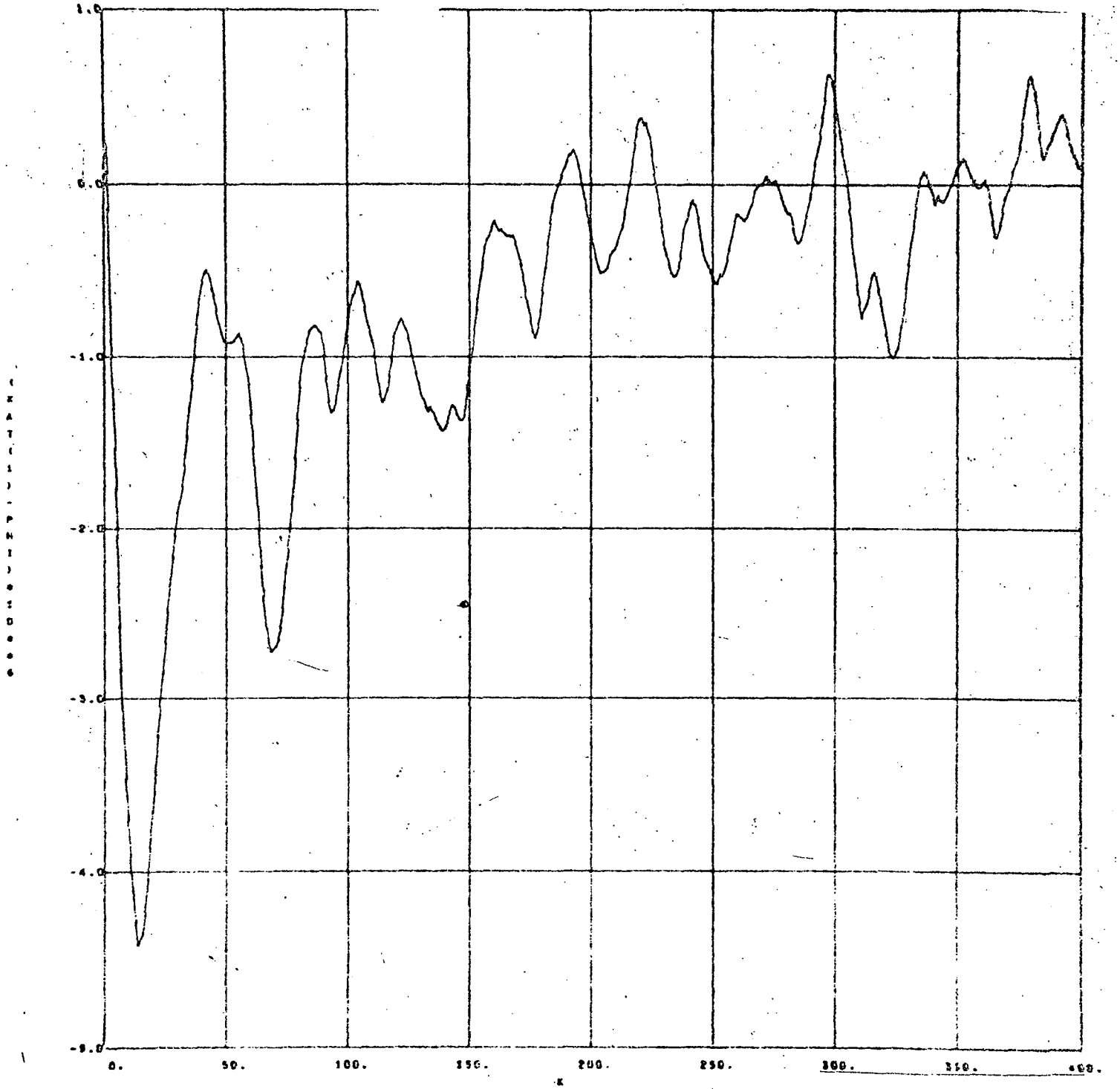

Sampling intervals

$\Delta t = .25$ sec.

Figure 4.7(a)

(stable)

Saturation Nonlinearity

$u_1 = 30.$

$b_\phi = 1($

$b_\theta = 1($

rad x 10^{-6} $(\theta)_{ANT} - (\theta)_T$

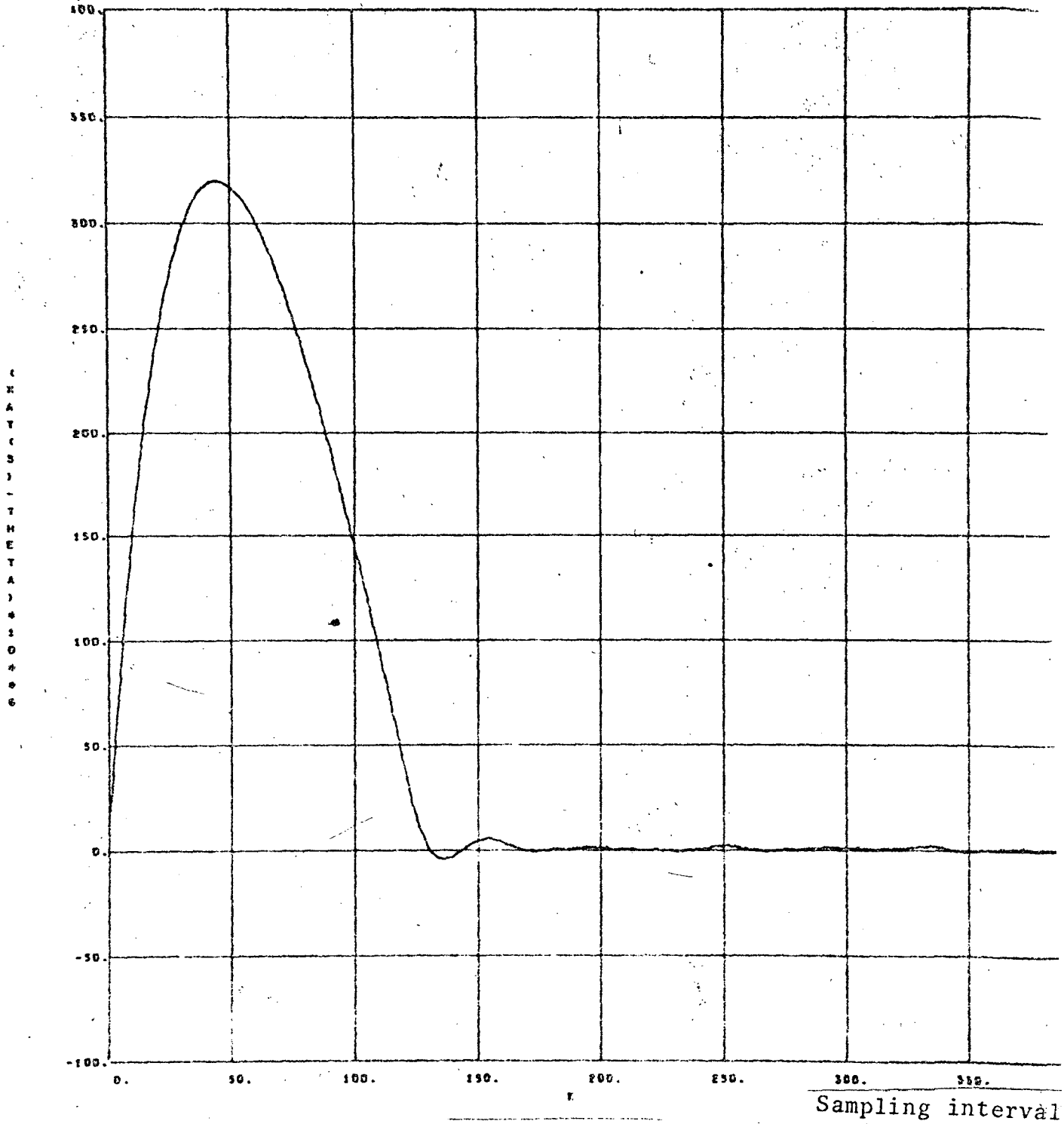

Figure 4.7(b)

Sampling interval

$\Delta t = .25$ sec.

(Stable)

Quantizer Nonlinearity

$u_1 = .002$

$b_\phi = 10^{-9}$

$b_\theta = 10^{-10}$

rad x 10^{-6} $(\phi)_{ANT} - (\phi)_T$

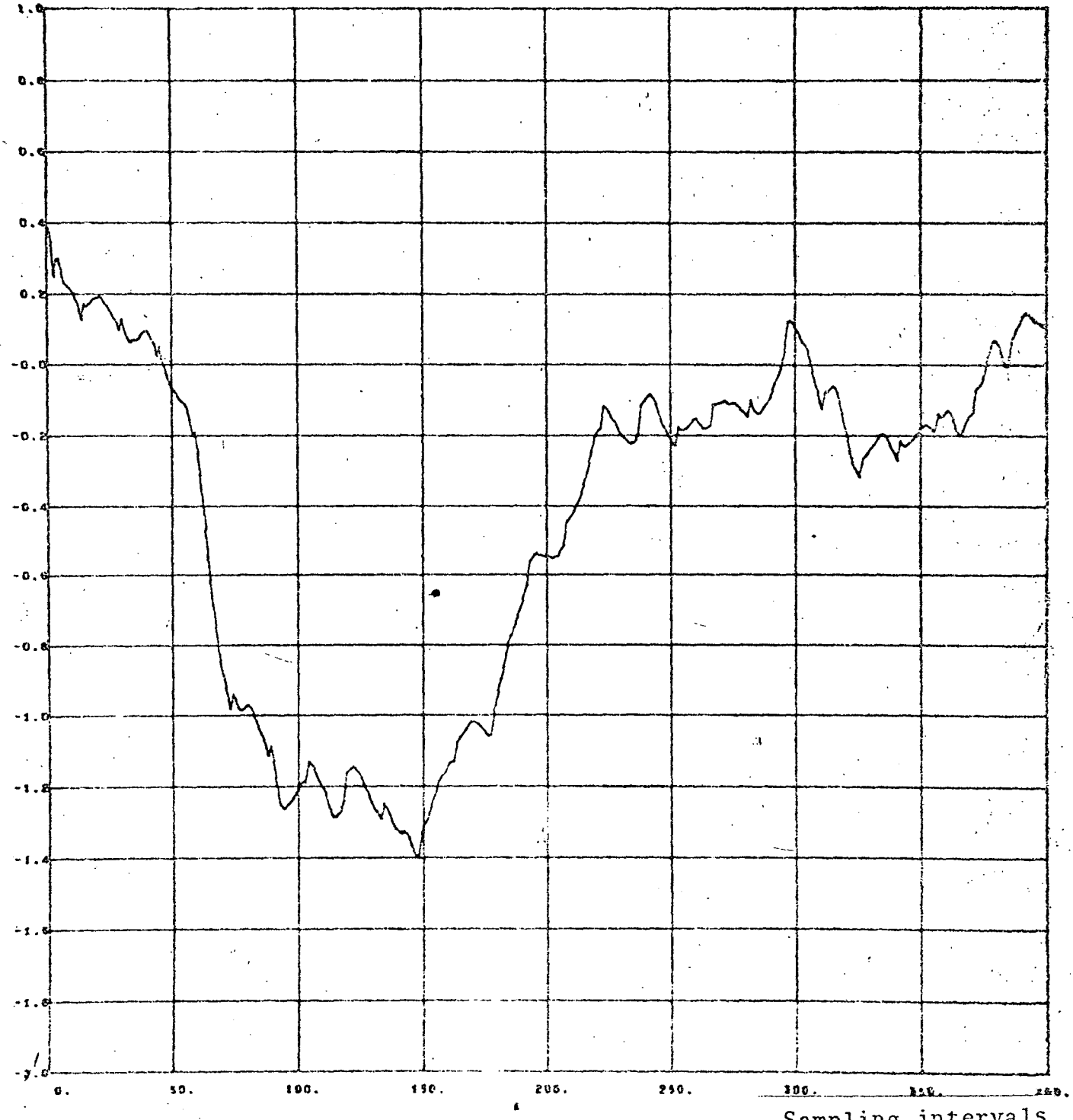

Sampling intervals

$\Delta t = .25$ sec.

Figure 4.8(a)

(Stable)

Quantizer Nonlinearity

$u_1 = .002$

$b_\phi = 10$

$b_\theta = 10$

rad x 10^{-6} $(\theta)_{ANT} - (\theta)_T$

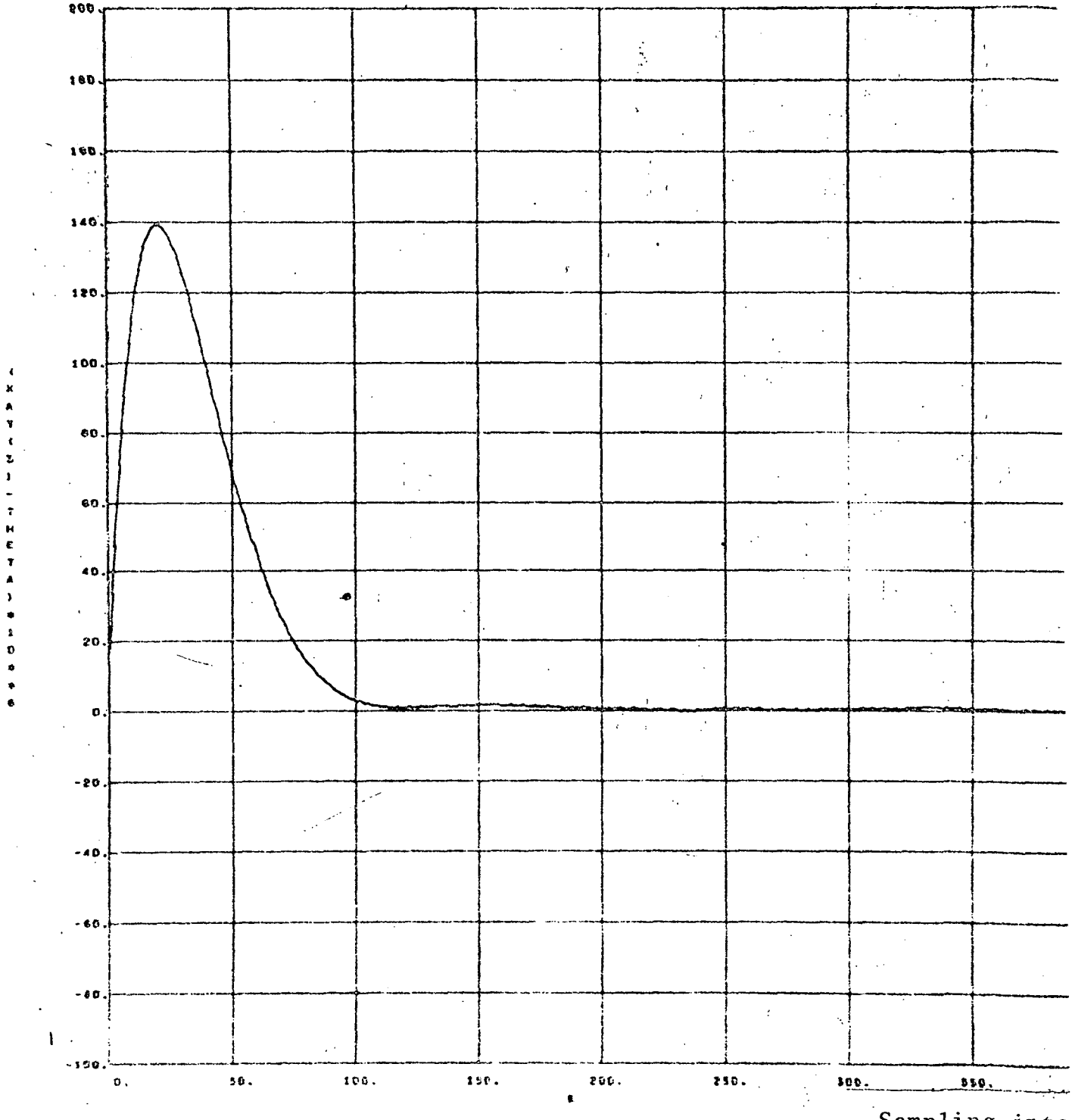

Figure 4.8(b)

Sampling inte

$\Delta t = .25$ sec.

(stable)

Quantizer Nonlinearity

$u_1 = .002$

$b_\phi = 10^{-11}$

$b_\theta = 10^{-12}$

rad x 10^{-6} $(\phi)_{ANT} - (\phi)_T$

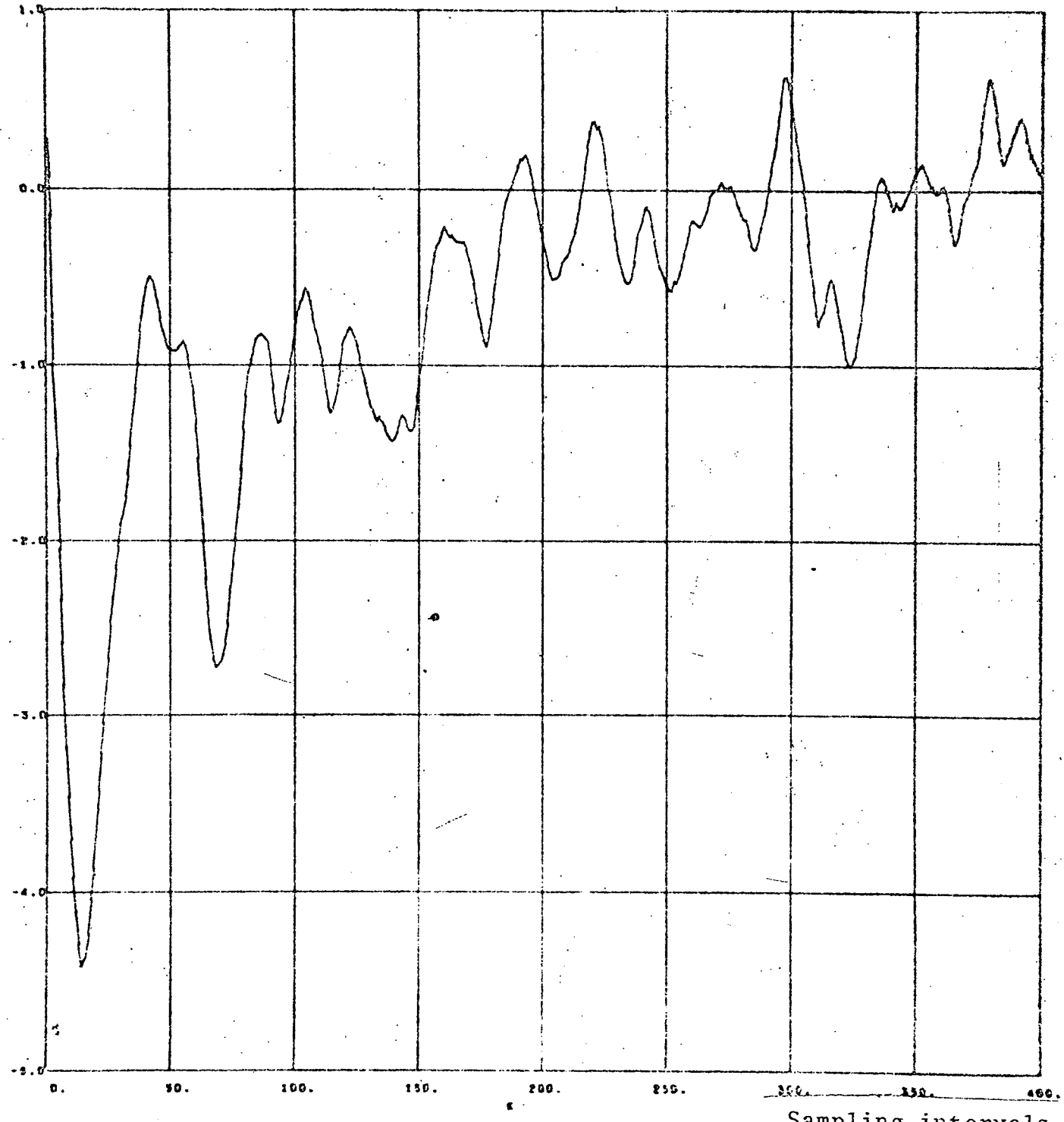

Sampling intervals

$\Delta t = .25$ sec.

Figure 4.9(a)

(stable)

Quantizer Nonlinearity

u_1 = .002

b_ϕ =

b_θ =

rad x 10^{-6}

$(\theta)_{ANT} - (\theta)_T$

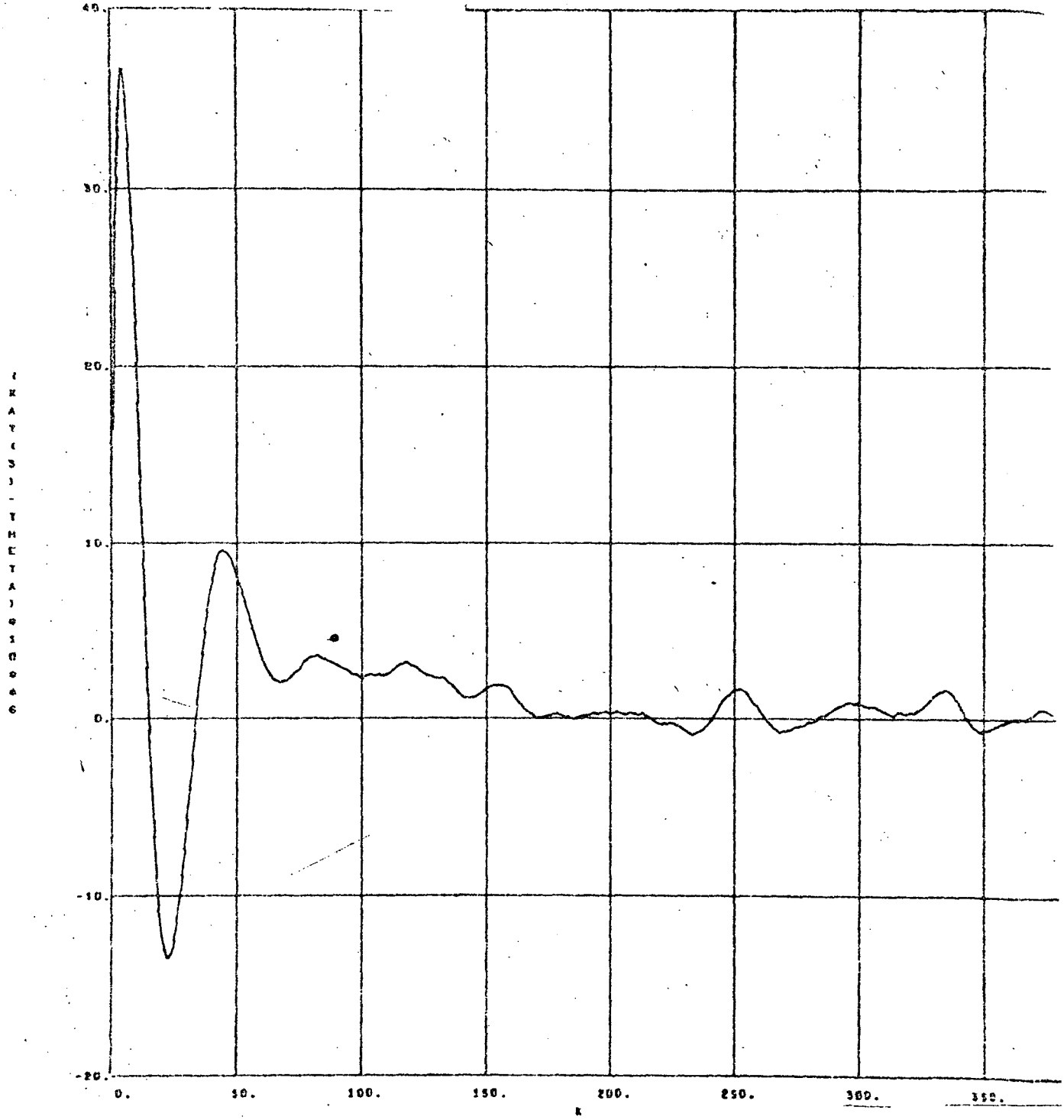

Sampling inter

Δt = .25 sec.

Figure 4.9(b)

Figures 4.4 and 4.5, were run with lower values of b_ϕ and b_ϕ by a factor of 100. The corresponding results are shown in Figures 4.6 and 4.7. As can be seen, there is no drastic difference in the system's performance. However, comparing Figure 4.4(a) with Figure 4.6(a) and Figure 4.5(a) with Figure 4.7(a), it appears that the undershoot in the ϕ channel is smaller for higher values of b_ϕ and b_Θ. The same applies to the settling value bounds; for higher values of b_ϕ and b_Θ they are lower. There is practically no difference in the behavior of the Θ channel.

The dead-zone nonlinearity, shown in Figure 4.2(b) was simulated with a small threshold value of $u_1 = .002$. The results turned out to be identical to the linear system, shown in Figure 4.1(a) - (f).

The quadratic form nonlinearity, shown in Figure 4.2(c) was tested for values of $u_1 = .002$ and $a = 1$. The system was unstable with the response similar to the one shown in Figure 4.3(a), (b).

The quantizer nonlinearity, shown in Figure 4.2(d), was simulated for the quatizing value of $u_1 = .002$, and for different values of b_ϕ and b_Θ. The results are shown in Figures 4.8 and 4.9. Comparing Figure 4.8(a) with Figure 4.9(a), it can be seen that for lower values of b_ϕ and b_Θ the undershoot in the ϕ channel is larger as is the settling value. On the other hand, as may be seen from Figures 4.8(b) and 4.9(b), for the Θ channel, for lower values of b_ϕ and b_Θ the overshoot is lower. The settling values appear to be the same. There is no undershoot for the higher values of b_ϕ and b_Θ.

An attempt to perform direct synthesis of single-loop control systems with the nonlinearity in the forward path is reported in Chapter 5. No linearization is performed and the nonlinearities are treated directly. The basic computational technique employed is that of Mathematical Programming. Stabilization of the systems involved is performed utilizing the criteria of Popov and Jury and Lee. Extension to multiloop systems with multiple nonlinearities is planned in future studies.

4.3 Simulation of the 40 Ft. Antenna

The data used in the simulation with the RATS program were as follows:

Initial satellite position and velocity in Earth centered coordinate system and their initial estimates:

		Actual	Estimated
x_{1e}	m	$.65700 \times 10^7$	$.65701 \times 10^7$
x_{2e}	m	0.	0.
x_{3e}	m	0.	0.
$\dot{x}_{1e}$	m/sec	0.	0.
$\dot{x}_{2e}$	m/sec	$.77891 \times 10^4$	$.77892 \times 10^4$
$\dot{x}_{3e}$	m/sec	0.	0.

The initial antenna state vector was:

	State No.	Actual	Estimated
Y Channel	1 (Y, rad)	-.13736	-.0022
	2 ($\dot{Y}$, rad/sec)	0.	0.
	3 (Y_m, rad)	-173.6	-172.7
	4 ($\dot{Y}_m$, rad/sec)	0.	0.
	5 (internal unidentified state)	0.	0.
	6 (disturbance)	0.	0.

	State No.	Actual	Estimated
X Channel	1 (X, rad)	-1.573	1.708
	2 ($\dot{X}$, rad/sec)	0.	0.
	3 (X_m, rad)	1341.	1341.
	4 ($\dot{X}_m$, rad/sec)	0.	0.
	5 (internal unidentified state)	0.	0.
	6 (disturbance)	0.	0.

Tracking station initial location, (See Figure A-1 in Reference [2]):

ψ = .0349 rad = 2°

δ = .24725 rad = 14.2°

The satellite is assumed to be in a circular orbit (≥ 200 N.M.) around the earth in the equatorial plane. The sampling period was T = 0.05 sec. and the program was run for a total of 5 seconds (100 sampling points).

The initial covariance matrix was:

$$P(o/o) = \text{diag}[.5, .5, 0, 10^{-18}, 10^{-18}, 0, \underbrace{10^{-9}, \ldots, 10^{-9}}_{\text{For all 12 antenna states}}]$$

The measurement noise covariance matrix was:

$$R = \text{diag}[.625, .4, .25, .18, .1, .1, .625, .4, .25, .18, .1] \times 10^{-2}$$

The state noise matrix Q was taken to be a diagonal matrix with all entries equal to 10^{-12}.

The results of the run, (pointing error) were as follows:

	X Channel	Y Channel
Initial Overshoot, deg.	190	7.7
Initial Undershoot, deg.	-24	-1.0
Acquisition Time (error $\leq 1°$), sec.	0.90	0.20
Steady State Error, deg.	0.001	0.004
Settling time (until steady state is reached), sec.	2.30	1.20

4.4 Simulation of the 30 Ft. Antenna

(SRI Pgm)

The ATRK30 program was run for the 30 Ft. antenna tracking station. The mission data were the same as in the simulations reported in Section 4.1. The only difference was in the plant which in this case was the 30 Ft. antenna control system, described in Chapter 3.

The results of the simulation, which was run for 100 sec. were as follows:

	X Channel		Y Channel	
	Estimator Controller	Autotrack	Estimator Controller	Autotrack
Initial Overshoot, deg.	.001	.055	0	0
Initial Undershoot, deg.	-.0003	0	-.0005	-.0002
Steady State Error, deg.	.00006	.052	.00006	.0001
Settling Time Sec.	40	50	40	90

REFERENCES

1. R.M. Dressler, E.C. Fraser, "Optical Communication and Tracking Systems," Stanford Research Institute, Final Report, October 1967, Contract NAS 12-59.

2. J. Peschon, et. al., "Research on the Design of Adaptive Control Systems," Final Report, Vol. 2, Ch. 7, Stanford Research Institute, September 1966, Contract NAS 12-59.

5.0 CONTROL INCLUDING NONLINEARITIES

5.1 Introduction

As one may see from the description in the previous chapers, the nonlinearities existing in the system state equations, have been treated by a first order linearization.

In this chapter, some direct methods of treating nonlinear systems are proposed, and some specific examples worked out. Initially, a method of computing the optimal control in a system containing a nonlinearity, using mathematical programming, is proposed. In the second part of the chapter a method of combining Popov's and Jury and Lee's stability criteria for nonlinear system with a nonlinear programming algorithm, is worked out in detail. This method may be used in automized stabilization and control of nonlinear systems in real time.

5.2 Optimal Control of Nonlinear Discrete Time Systems, Survey

After the formulation of the Maximum Principle for optimal control of continuous time systems was reported[1] considerable work was done in establishing a parallel version of the Maximum Principle for Discrete Time Systems, i.e., the so-called Discrete (or Digitized) Maximum Principle. The extension has been made in references[2] pt. III,[3-9] to mention only a few. In about all the references mentioned, necessary conditions for optimality have been derived. However, in every case one is faced with solving a two-point boundary-value problem. Indeed,

none of the authors quoted have implemented their results in practical computations. It has been one of the goals of this project to find an efficient computational solution for the design of optimal discrete-time control systems.

It has been found that at present the only way of getting computational results in the design of optimal discrete-time control systems, and especially in the case of nonlinear problems, would be by the use of mathematical programming. In the case of linear discrete-time systems, one may use the dynamic programming approach, for low-dimensioned systems, as was done by Tou,[10] for uniform sampling. A suboptimal solution for non-uniform sampling has been proposed by Brockstein and Kuo.[11] Although mathematical programming, in the nonlinear case, has its own computational difficulties, it is still the only method by which numerical results may be obtained with relatively little complexity. Similar ideas have also been expressed by J.B. Rosen.[12]

The use of mathematical programming should not be regarded as a complete alternative to the Maximum Principle. As a matter of fact, they are interrelated.

In a recent paper by Canon, Cullum and Polak,[13] general necessary conditions for optimal control have been developed. As particular cases of those conditions, the authors have demonstrated that it is possible to derive the Lagrange Multiplier's method, the Discrete Maximum Principle, [6,8] as well as the theorem of Kuhn and Tucker for nonlinear programming.[14] Similar results, showing the connection between the Kuhn-Tucker theorem and the Maximum

Principle have also been derived by L.W. Neustadt,[15] and by J.B. Pearson and R. Sridhar.[16] Perhaps one should regard mathematical programming as a way of computational realization of the necessary conditions of optimality, given by the Maximum Principle.

Linear and Quadratic Programming, which are particular cases of Mathematical Programming, have been previously applied in simple configurations of Linear Sampled Data Control Systems.[17-21] In this report the more general method of Nonlinear Programming[22,23] is applied to Nonlinear Nonuniformly sampled, Discrete Time Control Systems.[24,25]

5.3 Formulation of the Problem

The dynamic system under consideration is governed by the following set of state equations:

$$\underline{y}(i+1) = \underline{f}[\underline{y}(i),\underline{u}(i),i] \qquad (5\text{-}1)$$

$$i = 0,1,\ldots, N-1$$

where:

$\underline{y}(i)$ = n-dimensional state vector at the discrete time instant $t = t_i$

$\underline{u}(i)$ = m dimensional control vector at $t = t_i$

$\underline{f}$ = nonlinear, time-varying, n-dimensional vector function

N = maximal number of discrete time intervals considered; the intervals are in general unequal

At each discrete sampling time, the system may be subjected to an additional set of equality and inequality constraints:

$$h_j[\underline{y}(i),\underline{u}(i)] = 0; \quad j = 1,\ldots, p \tag{5}$$

$$g_k[\underline{y}(i),\underline{u}(i)] \geq 0; \quad k = 1,\ldots, q \tag{5}$$

where h_j, g_k are generally nonlinear functions.

It will be assumed that the initial state vector is specified:

$$\underline{y}(o) = \underline{y}_o \tag{5-}$$

The general optimal control problem for the discrete time system under consideration, could be formulated as follows:

Bring the system described by equations (5-1) from the initial state $\underline{y}_o$, into a target area described by:

$$\underline{a}[\underline{y}(n)] \geq 0 \tag{5-5}$$

where $\underline{a}$ is a ℓ-dimensional, nonlinear, vector function, so that the following performance index is minimized (or maximized):

$$J = \sum_{i=1}^{N} F\,[\underline{y}(i),\underline{u}(i-1),i] \tag{5-6}$$

where F is a nonlinear time-varying function, subject to the constraints (5-2), (5-3).

Considering the formualtion of the control problem, as well as the expressions involved, one may see, that it constitutes a classical mathematical programming problem with (5-6) serving as an objective function, (5-1), (5-2) as equality and (5-3), (5-5) as inequality constraints. A suitable algorithm is to be chosen for the numerical solution of this problem. In the following section, an example illustrating the method, is presented.

5.4 Computational Example

A part of a 40 ft. antenna tracking control system is considered. The system consists of a separable linear and nonlinear subsystem. The dynamics of the system are represented by the following set of difference equations:

$$\underline{y}(i+1) = A\,\underline{y}(i) + \underline{b}NL\,[u(i)] \tag{5-7}$$

where,

A = n x n constant matrix

$\underline{b}$ = n-dimensional constant vector

$u(i)$ = scalar control variable at $t = t_i$

NL = a nonlinear scalar function

The system under consideration is uniformly sampled. In view of this, one may now express the state vector at any time instant $t = t_N$, as[10]:

$$\underline{y}(N) = A^N\,\underline{y}(o) + \sum_{i=o}^{N-1} A^{N-i-1}\,\underline{b}NL[u(i)] \tag{5-8}$$

where $\underline{y}(o)$ is the initial state vector, assumed known.

The output of the system is represented by the first component of the state vector, y_1. The purpose of the control action is to bring the output y_1 to align with a prescribed reference position y_R. This control action, should be done with minimum expense of energy. Following these requirements the following performance index was formulated:

Minimize

$$J = \sum_{i=1}^{N} \left\{ \left[y_1(i) - y_R \right]^2 + W\, u^2(i-1) \right\} \qquad (5\text{-}9)$$

where W is a weighting factor, and N is the maximal number of sampling instants considered.

The meaning of the first term in the performance index in eq. (5-9), is minimization of the squared error, at any time instant considered, between the actual and the desired output position of the system. The second term, represents the minimum energy requirement.

From equation (5-8) it follows that:

$$y_1(i) = A_1^i \underline{y}(o) + \sum_{j=0}^{i-1} A_1^{i-j-1} \underline{b} NL[u(j)] \qquad (5\text{-}10)$$

where A_1 represents the first row of the matrix A.

Substituting eq. (5-10) into eq. (5-9), one obtains:

$$J = \sum_{i=1}^{N} \left\{ \left[A_1^i \underline{y}(o) + \sum_{j=o}^{i-1} A_1^{i-j-1} \underline{b} NL[u(j)] - y_R \right]^2 + W\, u^2(i-1) \right\} \tag{5-11}$$

As one may see from eq. (5-11), one has a nonlinear performance index, or objective function for the solution of this problem.

Additional constraints limiting the amplitude of the control signal were posed:

$$-u_m \leq u(i) \leq u_m \tag{5-12}$$

The objective function in eq. (5-11), along with the constraints in eq. (5-12), form a nonlinear programming problem, with N variables and 2N inequality constraints.

The algorithm applied for the solution of this problem, was the SUMT method,[26] on the IBM 360/91 computer system.

The actual system considered, was modeled as a third order system, for which:

$$A = \begin{bmatrix} -.114 & 1.000 & 0. \\ .233 & -.114 & 1. \\ -.275 & .233 & 0. \end{bmatrix} \quad \underline{b} = \begin{bmatrix} .179 \\ .550 \\ .115 \end{bmatrix}$$

The nonlinearity considered was of the saturation type, modeled by a hyperbolic tangent function:

$$NL(u) = S \tanh(u/S) \tag{5-13}$$

where S is the output of the nonlinearity at saturation, or in this case, when $u \to \infty$. On many occasions, a saturation is modeled using sharp corners at the passage from the linear region to saturation. In many practical systems, like in servo amplifiers, this passage is rather smooth, and the function in eq. (5-13) seems a suitable model to represent it. In this example, the saturation value was chosen to be S = 10.

The maximum allowed control signal amplitude, was fixed at $u_m = 10$. The initial state vector was:

$$\underline{y}(o) = \begin{bmatrix} .9 \\ 0 \\ 0 \end{bmatrix}$$

and the desired reference value, $y_R = 1.0$. The program was run for a total of 20 sampling periods, i.e., N = 20. The results are summarized in Table 5.1 and in Figures 5.1 and 5.2.

5.5 Automized Stabilization and Control

Automized stabilization and control is a problem of primary importance in the field of computer real-time process control. The problem is particularly difficult when one considers control of nonlinear processes. While there exist relatively easily programmable stability criteria for linear systems[2], the situation with nonlinear systems is entirely different. One could of course employ an approximate linearization of a nonlinear system and then apply stabilization algorithms suitable for linear systems. This kind of approach may be suitable to certain classes of systems, however it may involve untolerable errors in others. Therefore, there is a definite need in formulating stabilization algorithms directly applicable to nonlinear systems and at the same time - amenable to efficient computerization in real-time. This problem is, no doubt, of considerable interest in many industrial applications, however, to the best of the author's knowledge, the problem has not been treated and solved in the literature.

In this report, several stability criteria for nonlinear systems are reformulated in a form directly applicable to real-time stabilization and control of nonlinear systems, using a time-sharing digital computer system. Two basic configurations of computer control of nonlinear processes, are considered.

TABLE 5.1

SAMPLING INSTANT i	OUTPUT $y_1(i)$	CONTROL SIGNAL u_{i-1}	ERROR $e_i = y_1(i) - y_R$
1	.09494	1.1075	- .905063
2	1.22355	2.3787	.223548
3	1.04979	.5408	.049791
4	1.00955	1.3428	.009553
5	.97008	1.2791	- .029922
6	1.01657	1.2225	.016570
7	.96834	1.2601	- .031656
8	1.02376	1.2402	.023765
9	.97652	1.2814	- .023479
10	1.03857	1.2390	.038575
11	.96528	1.2212	- .034724
12	1.01545	1.2390	.015446
13	.97425	1.2528	- .025753
14	1.02848	1.2791	.028779
15	.98529	1.1200	- .014708
16	.99706	1.2555	- .002943
17	.98556	1.2476	- .014439
18	1.00052	1.2287	.000521
19	.97809	1.2304	- .021913
20	.99744	1.2589	- .002564

The total computing time was 12.19 sec. on the IBM 360/91 system. The value of the optimal performance index was:

$$J_o = .8803$$

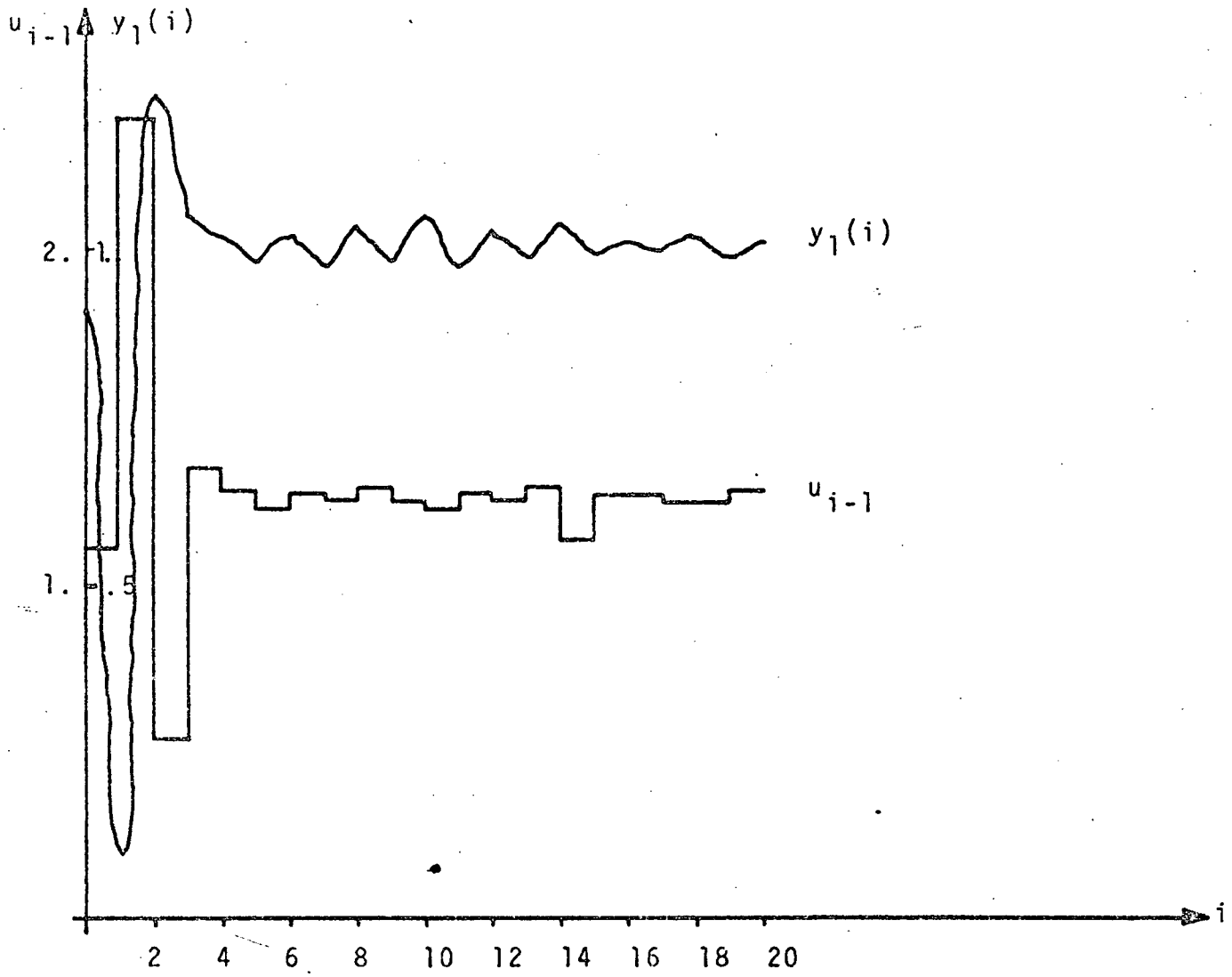

FIGURE 5.1 THE OUTPUT AND THE CONTROL SIGNAL

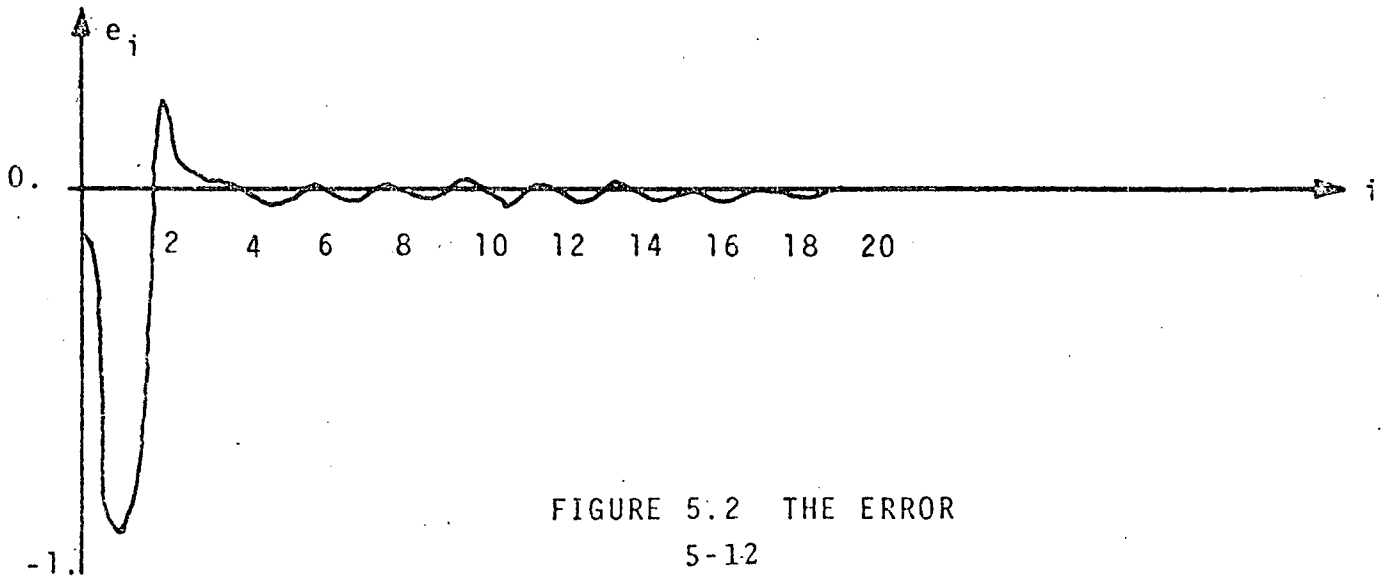

FIGURE 5.2 THE ERROR

(1) Parameter Adjustment Control. In this case, the parameters of the system may be adjusted through direct digital control. However, the computer system is actually outside of the control loop, which is a continuous, nonlinear feedback control system. The detailed treatment of this configuration has already been reported in detail previously,[28].

(2) Digitally Controlled System. The computer system is actually a part of the control loop in this case. To be more specific, the controller of the system is programmed on a real-time special purpose computer, or on a time-sharing extension of a universal computer system. The parameters of the controller are actually input data to the subroutine which realizes the digital controller. The system considered, is naturally, a sampled-data nonlinear control system.[34]

The basic algorithm proposed for the system of type (2) will be discussed in section 5.7 and an example presented in section 5.8. The stability criteria used were Popov's[29] for the system of type (1), and Jury and Lee's Lee's[30] for the system of type (2). The stability criteria are reformulated with respect to the particular process control configurations considered. As a result of the reformulation a nonlinear programming problem[22,23] is obtained. The SUMT algorithm, originated by Fiacco and McCormick[26] is then applied to the numerical solution of the problem. As a result of this calculation a set of the system's parameters is obtained, which stabilizes the system and satisfies a set of performance criteria at the same time.

It should be noted, that in the case of the system of type (2), the nonlinear programming problem derived, involved complex variables. This type of problem has not been reported as solved in previous publications. The SUMT algorithm was suitably modified for application to the solution of nonlinear programming problems involving complex variables. While applying the SUMT algorithm, there is the option of choosing various unconstrained minimization techniques. A comparative study involving the use of some of the available techniques has been conducted and will be described in section 5.9.

5.6 Parameter Adjustment Control

A general process control system with a nonlinearity is considered, as shown in Figure 5.3, $G(s,\underline{p})$ is the transfer function of the linear part of the system and it depends in general, on a parameter vector $\underline{p}$. The nonlinearity satisfies the following conditions:

a. $n(e)$ is defined and continuous for all values of e.

b. $n(o) = 0$ and $en(e) > 0$ for all $e \neq 0$.

One possibility of accomplishing computerized control of the system, is by adjusting the components of the parameter vector $\underline{p}$, through the scheme in Figure 5.4. In general, G may contain both the original plant as well as the controller.

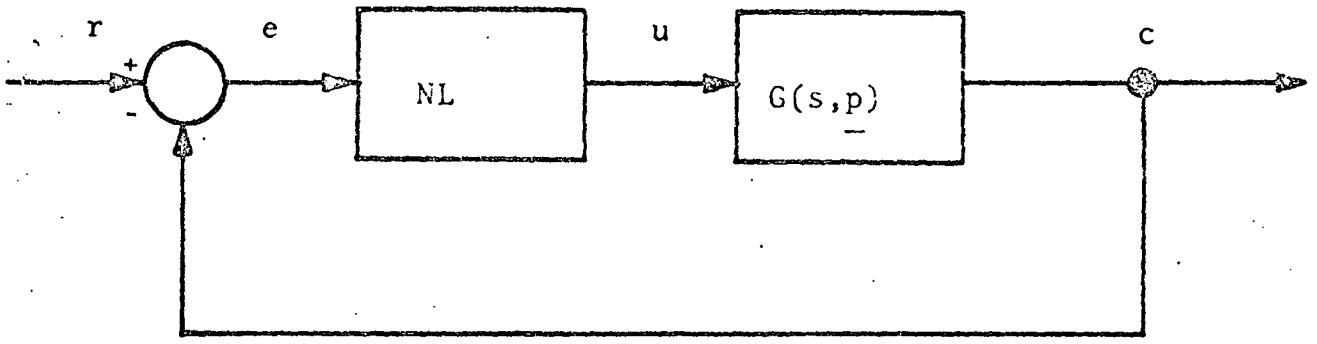

(a) System Block Diagram

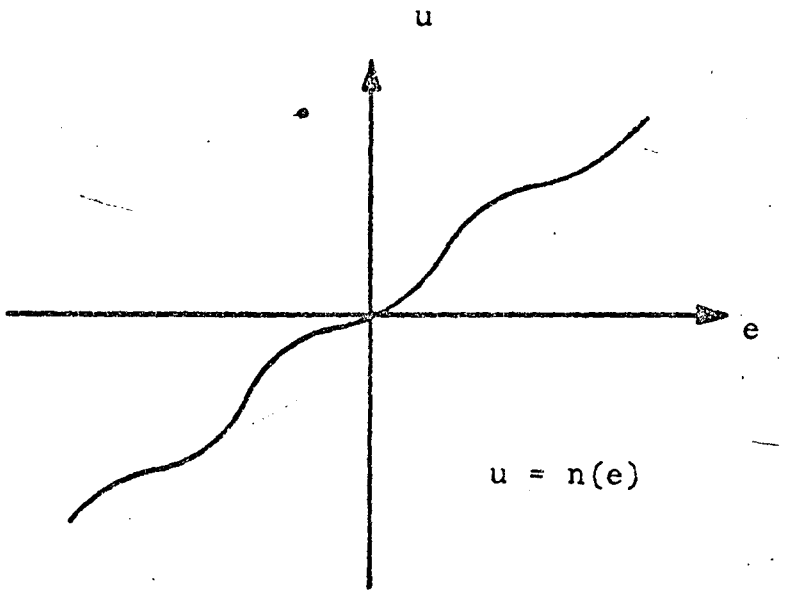

(b) The Nonlinearity

FIGURE 5.3 THE CONTROL SYSTEM

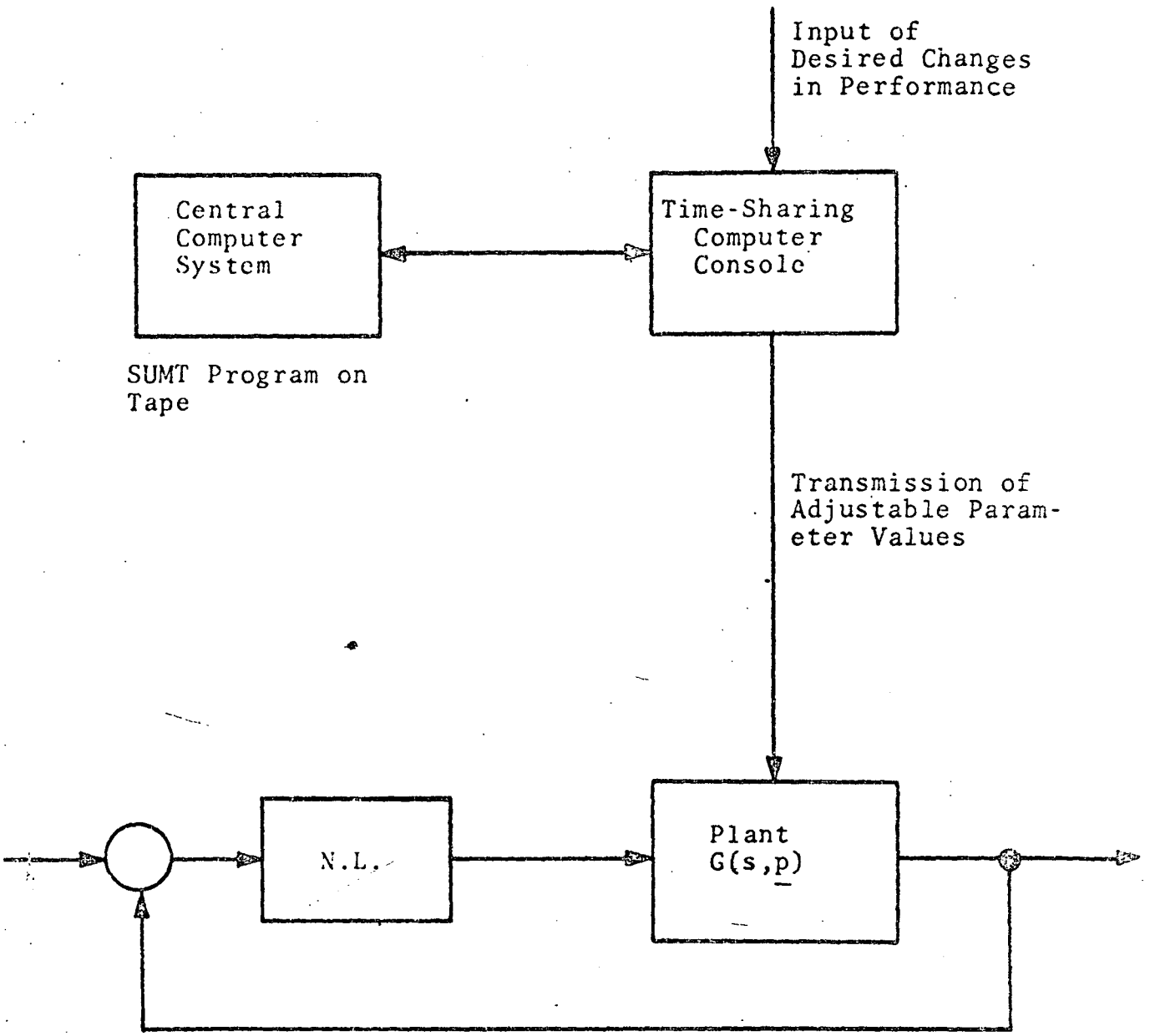

FIGURE 5.4 PARAMETER ADJUSTMENT

It may be required, that during the process, the system should work under varying performance criteria. At all times, stability is to be maintained, and the parameters $\underline{p}$ are to be adjusted accordingly by the computer. In view of the presence of the nonlinearity in the loop, classical methods of linear analysis[27] may not be used. The particular nonlinearity, which represents a wide class used in practice, corresponds to the conditions of Popov's[29] stability theorem. The theorem states that the system will be absolutely stable if for

$$0 \leq \frac{n(e)}{e} \leq K \tag{5-14}$$

There exists a non-negative real q such that

$$G_1(\omega,\underline{p}) - q\omega G_2(\omega,\underline{p}) + \frac{1}{K} > 0 \tag{5-15}$$

where

$$G = G_1 + jG_2$$

K is the maximal allowable instant gain (ratio between input and output) of the nonlinearity. Expression (5-15)

may usually be expanded into a set of inequalities which are functions or $\underline{p}$, K and q:

$$g_j(\underline{p},K,q) \geq 0 \tag{5-16}$$

$$q \geq 0$$

$$j = 1, \ldots, M$$

Formulating a general performance index

$$\text{Minimize (or Maximize) } J = f(\underline{p},K) \tag{5-17}$$

and adding any additional constraints, as required by various practical considerations, one would obtain a classical nonlinear programming[22,23] problem.

Example 1. A Third Order System. The transfer function of the linear part of the system is

$$G(s,\underline{p}) = \frac{1}{(s+a)\ (s^2+2\delta\omega_n s+\omega_n{}^2)} \tag{5-18}$$

$$a;\ \delta;\ \omega_n \geq 0$$

The parameter vector is

$$\underline{p} = \begin{bmatrix} a \\ \delta \\ \omega_n \end{bmatrix}$$

Introducing $x = 1/K$ and applying (5-15), one obtains[28]:

$$x\omega^6 + [x(a^2 - 2\omega_n^2 + 4\delta^2\omega_n^2) - q]\,\omega^4$$

$$+ [x(4\delta^2 a^2\omega_n^2 - 2a^2\omega_n^2 + \omega_n^4) + 2q\delta a\omega_n + q\omega_n^2$$

$$- 2\delta\omega_n - a]\,\omega^2 + (xa^2\omega_n^4 + a\omega_n^2) > 0 \qquad (5\text{-}19)$$

Since both x and q are non-negative, and since equation (5-19) contains terms of even order of ω only, the inequality (5-19) will be satisfied for all ω, if the following inequalities are satisfied[28]:

$$x(a^2 - 2\omega_n^2 + 4\delta^2\omega_n^2) - q \geq 0 \qquad (5\text{-}20)$$

$$x(4\delta^2 a^2\omega_n^2 - 2a^2\omega_n^2 + \omega_n^4) + 2q\delta a\omega_n + q\omega_n^2$$

$$- 2\delta\omega_n - a \geq 0 \qquad (5\text{-}21)$$

In addition the following constraints have been imposed:

$$\delta_{min} \leq \delta \leq \delta_{max}$$

$$a_{min} \leq a \leq a_{max}$$

$$\omega_n \leq \omega_{nmax} \qquad (5\text{-}22)$$

The performance index for this example was chosen according to the following considerations. On many occasions, one would like to adjust the system parameters, so that one could work with the maximal forward gain (which in this case happens to be K), and still retain the stability of the system. On the other hand, one may want to have the shortest possible rise time, which would require working with a low damping ratio δ. However, the requirement of maximizing K (or minimizing $x = 1/K$) would require a higher value of δ. The two requirements drive the optimization problem in opposite directions. In the combined performance index, one should assign an appropriate weighting factor to show the relative importance of both requirements. Since both x and δ are non-negative, the performance index could be chosen to be linear instead of quadratic:

$$\text{Minimize } J = cx + \delta \qquad (5\text{-}23)$$

As a result of maximizing K one may obtain the value of K at the limits of stability. In this case the result should be only indicative; it does not mean that the system should actually be working with this maximal value. The following limiting constraints were imposed, in addition to the stability constraints (5-20), (5-21):

$$.5 \leq \delta \leq .707$$

$$.1 \leq a \leq 1.$$

$$\omega \leq 3. \text{ rad/sec} \qquad (5\text{-}24)$$

The nonlinear programming problem was solved for different values of the weighting factor c.

The SUMT program[28] was used in the computations, performed on the IBM 360/91 computer. The results obtained are tabulated as follows:

c	.01	.02	.05	.10	.15	.18	.20	.50
x_{min}	4.00	4.00	.910	.312	.128	.081	.066	.064
K_{max}	.25	.25	1.100	3.200	7.810	12.35	15.15	15.61
δ	.5	.5	.612	.654	.676	.684	.687	.687
ω_n	.5	.5	1.414	1.861	2.420	2.783	2.972	2.999

a = 1. for all cases

For each value of c, the run time for the solution of the nonlinear programming problem was about 1.30 seconds. Each problem included five variables (x, a, δ, ω_n, q) and seven inequality constraints.

Example 2. A Fourth Order System. The general form of the fourth order system was chosen to be:

$$G(s,p) = \frac{1}{(s^2+2\delta_1\omega_{n1}s+\omega_{n1}^2)\ (s^2+2\delta_2\omega_{n2}s+\omega_{n2}^2)}$$

$$\delta_1;\ \delta_2;\ \omega_{n1};\ \omega_{n2} \geq 0 \qquad (5-$$

The adjustable parameter vector in this case is:

$$\underline{p} = \begin{bmatrix} \delta_1 \\ \omega_{n1} \\ \delta_2 \\ \omega_{n2} \end{bmatrix}$$

In the same manner as for the third order system, one obtains the following stability inequality constraints [28].

$$(2\delta_1^2-1)\ \omega_{n1}^2 + (2\delta_2^2-1)\ \omega_{n2}^2 \geq 0 \tag{5-26}$$

$$x\ [4\omega_{n1}^2\omega_{n2}^2\ (4\delta_1^2\delta_2^2-2\delta_1^2-2\delta_2^2+1) + \omega_{n1}^4 + \omega_{n2}^4]$$

$$+ 1 - 2q(\delta_1\omega_{n1}+\delta_2\omega_{n2}) \geq 0 \tag{5-27}$$

$$2x\omega_{n1}^2\omega_{n2}^2\ [(2\delta_1^2-1)\ \omega_{n2}^2 + (2\delta_2^2-1)\ \omega_{n1}^2]$$

$$+ 2\omega_{n1}\omega_{n2}q\ (\delta_1\omega_{n2}+\delta_2\omega_{n1})$$

$$- \omega_{n1}^2-\omega_{n2}^2-4\delta_1\delta_2\omega_{n1}\omega_{n2} \geq 0 \tag{5-28}$$

The performance index was:

$$\text{Minimize} \quad J = cx + \delta_1 + \delta_2$$

The additional constraints:

$$.5 \leq \delta_1 \leq 2.$$

$$.5 \leq \delta_2 \leq 2.$$

$$\omega_{n1} \leq 3. \text{ rad/sec.}$$

$$\omega_{n2} \leq 3. \text{ rad/sec.}$$

The results were as follows:

c	.01	.05	.10	.20	1.0
x_{min}	.251	.163	.138	.121	.100
K_{max}	3.98	6.14	7.25	8.26	10.0
δ_1	.708	.710	.712	.714	.723
ω_{n1}	2.999	2.999	3.0	3.0	3.0
δ_2	.5	.5	.5	.5	.5
ω_{n2}	.236	.398	.496	.611	.916

For each value of c, the run time for the solution of the nonlinear programming problem was about 1.45 seconds. Each problem had six variables (x, δ_1, ω_{n1}, δ_2, ω_{n2}, q) and nine inequality constraints.

5.7 Digitally Controlled System

The system under consideration is sketched in figure 5.5. The controller of the system is part of a digital computer. To be more precise, the digital controller is realized as a subroutine programmed on the computer used for the control purpose. Either a special purpose control computer or a time-sharing station connected to a central computer system may be used. For instance in the case of the digital control of the 40 ft. antenna tracking system, to be discussed in section 5.8, a SDS Sigma 5 computer is used, and the digital controller is programmed in assembly language.

The system considered (figure 5.5) is a sampled data nonlinear system. In this case, a different stability criterion should be used, namely the Jury and Lee criterion [30]. The following conditions are imposed on the nonlinearity:

a. $n(e)$ is continuous

b. $n(o) = 0$

c. $K > \frac{n(e)}{e} > 0$, for $e \neq 0$

d. $\frac{dn(e)}{de} < K'$

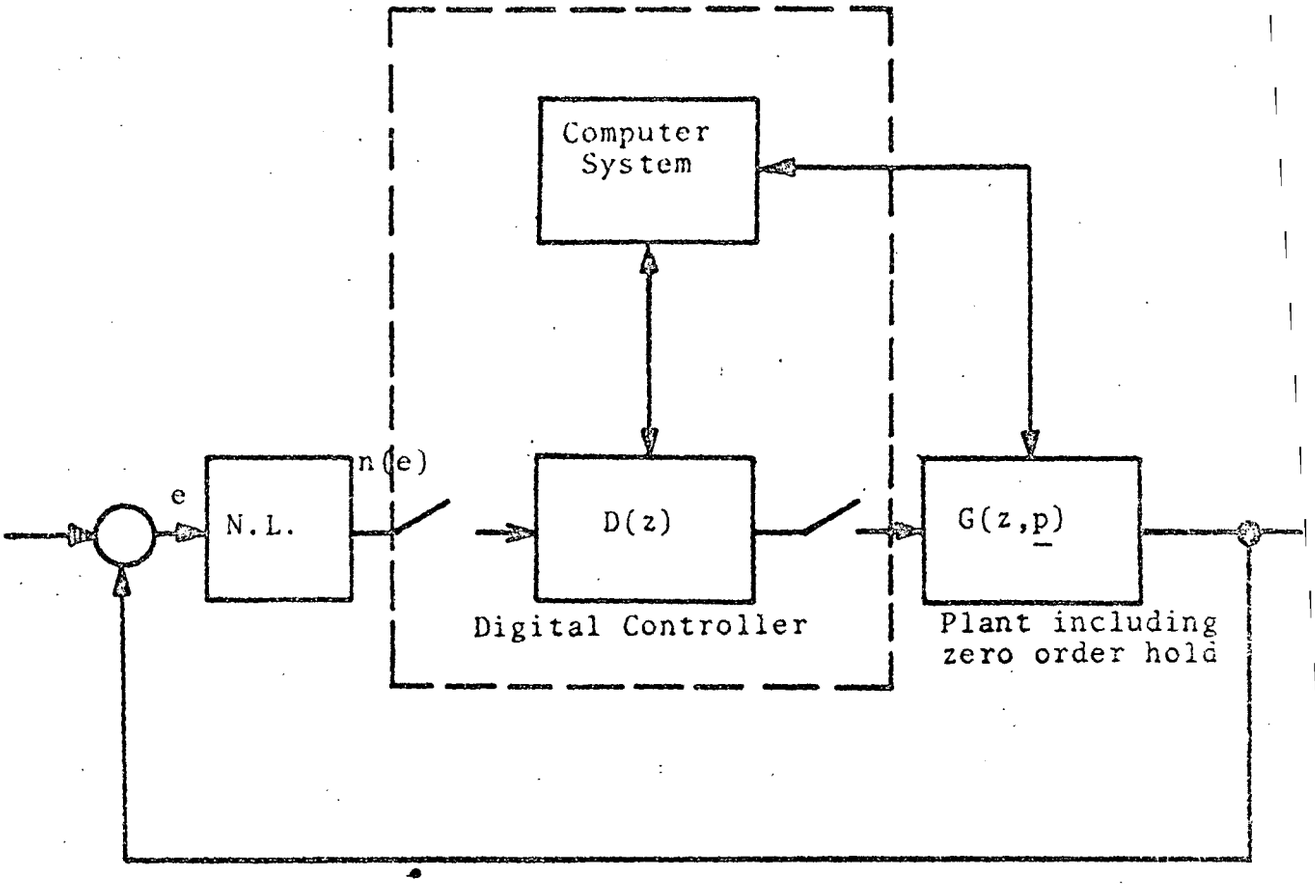

FIGURE 5.5 DIGITALLY CONTROLLED SYSTEM

If $G^*(z)$ is the overall z-transfer function of the linear subsystem, including the controller, the Jury and Lee theorem states that the system is absolutely stable if a q exists such that:

$$JL(z) \equiv \mathrm{Re}\{G^*(z)\ [1+q(z-1)]\} + \frac{1}{K} - \frac{K'|q|}{2} |(z-1)G^*(z)|^2 \geq 0 \qquad (5\text{-}30)$$

is satisfied on the unit circle $z = \exp(j\omega T)$, where T is the sampling period.

The computational algorithm in this case, would have to run in two phases:

(1) Establish, for which value of z, does the left side of inequality (5-30) have the minimal value.

(2) Substitute the value of z obtained in phase (1) into inequality (5-30), and use it as a basis for the nonlinear programming problem to establish the optimal parameters that would stabilize the system. Of course, one has to formulate a suitable performance index and one may pose additional constraints.

This algorithm may be applied to a variety of digitally controlled systems. For instance, it could be used in automized stabilization and control of antenna tracking systems. Two examples simulating the implementation of this algorithm are presented in section 5.8. A flow chart illustrating the proposed algorithm is sketched in figure 5.6.

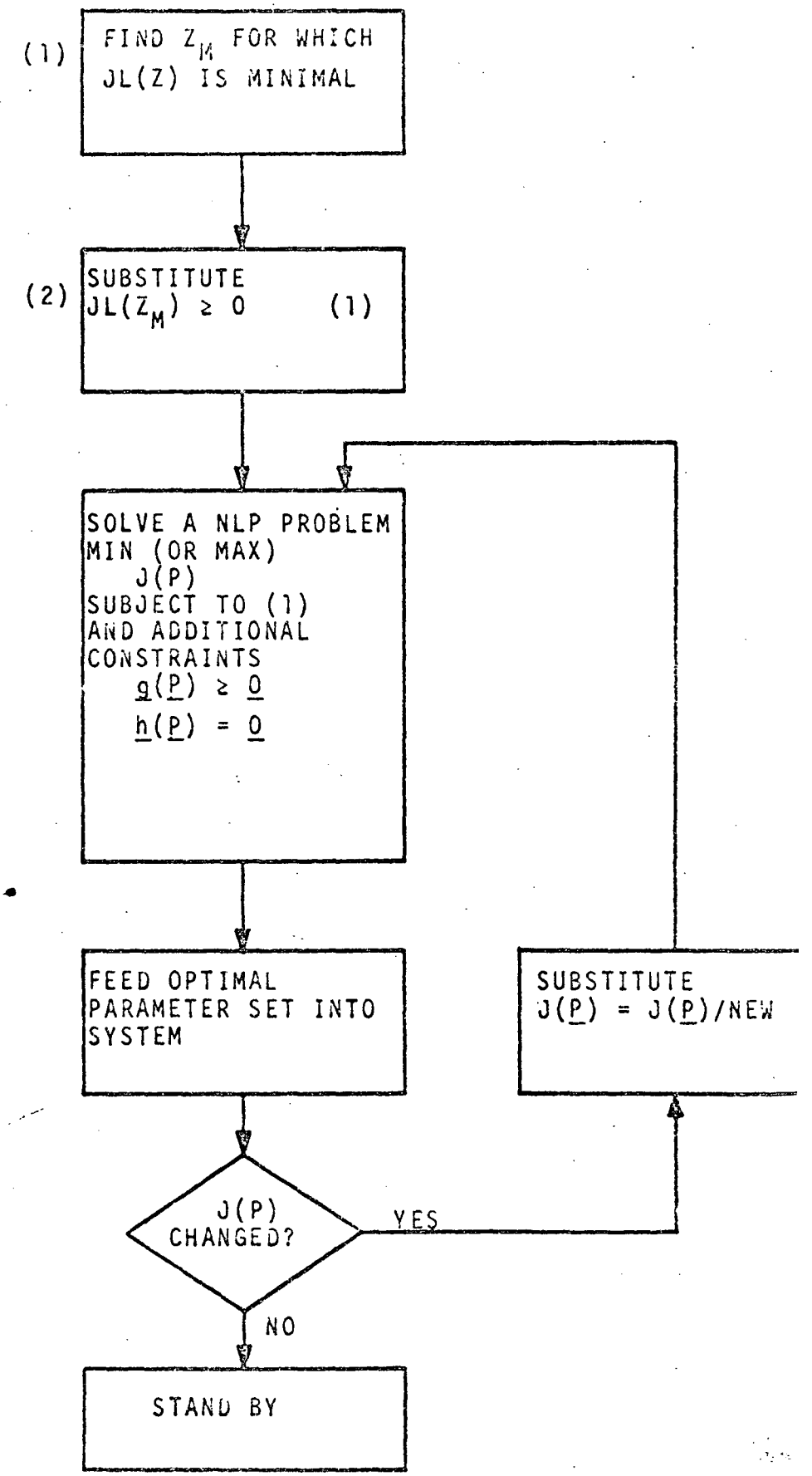

FIGURE 5.6 THE ALGORITHM FOR THE DIGITALLY CONTROLLED SYSTE

5.8 Digitally Controlled Antenna Tracking System

As an illustrative example of the stabilization algorithm proposed, the case of computer control of a 40 foot antenna tracking system of the NASA Goddard Space Flight Center was chosen. The basic system configuration is sketched in figure 5.7. The z-transform transfer function of the linear part of the plant, including a zero-order-hold, is:

$$G(z) = \frac{.179z^2 + .55z + .115}{z^3 - .114z^2 + .233z - .275}$$

The nonlinearity is assumed to satisfy all the conditions specified in section 5.7. Otherwise, no particular configuration is assumed for the nonlinearity, which makes the solution applicable to a wide class of system.

The digital controller was chosen to be of second order:

$$D(z) = \frac{a_o z^2 + a_1 z + a_2}{z^2 + b_1 z + b_2} = \frac{a_o + a_1 z^{-1} + a_2 z^{-2}}{1 + b_1 z^{-1} + b_2 z^{-2}}$$

The parameters of the digital controller, a_o, a_1, a_2, b_1, b_2 are unknown variables and should be established in the process of the solution. The digital controller may be programmed on a digital computer according to well established methods[31]. The choice of a second order controller is somewhat arbitrary and rather based on experience. There is no loss of generality in this choice,

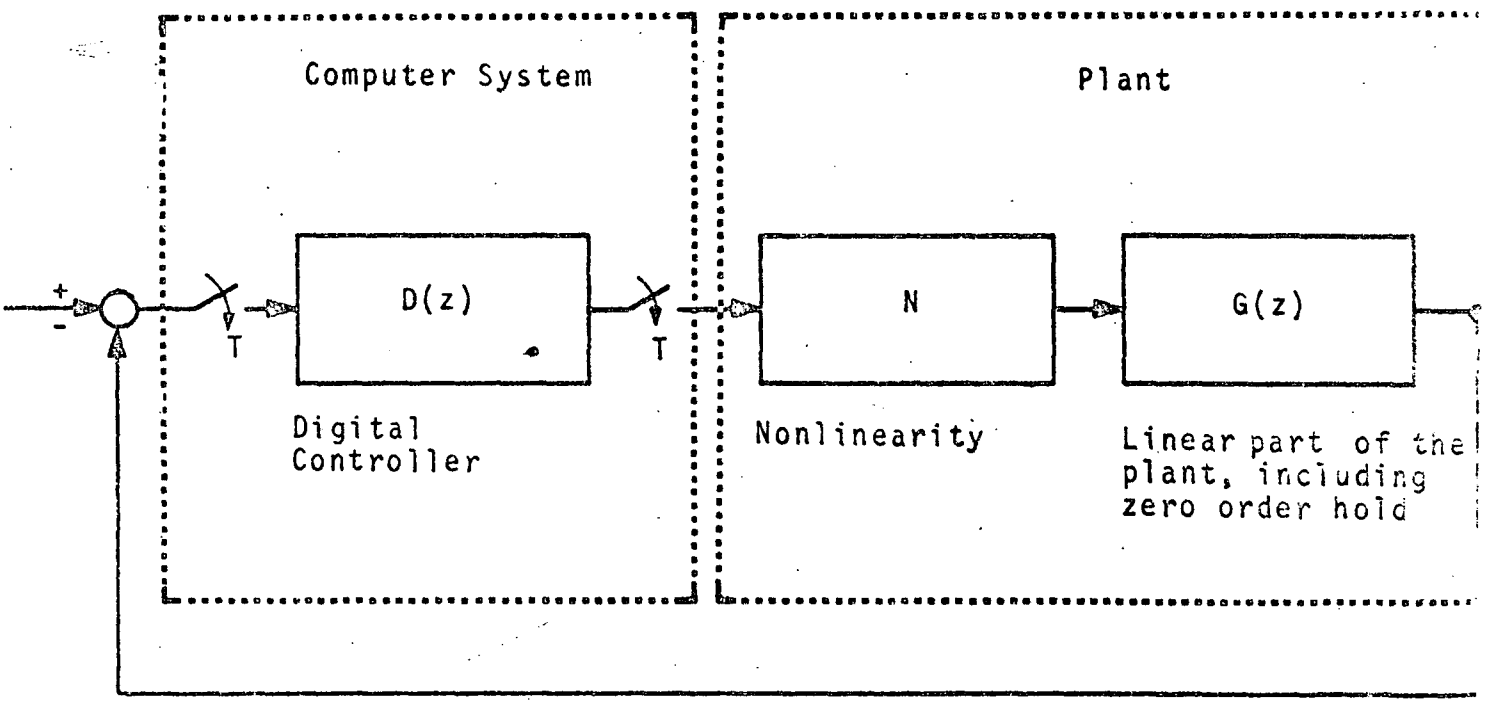

FIGURE 5.7 ANTENNA TRACKING SYSTEM CONFIGURATION

since the same method would apply to any order of D(z). The only difference it would make is in the number of variables. One should, of course, try to solve a problem with a minimal number of unknowns, so one would not want to make the order of D(z) too high. Since the plant is of third order, it is reasonable to choose the controller of one order less. Anyway, the choice of the order of D(z) is a minor issue of this work; what is important, is the method of establishing the actual values of its parameters. These parameters are physically input data to the subroutine which realizes D(z). The communication between the controller and the continuous time plant is accomplished through A/D and D/A converters.

The transfer function of the whole linear subsystem, which includes the plant and the controller, is:

$$G^*(z) = D(z)\,G(z) =$$

$$= \frac{\left(a_o+a_1z^{-1}+a_2z^{-2}\right)\left(.179z^{-1}+.55z^{-2}+.115z^{-3}\right)}{\left(1+b_1z^{-1}+b_2z^{-2}\right)\left(1-.114z^{-1}+.233z^{-2}-.2752^{-3}\right)} \qquad (5\text{-}33)$$

As mentioned in section 5.7, the first part of the algorithm involves finding the value of z for which the left side of inequality (5-30) is minimal. In other words, one would like to find the value of z for the worst case when the stability of the system is mostly "threatened." It should be remembered, that the left side of (5-30), JL(z), should be non-negative in order to satisfy the

stability criterion. According to this criterion, z is restricted to be on the unit circle in the complex z-plane, i.e.,

$$z = e^{j\omega T} \tag{5}$$

or

$$|z| = 1 \tag{5}$$

One of the simplest ways of finding the value z_m which minimized JL(z), is by direct search, since only one independent variable z is involved. The restrictions in (5-34) or (5-35) should of course be preserved. This is done simply by performing the search using the real value of z, Re(z), as an independent variable, and then computing the imaginary value of z by:

$$Im(z) = \sqrt{1 - Re^2(z)} \tag{5}$$

In this example the search was performed by direct scanning over the values of Re(z) at a fixed interval. Of course, one may use more sophisticated search methods if desired. The search took 0.3 seconds on the IBM 360/91 system. The results obtained were:

$$z_m = -.270 + j.963$$

$$JL(z_m) = -7110.0 \tag{5}$$

The same problem was also solved as a nonlinear programming problem using the SUMT[26] method. The nonlinear programming problem was formulated as:

$$\text{Min} \left\{ JL(z, K, K', q) \;\middle|\; |K| \leq K_{max};\ |K'| \leq K'_{max};\ |q| \leq q_{max};\ |z| = 1 \right\} \tag{5-38}$$

As one may see, the objective function in this problem depends explicitly on a complex variable z and on a complex function G(z). (See equation 5-30). In this problem G(z) is used instead of G*(z) in equation (5-30). For the purpose of the numerical solution, instead of z, one works with two variables x_1, x_2, which are the real and imaginary parts of z:

$$z = x_1 + jx_2 \tag{5-39}$$

The complexity of z and its connection with x =Re(z) is stipulated in the program by the following two FORTRAN IV statements:

```
COMPLEX    Z
EQUIVALENCE (Z, X(1))
```

This automatically implies that $X(2) \equiv x_2$ is the imaginary part of z.

The conditions in equations (5-34) or (5-35) were taken care of by imposing an explicit equality constraint.

$$x_1^2 + x_2^2 - 1 = 0 \tag{5-40}$$

Although the constraints in this case (see equations (5-38) and (5-40)) are very simple, the objective function $JL(x_1, x_2, K, K', q)$ is a very complicated function of all the five variables of the problem. Although JL itself is real, it does depend on complex values z and G(z) explicitly, which makes the numerical solution of the nonlinear programming problem quite difficult. In this case, a special technique of unconstrained minimization, developed by Fiacco and McCormick[26] was adopted. This technique does not require the explicit calculation of the derivatives of the functions involved. This property is important in this solution, considering the complexity of the JL function. The solution obtained in this case was:

$$z_m = -.288 + j.958$$

$$JL(z_m) = -7101.0$$

$$K = 48.4 \qquad (5$$

$$K' = q = 100.0$$

This example ran for about 28 seconds on the same system. One may argue that the SUMT run was unnecessary, however one would not be able to perform the search without the appropriate values of K, K' and q, which were obtained in the SUMT run. The search performed after that is needed, since the particular algorithm employed in conjunction with SUMT is known for its lack of precision, whenever complicated functions are involved. Still, by comparing the

results in equations (5-37) and (5-41), one may see that they are not too far apart, (.13% for $JL(z_m)$). Obviously, the result of the search, equation (5-37), was picked, since in it $JL(z_m)$ is smaller. The search revealed that the value of JL(z) is quite flat in that region;

$$JL[Re(z) = -.30] = -7074.2$$

$$JL[Re(z) = -.25] = -7078.5$$

So, that precision within the second significant figure of Re(z) is not critical.

The value of z_m in equation (5-37) was used in equations (5-30) and (5-33). This time, the value of G*(z) of equation (5-33) was substituted into JL in equation (5-30).

Now one forms a new nonlinear programming problem:

$$\text{Min} \left\{ J(K,K') \,\middle|\, JL(K,K',2,a_o,a_1,a_2,b_1,b_2) \geq 0;\ \underline{p} \varepsilon P \right\} \qquad (5\text{-}42)$$

where

$\underline{p} = [K,K',q,a_o,a_1,a_2,b_1,b_2]$ is the parameter vector in this example.

P is a closed set; in this case the values of all of the parameters involved were limited in size. The limit imposed on all parameters in this case was:

$$|p_i| \leq 100.0; \quad i = 1, \ldots, 8 \qquad (5\text{-}43)$$

The performance criterion in this case was of the form

$$\text{Max} \quad J = K + w\,K' \tag{5-4a}$$

where w is a weighting factor, in this case chosen as w=1. The meaning of the problem is that one would like to find a set of parameters $\underline{p}$, which would permit operating the system with maximum values of K and K' while keeping the system stable.

Since the SUMT program is geared to solve minimization problems the performance criterion is reformulated:

$$\text{Min} \quad J(K, K') = -K - wK' \tag{5-4b}$$

The results obtained in this run, which took 5 seconds on the IBM 360/91 system, were:

$K = K' = 100.0$ (i.e., working at the limit)

$q = 15.0$

$a_o = .131$

$a_1 = .063$ $\qquad$ $b_1 = .100$

$a_2 = .129$ $\qquad$ $b_2 = .094$

Or, in other words, the digital controller is:

$$D(z) = \frac{.131 + .063z^{-1} + .129z^{-2}}{1 + .100z^{-1} + .094z^{-2}} \qquad (5\text{-}46)$$

The actual value of JL for the mentioned parameters was 0.08. This is quite close to the stability limit of zero. Therefore, in actual operation, one should work with somewhat lower values of K and/or K'. In solving problems like this, one should set an a priori limit of K and K' about 20% higher than really desired. It should be stressed, that the search for z_m is done unfrequently, and that only if there is a considerable change in the plant's parameters. In view of the short computing times for the parameters of the digital controller, this algorithm could definitely be employed in real-time control of processes, where changes in system requirements do not occur more often than about every 10 seconds. This could indeed cover a very wide class of computer controlled processes.

5.9 Comparative Study of Minimization Techniques

In real-time computer control the computational efficiency of the algorithms used is of crucial importance. The SUMT program, proposed for use in computer controlled algorithms involves the sequential use of unconstrained minimization techniques. There is a wide variety of available techniques[26,32] that could be used. In order to evaluate their effectiveness for the particular class of problems discussed in this report, a comparative study was performed. As an example, the fourth order system, discussed in section 5.6, was chosen. The methods tested could be classified within the gradient methods using variable metrics.[26,32,33]

To describe the methods used, the following notation is introduced:

$\underline{x}_i$ = the solution vector at iteration i, of dimension n.

$f(\underline{x})$ = the objective function.

∇f_i = the gradient of the objective function at point $\underline{x}_i$.

$\underline{r}_i$ = the unit vector in the direction of the next step from $\underline{x}_i$.

d_i = the step size of the next step from $\underline{x}_i$.

$\underline{s}_i = \underline{x}_{i+1} - \underline{x}_i = d_i \underline{r}_i$

$\underline{y}_i = \nabla f_{i+1} - \nabla f_i$

$A = [\partial^2 f / \partial x_i \partial x_j]$ = the Hessian matrix

$Y_i = [\underline{y}_0, \underline{y}_1, \cdots, \underline{y}_{i-1}]$

$$\underline{r}_i = H_i \nabla f_i$$

H_i = the metric

The methods tested on the IBM 360/91 system and the appropriate results are tabulated as follows:

METHOD	THE RECURSIVE FORMULA	NUMBER OF ITERATIONS	COMPUTING TIME IN SEC.
1. Newton Raphson	$H_i = A^{-1}\ (\underline{x}_i)$	61	1.40
2. Reduced Gradient Projection	$\underline{r}_{i+1} = \begin{bmatrix} -Y_1^{-1}Y_2 \\ I_n \end{bmatrix} \begin{bmatrix} -Y_1^{-1}Y_2 \\ I_n \end{bmatrix}^T \nabla f_{i+1}; Y_{i+1} r_{i+1} = 0$	114	2.10
3. Projected Gradient	$H_{i+1} = H_i + \frac{(H_i \gamma_i)\ (H_i \gamma_i)^T}{\gamma_i^T H_i \gamma_i}$	156	2.93
4. Unsymmetric Variable Metric 1.	$H_{i+1} = H_i + \frac{(\underline{s}_i - H_i \gamma_i)\ (H_i \gamma_i)^T}{\gamma_i^T H_i \gamma_i}$	344	6.13
5. Modified Fletcher-Powell	$H_{i+1} = H_i + \frac{(\underline{s}_i - H_i \gamma_i)\ (\underline{s}_i - H_i \gamma_i)^T}{\gamma_i^T\ (\underline{s}_i - H_i \gamma_i)}$	354	6.63
6. Fletcher-Reeves	$\underline{r}_{i+1} = -\nabla f_{i+1} + \underline{r}_i \frac{\nabla f_{i+1}^T\ \nabla f_{i+1}}{\nabla f_i^T\ \nabla f_i}$	399	7.66
7. Unsymmetric Variable Metric 2	$H_{i+1} = H_i + \frac{(\underline{s}_i - H_i \gamma_i)\underline{s}_i^T}{\underline{s}_i^T \gamma_i}$	580	9.67
8. Fletcher-Powell-Davidon	$H_{i+1} = H_i - \frac{(H_i \gamma_i)\ (H_i \gamma_i)^T}{\gamma_i^T H_i \gamma_i} + \frac{\underline{s}_i \underline{s}_i^T}{\underline{s}_i^T \gamma_i}$	2015	32.24
9. Steepest Descent	$H_i = I_n$	4141	57.53

In the majority of the methods, $H_0 = I_n$, and H_i is being reset to H_0 after every n-1, or n, or n+1 steps.

The reader should be cautioned not to interpret these results in a universal manner. They only mean that for the particular type of problem under consideration, the Newton-Raphson technique proved to be the most effective. For a different problem, the results may be different.

5.10 Conclusion

It was demonstrated that Popov's or Jury and Lee's stability criteria could be reformulated and combined with a nonlinear programming technique in order to generate an algorithm for digital computer, real-time control of nonlinear processes. The computing times in the simulated cases, turned to be quite small; less than 2 seconds in the case of Popov's criterion, and about 5 seconds in the case of Jury and Lee's. It is easy to see that the same algorithm may readily be applied to higher order systems. It would of course involve more variables and more computing time. This aspect should be investigated in more detail in future studies. There is no restriction whatsoever on the performance criterion to be used.

The algorithm proposed, should be applied to other kinds of nonlinear process control systems and actually implemented in real-time, as a natural extension of this study.

REFERENCES

1. Pontragin, L.S., Boltianskii, V.G., Gamkrelidze, R.V., Mishchenko, E.F., The Mathematical Theory of Optimal Processes, Interscience, New York, N.Y., 1962.

2. Rozonoer, L.I., "L.S. Pontriagin's Maximum Principle in the Theory of Optimum Systems," Automation & Remote Control, 20, I, 1288-1302; II, 1405-1421; III, 1517-1532, 1959.

3. Chang, S.S.L., "Digitized Maximum Principle," IRE Proc., 48, 2030-2031, 1960.

4. Katz, S., "A Discrete Version of Pontriagin's Maximum Principle," J. of Electronics and Control, 13, 179-184, 1962.

5. Fan, L.T., Wang, C.S., The Discrete Maximum Principle, John Wiley and Sons, New York, N.Y., 1964.

6. Halkin, H., Jordan, B.W., Polak, E., Rosen, J.B., "Theory of Optimum Discrete Time Systems," 3rd IFAC Conference, London, England, 1966.

7. Pearson, J.D., "The Discrete Maximum Principle, Intr. J. of Control, 2, 117-124, 1965.

8. Holtzman, J.M., "Convexity and the Maximum Principle for Discrete Systems," IEEE Trans., AC-11, 30-35, 1966.

9. Propoi, A.I., "A Problem of Optimal Discrete Control," Sovient Physics - Doklady, 9, 1040-1042, 1965.

10. Tou, J.T., Optimum Design of Digital Control Systems, Academic Press, New York, N.Y., 1963.

11. Brockstein, A.J., Kuo, B.C., "Optimum Control of Multivariable Sampled Data Systems with Adaptive Sampling," 1967 JACC, 366-372, Philadelphia, Pa.

12. Rosen, J.B., "Optimal Control and Convex Programming," MRC Technical Report 547, University of Wisconsin, Feb. 1965.

13. Canon, M.D., Cullum, C., Polak, E., "Constrained Minimization Problems in Finite Dimensional Spaces," J. SIAM Control, 4, 528-547, 1966.

14. Kuhn, M.W., Tucker, A.W., "Nonlinear Programming," Proceedings of the Second Berkeley Symposium on Mathematical Statistics and Probability, 481-492, University of California Press, Berkeley, California, 1951.

15. Neustadt, L.W., "An Abstract Variational Theory with Applications to a Broad Class of Optimization Problems, pt. I. General Theory," J. SIAM Control, 4, 505-527, 1966.

16. Pearson, J.B., Sridhar, R., "A Discrete Optimal Control Problem," IEEE Trans., AC-11, 171-174, 1966.

17. Porcelli, G., Fegley, K.A., "Optimal Design of Digitally Compensated Systems by Quadratic Programming," J. Franklin Inst., 282, 303-317, 1966.

18. Torng, H.C., "Optimization of Discrete Control Systems Through Linear Programming," J. Franklin Inst., 277, 28-44, 1964.

19. Canon, M.D., Eaton, J.H., "A New Algorithm for a Class of Quadriatic Programming Problems with Application to Control," J. SIAM Control, 4, 34-45, 1966.

20. Kim, M., "On Optimum Control of Discrete Systems," Pt. 1, ISA Trans., 5, 93-98, 1966.

21. Tabak, D., "Optimization of Nuclear Reactor Fuel Recycle via Linear and Quadratic Programming," IEEE Trans., NS-15, pp. 60-64, Feb. 1968.

22. Hadley, G., Nonlinear and Dynamic Programming, Addison Wesley, Reading, Mass., 1964.

23. Zoutendijk, G., "Nonlinear Programming: A Numerical Survey," J. SIAM Control, 4, 194-210, 1966.

24. Tabak, D., "Application of Mathematical Programming in the Design of Optimal Control Systems," Ph.D. thesis, University of Illinois, Urbana, Illinois, Feb. 1968.

25. Tabak, D., B.C. Kuo, "Application of Mathematical Programming in the Design of Optimal Control Systems," International J. of Control, Oct. 1969.

26. Fiacco, A.V., McCormick, G.P., "Nonlinear Programming: Sequential Unconstrained Minimization Techniques," Wiley, N.Y., 1968.

27. Kuo, B.C., "Automatic Control Systems," 2nd edition, Prentice-Hall, Englewood Cliffs, N.J., 1967.

28. Tabak, D., "Computer Control of Nonlinear Systems with Varying Performance Criteria," Invited paper for 1969 JACC, Boulder, Colorado, August 1969. (To appear in Int. J. Control).

29. Popov, V.M., "Absolute Stability of Nonlinear Systems of Automatic Control," Automation and Remote Control, 22, pp. 857-875, August 1961.

30. Jury, E.I., B.W. Lee, "On the Stability of a Certain Class of Nonlinear Sampled - Data Systems," IEEE Trans. Automatic Control, AC-9, pp. 51-61, January 1964.

31. Kuo, B.C., "Analysis and Synthesis of Sampled Data Control Systems," Prentice Hall, Englewood Cliffs, N.J., 1963.

32. Kowalik, J., M.R. Osborne, "Methods for Unconstrained Optimization Problems," American Elsevier, N.Y., 1968.

33. Pearson, J.D., "On Variable Metric Methods of Minimization," Research Analysis Corporation Technical Paper, RAC-TP-302, McLean, Va., February 1968.

34. Tabak, D., "An Algorithm for Nonlinear Process Stabilization and Control," IEEE Computer Group Conference, June 1969, Minneapolis, pp. 82-86.

6. Conclusions

It was demonstrated by the simulations performed that optimal estimation-control techniques can be applied to antenna tracking systems. Using the optimal estimator-controller configuration, the system errors are estimated and proper correction in the controller is performed. As a result, at least under ideal conditions, a much smaller pointing error is obtained. In the simulation of the telescopic tracker, the ratio between the autotrack and the optimal estimator-controller error was 20 to 40. In the simulation of the 30 ft antenna, the ratio was up to 850 for the simulated Mars mission. In the near Earth Trajectory simulation 200 N.M. circular orbit with the 40 ft antenna a steady state pointing error of 0.001 to 0.004 degrees was achieved. Present standards for near-Earth missions are approximately ten times higher.

It was shown that insertion of certain types of nonlinearities in the control loop of the tracking system causes instability. It is also a fact that nonlinearities are inherent in the actual tracking systems, as the 40 ft antenna system. It was further shown that using the mathematical programming approach the optimal control signal can be synthesized, taking into account the existing nonlinearities as they are, without resorting to approximate linearizations.

Further work is recommended in the following areas:

1. Work out actual implementation of optimal estimator-controller, in real-time, connecting specific computers to specific tracking systems.

2. Continue investigation of actual implementation of nonlinear synthesis.

3. Apply the same methods to a wider area of different systems. One possible area of immediate interest would be optical tracking systems.

MEMORANDUM 7

APPLICATION OF OPTIMUM ESTIMATION AND CONTROL THEORY TO SATELLITE TRACKING PROBLEMS

I INTRODUCTION

The purpose of this memorandum is to derive optimum (approximately) estimation and control techniques for the satellite tracking problem. The problem is nonlinear, as will become apparent in subsequent sections. Some preliminary studies are described in Refs. 1 and 2.* The present study has resulted in the development of a digital computer program that implements the operation of the optimal estimator and controller in conjunction with the satellite tracking system.

A solution to the problem can be obtained by solving the estimation and control portions separately. Since the satellite tracking problem is nonlinear, the assumption that the estimation and control portions separate may not be optimal in the strictest sense;[3] however, since the estimation and control portions are weakly coupled (as will be seen in subsequent sections), the assumption of separation is quite reasonable.

The estimator, which generates an optimum estimate of the present state of the system (satellite and antenna control system), is derived in Sec. III. The estimation problem is solved by employing the extended Kalman filter, which necessitates the linearization of the satellite equations and the measurement equations.

The estimate of the system state is then employed in the controller to compute the optimum control with respect to the given performance criterion. The control problem is solved in Sec. IV by making the appropriate linearization and applying some new results in the theory of linear optimal control.

* References are listed at the end of the memorandum.

II PROBLEM FORMULATION

Figure 1 is a block diagram of the satellite tracking system. The mathematical models for the various parts of the system are given below.

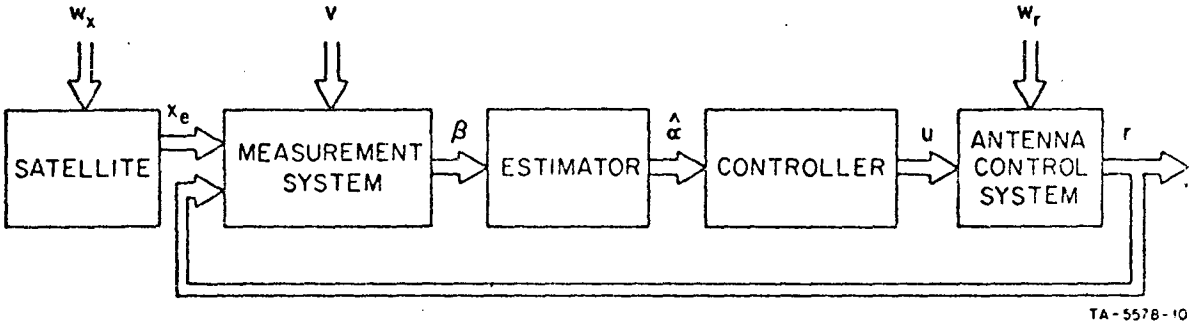

FIG. 1 SATELLITE TRACKING SYSTEM

A. SATELLITE*

$$\ddot{x}_{1_e} = -\frac{\mu_e x_{1_e}}{r_e^3} \quad ,$$

$$\ddot{x}_{2_e} = -\frac{\mu_e x_{2_e}}{r_e^3} \quad , \tag{1}$$

$$\ddot{x}_{3_e} = -\frac{\mu_e x_{3_e}}{r_e^3} \quad ,$$

where

$$r_e = \left(x_{1_e}^2 + x_{2_e}^2 + x_{3_e}^2\right)^{1/2} \quad ,$$

*The term "satellite" does not necessarily mean a near-earth satellite; it could, for instance, refer to a deep-space probe.

μ_e = the product of the universal gravitational constant and the mass of the earth,

x_{1_e}, x_{2_e}, x_{3_e} = the position coordinates of the satellite with respect to an earth-centered Cartesian coordinate system. (The 3_e axis is coincident with the earth's polar axis, and the 1_e and 2_e axes lie in the equatorial plane, completing a right-handed orthogonal set.)

It should be noted that the above differential equations (1) merely give an approximate description of the motion of the satellite, and are used only to obtain the solutions to the estimation and control portions of the problem. The actual* trajectory of the satellite is generated by a more exact computer program model developed at NASA Ames Research Center, Mountain View, California.

The differential equations (1) can be put into state variable form upon definition of the following variables:

$$\begin{aligned} \alpha_1 &= x_{1_e} , \\ \alpha_2 &= x_{2_e} , \\ \alpha_3 &= x_{3_e} , \\ \alpha_4 &= \dot{x}_{1_e} , \\ \alpha_5 &= \dot{x}_{2_e} , \\ \alpha_6 &= \dot{x}_{3_e} . \end{aligned} \tag{2}$$

Combining Eqs. (1) and (2) yields

$$\begin{aligned} \dot{\alpha}_1 &= \alpha_4 , \\ \dot{\alpha}_2 &= \alpha_5 , \\ \dot{\alpha}_3 &= \alpha_6 , \end{aligned}$$

* The term "actual" refers to the trajectory to be tracked by the antenna in the computer simulation.

$$\dot{\alpha}_4 = \frac{-\mu_e \alpha_1}{r_e^3} \quad ,$$

$$\dot{\alpha}_5 = \frac{-\mu_e \alpha_2}{r_e^3} \quad ,$$

$$\dot{\alpha}_6 = \frac{-\mu_e \alpha_3}{r_e^3} \quad , \tag{3}$$

where

$$r_e = (\alpha_1^2 + \alpha_2^2 + \alpha_3^2)^{1/2} \quad .$$

After defining the six-dimensional state vector of the satellite as

$$x_e = \begin{bmatrix} \alpha_1 \\ \vdots \\ \alpha_6 \end{bmatrix} \quad , \tag{4}$$

the differential equations (3) can be rewritten concisely as

$$\dot{x}_e = f(x_e) \quad , \tag{5}$$

where $f(x_e)$ is a six-dimensional vector function of x_e as given by Eqs. (3).

Equation (5) is a nonlinear differential equation; however, in order to take advantage of certain results in the theory of linear estimation and control, it is necessary to linearize this equation. This concept will be clarified in Secs. III and IV. Linearization of Eq. (5) is achieved by considering x_e to be composed of some nominal trajectory x_e^o and a perturbation from the nominal $\tilde{x}_e$:

$$x_e = x_e^o + \tilde{x}_e \quad . \tag{6}$$

Upon expanding Eq. (5) in a Taylor series about x_e^o and neglecting second and higher-order terms, the linear perturbation equation is found to be:

$$\dot{\tilde{x}}_e = \mathcal{J}(x_e^o)\tilde{x}_e \quad , \tag{7}$$

where

$$\dot{x}_e^o = f(x_e^o) \quad ,$$

$$\mathfrak{J}(x_e^o) = \left.\frac{\partial f}{\partial x_e}\right|_{x_e^o} = \left[\frac{\partial f_i}{\partial x_j}\right]_{x_e^o} .$$

$$\mathfrak{J}(x_e^o) = \begin{bmatrix} 0 & 0 & 0 & 1 & 0 & 0 \\ 0 & 0 & 0 & 0 & 1 & 0 \\ 0 & 0 & 0 & 0 & 0 & 1 \\ \dfrac{\mu_e(2\alpha_1^2 - \alpha_2^2 - \alpha_3^2)}{r_e^5} & \dfrac{3\mu_e\alpha_1\alpha_2}{r_e^5} & \dfrac{3\mu_e\alpha_1\alpha_3}{r_e^5} & 0 & 0 & 0 \\ \dfrac{3\mu_e\alpha_2\alpha_1}{r_e^5} & \dfrac{\mu_e(2\alpha_2^2 - \alpha_1^2 - \alpha_3^2)}{r_e^5} & \dfrac{3\mu_e\alpha_2\alpha_3}{r_e^5} & 0 & 0 & 0 \\ \dfrac{3\mu_e\alpha_3\alpha_1}{r_e^5} & \dfrac{3\mu_e\alpha_3\alpha_2}{r_e^5} & \dfrac{\mu_e(2\alpha_3^2 - \alpha_1^2 - \alpha_2^2)}{r_e^5} & 0 & 0 & 0 \end{bmatrix}_{x_e^o} \quad (8)$$

Since the problem is to be simulated on a digital computer, it is essential to convert the differential equation (7) into an equivalent difference equation. This can be done by noting that the time derivative is approximately given by

$$\dot{\tilde{x}}_e(k-1) = \frac{\tilde{x}_e(k) - \tilde{x}_e(k-1)}{\Delta t} \quad ,$$

or

$$\tilde{x}_e(k) = \tilde{x}_e(k-1) + \dot{\tilde{x}}_e(k-1)\Delta t \quad , \qquad (9)$$

where

$\tilde{x}_e(k\Delta t)$ is defined as $\tilde{x}_e(k)$, and Δt is the time increment.

Substituting Eq. (7) into (9) gives

$$\tilde{x}_e(k) = \{I + \mathfrak{J}[x_e^o(k-1)]\Delta t\}\tilde{x}_e(k-1) \quad , \tag{10}$$

where the transition matrix is given by

$$\Phi_x(k-1) = I + \mathfrak{J}[x_e^o(k-1)]\Delta t \quad . \tag{11}$$

Since Eq. (10) is only an approximate mathematical model of the satellite motion, a random forcing term will be included as follows in order to account for the imprecise nature of this model:

$$\tilde{x}_e(k) = \Phi_x(k-1)\tilde{x}_e(k-1) + \Gamma_x(k-1)w_x(k-1) \quad , \tag{12}$$

where

$$\Gamma_x(k-1) = \Gamma_x = \begin{bmatrix} 0 & 0 & 0 \\ 0 & 0 & 0 \\ 0 & 0 & 0 \\ 1 & 0 & 0 \\ 0 & 1 & 0 \\ 0 & 0 & 1 \end{bmatrix} \quad , \quad w_x(k-1) = \begin{bmatrix} w_{x_1}(k-1) \\ w_{x_2}(k-1) \\ w_{x_3}(k-1) \end{bmatrix} \quad .$$

It is assumed that the random forcing term $w_x(k-1)$ is white* gaussian noise with zero mean and covariance $Q_x(k-1) = E[w_x(k-1)w_x^T(k-1)]$.

B. ANTENNA CONTROL SYSTEM

The antenna control system consists of two channels—elevation and azimuth. The elevation channel, which includes the antenna dynamics, is illustrated schematically in Fig. 2; the azimuth channel has a similar configuration. In this study, the analysis is carried through for an electric drive; a hydraulic drive could be considered in an analogous manner.

---

* The statement that a random quantity z is white implies that $E[z(i)z^T(j)] = 0$ for $i \neq j$; i.e., z is uncorrelated for different sample times.

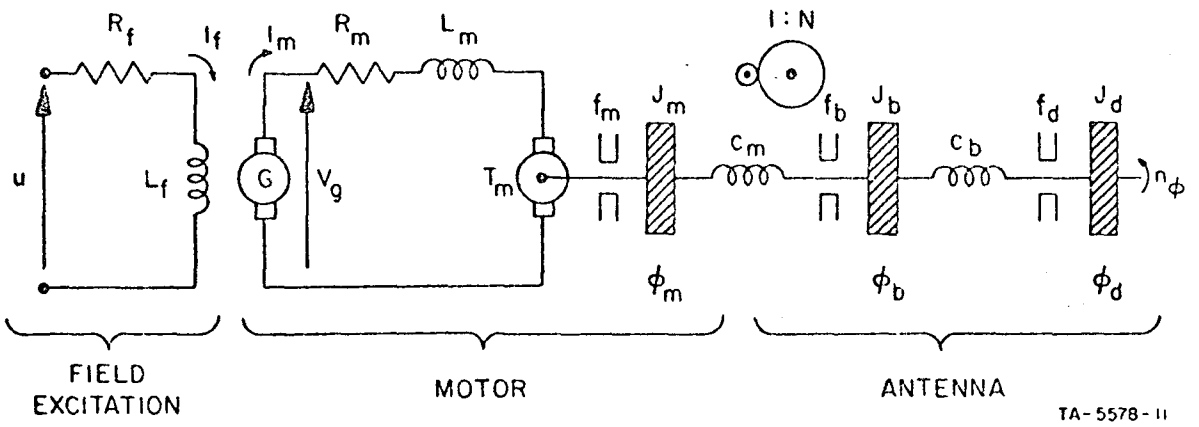

FIG. 2 SCHEMATIC DIAGRAM OF ANTENNA CONTROL SYSTEM (Elevation Channel)

It is assumed that the elevation channel is linear (for suitably small signals) and is described by the following:

$$
\begin{aligned}
L_f \dot{I}_f + R_f I_f &= u_\phi \quad , \\
V_g &= k_f I_f \quad , \\
L_a \dot{I}_a + R_a I_a &= V_g - k_a \dot{\phi}_a \quad , \\
T_a &= k_a I_a \quad , \\
J_a \ddot{\phi}_a + f_a \dot{\phi}_a + c_a\left(\phi_a - N\phi_b\right) &= T_a \quad , \\
J_b \ddot{\phi}_b + f_b \dot{\phi}_b + c_b\left(\phi_b - \phi_d\right) + N^2 c_a\left(\phi_b - \frac{1}{N}\phi_a\right) &= 0 \quad , \\
J_d \ddot{\phi}_d + f_d \dot{\phi}_d + c_b\left(\phi_d - \phi_b\right) &= n_\phi \quad ,
\end{aligned}
\tag{13}
$$

where

u_ϕ = control variable
L_f = field inductance
R_f = field resistance
I_f = field current
k_f = field proportionality constant
V_g = generator voltage
L_a = motor inductance
R_a = motor resistance
I_a = motor current

k_m = motor proportionality constant

T_m = motor torque

J_m = moment of inertia of motor

f_m = damping of motor

c_m = gear spring constant of motor (referred to the motor shaft)

N = gear ratio

ϕ_m = motor angle

J_b = moment of inertia of antenna base

f_b = damping of antenna base

c_b = spring constant of antenna

ϕ_b = angle of antenna base or angle of antenna's mechanical axis

J_d = moment of inertia of antenna dish

f_d = damping of antenna dish

ϕ_d = angle of antenna dish or angle of antenna's electrical axis

n_ϕ = random disturbance (noise) due to wind gusts.

It should be noted that this model of the antenna considers the first bending mode. For large antennas this effect is quite significant.

It has been shown[4] that the power spectral density of the wind disturbance n_ϕ is approximately equal to

$$\mathcal{S}n_\phi(s) = \frac{1}{-s^2 + a_\phi^2} .$$

The noise n_ϕ can be considered as the output of a filter having the transfer function

$$\frac{1}{s + a_\phi}$$

and subjected to white noise w_ϕ, where $\mathcal{S}w_\phi(s) = 1$. This step is necessary in order to put the problem in the appropriate form for the relevant theory. In the time domain, n_ϕ and w_ϕ are related by

$$\dot{n}_\phi = -a_\phi n_\phi + w_\phi \quad . \tag{14}$$

The differential equations (13) and (14) can be put into state variable form by defining the following variables:

$$\alpha_7 = I_f$$

$$\alpha_8 = I_m$$

$$\alpha_9 = \phi_m$$

$$\alpha_{10} = \dot{\phi}_m$$

$$\alpha_{11} = \phi_b$$

$$\alpha_{12} = \dot{\phi}_b$$

$$\alpha_{13} = \phi_d$$

$$\alpha_{14} = \dot{\phi}_d$$

$$\alpha_{15} = n_\phi \quad . \qquad (15)$$

Upon denoting the nine-dimensional state vector of the elevation channel as

$$r_\phi = \begin{bmatrix} \alpha_7 \\ \cdot \\ \cdot \\ \cdot \\ \alpha_{15} \end{bmatrix} , \qquad (16)$$

the differential equations (13) and (14) can be rewritten concisely as

$$\dot{r}_\phi = F_\phi r_\phi + D_\phi u_\phi + G_\phi w_\phi \quad , \qquad (17)$$

where

$$F_\phi = \begin{bmatrix} -\frac{R_f}{L_f} & 0 & 0 & 0 & 0 & 0 & 0 & 0 & 0 \\ \frac{k_f}{L_m} & -\frac{R_m}{L_m} & 0 & -\frac{k_m}{L_m} & 0 & 0 & 0 & 0 & 0 \\ 0 & 0 & 0 & 1 & 0 & 0 & 0 & 0 & 0 \\ 0 & -\frac{k_m}{J_m} & -\frac{c_m}{J_m} & -\frac{f_m}{J_m} & -\frac{c_m N}{J_m} & 0 & 0 & 0 & 0 \\ 0 & 0 & 0 & 0 & 0 & 1 & 0 & 0 & 0 \\ 0 & 0 & -\frac{c_m N}{J_b} & 0 & -\frac{N^2 c_m + c_b}{J_b} & -\frac{f_b}{J_b} & -\frac{c_b}{J_b} & 0 & 0 \\ 0 & 0 & 0 & 0 & 0 & 0 & 0 & 1 & 0 \\ 0 & 0 & 0 & 0 & -\frac{c_b}{J_d} & 0 & -\frac{c_b}{J_d} & -\frac{f_d}{J_d} & \frac{1}{J_d} \\ 0 & 0 & 0 & 0 & 0 & 0 & 0 & 0 & -a_\phi \end{bmatrix}$$

$$D_\phi = \begin{bmatrix} L_f^{-1} \\ 0 \\ \vdots \\ 0 \end{bmatrix}, \quad G_\phi = \begin{bmatrix} 0 \\ \vdots \\ 0 \\ 1 \end{bmatrix}.$$

The digital computer simulation of the problem necessitates the conversion of the differential equation (17) into an equivalent difference equation. This can be accomplished by solving Eq. (17) with an arbitrary initial condition $r_\phi(t')$:

$$r_\phi(t) = \exp[F_\phi(t - t')]r_\phi(t') + \int_{t'}^{t} \exp[F_\phi(t - \tau)]D_\phi u_f(\tau)d\tau$$

$$+ \int_{t'}^{t} \exp[F_\phi(t - \tau)]G_\phi w_\phi(\tau)d\tau \quad . \qquad (18)$$

With $t = k\Delta t$ and $t' = (k - 1)\Delta t$, and with u_ϕ and w_ϕ assumed to be constant over the time interval $[(k - 1)\Delta t, k\Delta t]$, Eq. (18) becomes

$$r_\phi(k) = \Phi_\phi(k - 1)r_\phi(k - 1) + \Lambda_\phi(k - 1)u_\phi(k - 1) + \Gamma_\phi(k - 1)w_\phi(k - 1) \quad , \tag{19}$$

where

$$\Phi_\phi(k - 1) = \Phi_\phi = \exp\,[F_\phi \Delta t] = \sum_{i=0}^{\infty} \frac{F_\phi^i \cdot (\Delta t)^i}{i!} \quad ,$$

$$\Delta_\phi(k - 1) = \Lambda_\phi = \int_{(k-1)\Delta t}^{k\Delta t} \exp\,[F_\phi(k\Delta t - \tau)]\,d\tau D_\phi$$

$$= \left[\sum_{i=0}^{\infty} \frac{F_\phi^i \cdot (\Delta t)^{i+1}}{(i + 1)!}\right] D_\phi \quad ,$$

$$\Gamma_\phi(k - 1) = \Gamma_\phi = \int_{(k-1)\Delta t}^{k\Delta t} \exp\,[F_\phi(k\Delta t - \tau)]\,d\tau G_\phi$$

$$= \left[\sum_{i=0}^{\infty} \frac{F_\phi^i \cdot (\Delta t)^{i+1}}{(i + 1)!}\right] G_\phi \quad , \tag{20}$$

and $r_\phi(k\Delta t)$ is defined as $r_\phi(k)$.

The azimuth channel has the same form as the elevation channel, which is described by the differential equation (17). The only difference between the two channels is that the moments of inertia of the antenna (in azimuth) are functions of the elevation angles. Since the rates of change for these moments of inertia are slow with respect to the control system time constants, it will be assumed that they can be treated as time-varying functions. Hence, the azimuth channel can be described by a differential equation that is analogous to Eq. (17):

$$\dot{r}_\theta = F_\theta(t)r_\theta + D_\theta u_\theta + G_\theta w_\theta \quad , \tag{21}$$

where

$$r_\theta = \begin{bmatrix} \alpha_{16} \\ \cdot \\ \cdot \\ \cdot \\ \alpha_{24} \end{bmatrix} \tag{22}$$

is the nine-dimensional state vector of the azimuth channel and is entirely analogous to r_ϕ as defined by Eqs. (15) and (16). The matrices $F_\theta(t)$, D_θ, and G_θ have the identical form of the corresponding matrices defined in Eq. (17), the time dependence in $F_\theta(t)$ being due to the time-varying moments of inertia.

The differential equation (21) can be converted into an equivalent difference equation by assuming that F_θ, in addition to u_θ and w_θ, is constant over the interval $[(k-1)\Delta t,\ k\Delta t]$:

$$r_\theta(k) = \Phi_\theta(k-1)r_\theta(k-1) + \Delta_\theta(k-1)u_\theta(k-1) + \Gamma_\theta(k-1)w_\theta(k-1) \quad , \tag{23}$$

where

$$\Phi_\theta(k-1) = \sum_{i=0}^{\infty} \frac{F_\theta^i(k-1)\cdot(\Delta t)^i}{i!}$$

$$\Delta_\theta(k-1) = \left[\sum_{i=0}^{\infty} \frac{F_\theta^i(k-1)\cdot(\Delta t)^{i+1}}{(i+1)!}\right] D_\theta$$

$$\Gamma_\theta(k-1) = \left[\sum_{i=0}^{\infty} \frac{F_\theta^i(k-1)\cdot(\Delta t)^{i+1}}{(i+1)!}\right] G_\theta \quad , \tag{24}$$

and $r_\theta(k\Delta t)$ is defined as $r_\theta(k)$.

Hence, the antenna control system (elevation and azimuth channels) is described by

$$r(k) = \Phi_r(k-1)r(k-1) + \Delta_r(k-1)u(k-1) + \Gamma_r(k-1)w_r(k-1) \quad , \tag{25}$$

where

$$r(k-1) = \begin{bmatrix} r_\phi(k-1) \\ r_\theta(k-1) \end{bmatrix}$$

$$\Phi_r(k-1) = \begin{bmatrix} \Phi_\phi & 0 \\ 0 & \Phi_\theta(k-1) \end{bmatrix}$$

$$u(k-1) = \begin{bmatrix} u_\phi(k-1) \\ u_\theta(k-1) \end{bmatrix}$$

$$\Delta_r(k-1) = \begin{bmatrix} \Delta_\phi & 0 \\ 0 & \Delta_\theta(k-1) \end{bmatrix}$$

$$w_r(k-1) = \begin{bmatrix} w_\phi(k-1) \\ w_\theta(k-1) \end{bmatrix}$$

$$\Gamma_r(k-1) = \begin{bmatrix} \Gamma_\phi & 0 \\ 0 & \Gamma_\theta(k-1) \end{bmatrix} .$$

In addition, it is assumed that $w_r(k-1)$ is white gaussian noise with zero mean and covariance $Q_r(k-1) = E[w_r(k-1)w_r^T(k-1)]$. The matrices Φ_r, Δ_r, and Γ_r can be computed with an arbitrary degree of accuracy by taking a suitably large (but finite) number of terms in the series expansions of Eqs. (20) and (24).

C. MEASUREMENT SYSTEM

The state of the satellite tracking system, which consists of the satellite (x_e) and the antenna control system (r), may be defined by the 24-dimensional vector

$$\alpha = \begin{bmatrix} x_e \\ r \end{bmatrix} = \begin{bmatrix} \alpha_1 \\ . \\ . \\ . \\ \alpha_{24} \end{bmatrix} . \qquad (26)$$

The measurement system, which includes the monopulse receiver*, is defined by the 15-dimensional measurement vector

* The monopulse receiver and its associated demodulating equipment measures the elevation and azimuth components of the difference between the angle of the antenna's electrical axis and the satellite angle. It is assumed that this difference is suitably small so that the operation of the monopulse receiver is linear.

$$\beta(k) = \begin{bmatrix} \alpha_7(k) \\ \vdots \\ \alpha_{12}(k) \\ \alpha_{16}(k) \\ \vdots \\ \alpha_{21}(k) \\ \phi_d(k) - \phi_s[\alpha(k),k] \\ \theta_d(k) - \theta_s[\alpha(k),k] \\ \dot{\rho}_s[\alpha(k),k] \end{bmatrix} + v(k) = h[\alpha(k),k] + v(k) \quad , \quad (27)$$

where

$\phi_s[\alpha(k),k]$ = elevation angle of satellite

$\theta_s[\alpha(k),k]$ = azimuth angle of satellite

$\dot{\rho}_s[\alpha(k),k]$ = range rate of satellite

$\phi_d(k) = \alpha_{13}(k)$, $\theta_d(k) = \alpha_{22}(k)$

$v(k)$ = measurement noise, which is assumed to be a white gaussian random process with zero mean and covariance $R(k) = E[v(k)v^T(k)]$.

The expressions ϕ_s, θ_s, and $\dot{\rho}_s$ (which are time-varying, nonlinear functions) are derived in Appendix A and given by Eqs. (A-6), (A-7), and (A-9), respectively. Figures A-1, A-2, and A-3 in Appendix A illustrate the geometry of the satellite tracking problem. It should be pointed out that this study considers the relative motion of the antenna with respect to the satellite as the earth rotates on its axis.

Since the measurement equation (27) is nonlinear, it is necessary, as before, to perform a linearization. Consider α to be composed of some nominal trajectory α^o and a perturbation from the nominal $\tilde{\alpha}$:

$$\alpha = \alpha^o + \tilde{\alpha} \quad . \quad (28)$$

Similarly, let β be given as follows:

$$\beta = \beta^{o} + \tilde{\beta} \quad . \tag{29}$$

Expanding Eq. (27) in a Taylor series about α^{o} and neglecting second and higher-order terms, the linear perturbation equation is

$$\tilde{\beta}(k) = H[\alpha^{o}(k),k]\tilde{\alpha}(k) + v(k) \quad , \tag{30}$$

where

$$\beta^{o}(k) = h[\alpha^{o}(k),k] \quad ,$$

$$H[\alpha^{o}(k),k] = \left.\frac{\partial h}{\partial \alpha}\right|_{\alpha^{o}(k),k} = \left[\frac{\partial h_i}{\partial \alpha_j}\right]_{\alpha^{o}(k),k} \quad .$$

From Eqs. (26) and (27), it can be demonstrated that

$$H[\alpha^{o}(k),k] \triangleq H(k) = \left[\begin{array}{c|c|c} \bigcirc & \mathrm{I} & \bigcirc \\ (6\times 6) & (6\times 6) & (6\times 12) \\ \hline \bigcirc & \mathrm{I} & \bigcirc \\ (6\times 15) & (6\times 6) & (6\times 3) \\ \hline \begin{array}{cccccc} a_1 & a_2 & a_3 & 0 & 0 & 0 \\ b_1 & b_2 & b_3 & 0 & 0 & 0 \\ c_1 & c_2 & c_3 & d_1 & d_2 & d_3 \end{array} & \begin{array}{c} 0\ldots 0\,1\,0\,0 \\ 0\quad\ldots\quad 0 \\ 0\quad\ldots\quad\quad \end{array} & \begin{array}{c} 0\quad\ldots\quad 0 \\ 0\ldots 0\,1\,0\,0 \\ \ldots\quad 0 \end{array} \end{array}\right]_{\alpha^{o}(k),k} \tag{31}$$

where the a_i, b_i, c_i, and d_i are derived in Appendix B and given by Eqs. (B-5) through (B-8).

D. ESTIMATOR AND CONTROLLER

The function of the estimator is to generate an optimum estimate of the present state α from the measurement β, which is corrupted by noise. This estimate is then employed in the controller to compute the optimum control with respect to the given performance criterion. The estimation and control equations are obtained in Secs. III and IV, respectively.

III ESTIMATION EQUATIONS

In this section the estimation problem is solved by employing the extended Kalman filter. This concept is an application to nonlinear systems of work done by Kalman in linear estimation theory.[5] The derivation of the extended (or linearized) Kalman filter is presented in Memorandum 6[6] and hence will not be repeated here. This approach has been successfully applied at SRI to missile tracking problems, including the identification of unknown aerodynamic parameters.[7]

From Eqs. (12) and (25), the random disturbance acting upon the satellite tracking system is given by the five-dimensional vector

$$w(k) = \begin{bmatrix} w_x(k) \\ \\ w_r(k) \end{bmatrix} ,$$

which is white gaussian noise with

$$E[w(k)] = 0 ,$$

$$E[w(k)w^T(k)] = Q(k) = \begin{bmatrix} Q_x(k) & 0 \\ \\ 0 & Q_r(k) \end{bmatrix} .$$

The measurement noise $v(k)$ has been defined in Eq. (27). The initial state $\alpha(0)$ is a gaussian random variable with

$$E[\alpha(0)] = \hat{\alpha}(0/0) ,$$

$$E[\{\alpha(0) - \hat{\alpha}(0/0)\}\{\alpha(0) - \hat{\alpha}(0/0)\}^T] = P(0/0) .$$

Furthermore, it is assumed that $w(k)$, $v(k)$, and $\alpha(0)$ are uncorrelated.

The resulting estimation equations can be considered as consisting of two parts: prediction and correction (or regression).*

A. PREDICTION

Given the estimate of the system state at the k-1th instant $[\hat{\alpha}(k - 1/k - 1)]$, the predicted system state for the kth instant $[\hat{\alpha}(k/k - 1)]$ is obtained from Eqs. (9) and (25):

$$\hat{\alpha}(k/k-1) \begin{cases} \hat{x}_e(k/k-1) = \hat{x}_e(k-1/k-1) + f[\hat{x}_e(k-1/k-1)]\Delta t & ,\dagger \\ \hat{r}(k/k-1) = \Phi_r(k-1)\hat{r}(k-1/k-1) + \Delta_r(k-1)u(k-1) & , \end{cases} \tag{32}$$

with the covariance of the error in this prediction given by

$$P(k/k-1) = \Phi(k-1)P(k-1/k-1)\Phi^T(k-1) + \Gamma(k-1)Q(k-1)\Gamma^T(k-1) \quad , \tag{33}$$

where

$$\Gamma(k-1) = \begin{bmatrix} \Gamma_x & 0 \\ 0 & \Gamma_r(k-1) \end{bmatrix} \quad ,$$

$$\Phi(k-1) = \begin{bmatrix} \Phi_x(k-1) & 0 \\ 0 & \Phi_r(k-1) \end{bmatrix} \quad ,$$

and $\Phi_x(k - 1)$ is obtained from Eqs. (7), (8), and (11) by linearization about the estimate $\hat{\alpha}(k - 1/k - 1)$ [or $\hat{x}_e(k - 1/k - 1)$]; *i.e.*,

$$\Phi_x(k-1) = I + \mathfrak{J}[\hat{x}_e(k-1/k-1)]\Delta t \quad .$$

It should be noted that $w(k - 1) = 0$ in Eq. (32), since $E[w(k - 1)] = 0$.

---

* The following notation will be employed:

$\hat{\alpha}(i/j) \triangleq E[\alpha(i)/\beta(j), \ldots, \beta(1), u(j-1), \ldots, u(0)]$,

$P(i/j) \triangleq E[\{\alpha(i) - \hat{\alpha}(i/j)\}\{\alpha(i) - \hat{\alpha}(i/j)\}^T/\beta(j), \ldots, \beta(1), u(j-1), \ldots, u(0)]$.

These expectations are conditioned on the previous measurements and inputs.

† The nonlinear differential equation for x_e may be integrated by a more accurate method if necessary.

B. CORRECTION

The prediction $\hat{\alpha}(k/k-1)$ is then "corrected" by using the actual measurement at the kth instant $[\beta(k)]$ and the predicted measurement for the kth instant $[\hat{\beta}(k/k-1)]$, which is obtained from Eq. (27):

$$\hat{\beta}(k/k-1) = h[\hat{\alpha}(k/k-1), k] \quad . \tag{34}$$

It should be noted that $v(k) = 0$ in Eq. (34), since $E[v(k)] = 0$.

Hence, the estimate of the system state at the kth instant is given by

$$\hat{\alpha}(k/k) = \hat{\alpha}(k/k-1) + W(k)[\beta(k) - \hat{\beta}(k/k-1)] \quad , \tag{35}$$

where the weighting matrix

$$W(k) = P(k/k-1)H^T(k)[R(k) + H(k)P(k/k-1)H^T(k)]^{-1} \quad , \tag{36}$$

and $H(k)$ is obtained from Eqs. (30) and (31) by linearization about the prediction $\hat{\alpha}(k/k-1)$; *i.e.*,

$$H(k) = H[\hat{\alpha}(k/k-1), k] = \left.\frac{\partial h}{\partial \alpha}\right|_{\hat{\alpha}(k/k-1),k} \quad .$$

The covariance of the error in the estimate $\hat{\alpha}(k/k)$ is

$$\begin{aligned} P(k/k) &= [I - W(k)H(k)]P(k/k-1) \\ &= P(k/k-1) - P(k/k-1)H^T(k)[R(k) + H(k)P(k/k-1)H^T(k)]^{-1}H(k)P(k/k-1) \quad . \end{aligned} \tag{37}$$

The extended Kalman filter [Eqs. (32) through (37)], which is depicted in Fig. 3, gives the solution to the estimation problem. Obviously, this solution can be readily implemented on a digital computer. However, since the overall system is not linear, the solution is

---

* From Eqs. (B-5) through (B-8), together with Eq. (31), it is obvious that $H(k)$ is actually evaluated at the prediction $\hat{\alpha}(k/k-1)$.

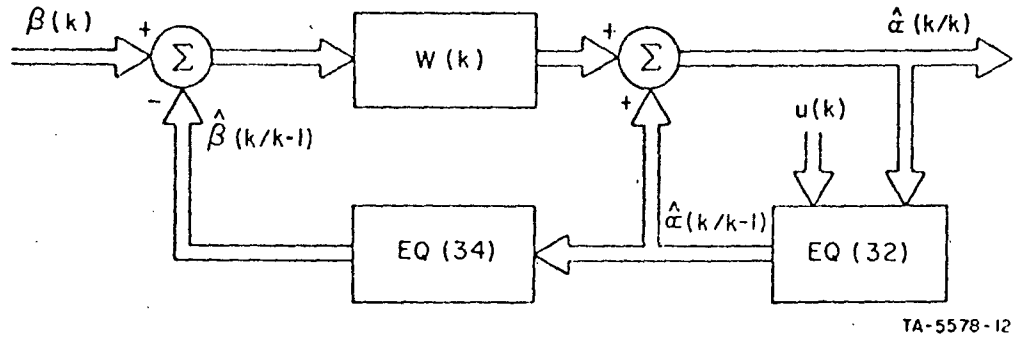

FIG. 3 BLOCK DIAGRAM OF THE ESTIMATOR

suboptimal. Intuitively, this approach seems to be quite reasonable, but its validity has not been rigorously established. The extent to which this solution to the estimation problem differs from the optimum is mainly dependent upon the accuracy of the linearization of Eq. (5), the differential equation for x_c, and of Eq. (27), the measurement equation. There are many questions pertaining to this subject that remain to be answered.

It should be noted that in the derivation of the extended Kalman filter, the nonlinear equations (5) and (27) were used in Eqs. (32) and (34) to obtain the predicted state and the predicted measurement. The linearization of Eqs. (5) and (27), in order to obtain Φ_x and H, is only employed to calculate the covariance matrices P and the weighting matrix W.

IV CONTROL EQUATIONS

In this section the control problem is solved by application of linear optimal control theory. Consider the performance criterion

$$J = E\left[\sum_{k=0}^{M}\{[\phi_b(k)-\phi_s(k)]^2+[\theta_b(k)-\theta_s(k)]^2+\gamma[u_\phi^2(k)+u_\theta^2(k)]\}\right] \quad . \tag{38}$$

This performance criterion corresponds to tracking for the purpose of gathering satellite position data. The cost associated with control (where $\gamma \geq 0$) is essential in order to guarantee that u_ϕ and u_θ do not become too large, which, in turn, could cause certain state variables of the antenna control system to exceed their permissibles range of values (*e.g.*, the motor speed and torque are bounded because of physical considerations). However, the actual performance of the satellite tracking system is determined by the first two terms in Eq. (38).

To use the results of linear optimal control theory, it is necessary for the performance criterion J to be quadratic in the system state α. However, this condition is not satisfied, since ϕ_s and θ_s are nonlinear functions of α (or x_e), as shown by Eqs. (A-6) and (A-7). The criterion J can be put into the appropriate form by linearization of $\phi_s(k)$ about the estimate $\hat{\alpha}(k/k)$ [or $\hat{x}_e(k/k)$]. After writing Eqs. (A-6) and (A-7) as Taylor series expansions about $\hat{x}_e(k/k)$ and neglecting second and higher-order terms,

$$\begin{aligned}\phi_s(k) &= \hat{\phi}_s(k/k) + \underline{a}^T(k)\,\tilde{x}_e(k)\\ \theta_s(k) &= \hat{\theta}_s(k/k) + \underline{b}^T(k)\,\tilde{x}_e(k)\end{aligned} \quad , \tag{39}$$

where

$$x_e(k) = \hat{x}_e(k/k) + \tilde{x}_e(k) \tag{40}$$

$$\hat{\phi}_s(k/k) = \phi_s[\hat{x}_e(k/k), k]$$

$$\hat{\theta}_s(k/k) = \theta_s[\hat{x}_e(k/k), k] \quad ,^*$$

$$\underline{a}(k) = \left[\begin{array}{c} -a_1 \\ -a_2 \\ -a_3 \\ 0 \\ 0 \\ 0 \end{array}\right]_{\hat{x}_e(k/k),\,k} \quad , \quad \underline{b}(k) = \left[\begin{array}{c} -b_1 \\ -b_2 \\ -b_3 \\ 0 \\ 0 \\ 0 \end{array}\right]_{\hat{x}_e(k/k),\,k} \quad ,$$

in which the a_i and b_i are given by Eqs. (B-5) and (B-6).

The state of the antenna control system can be defined by the 26-dimensional vector

$$\underline{\alpha} = \left[\begin{array}{c} \hat{\phi}_s \\ \hat{\theta}_s \\ \tilde{x}_e \\ r \end{array}\right] \quad , \tag{41}$$

which contains α (with x_e linearized) and is augmented by $\hat{\phi}_s$ and $\hat{\theta}_s$. The dynamics of $\tilde{x}_e$ and r are given by Eqs. (12) and (25), respectively; there are no dynamics associated with $\hat{\phi}_s$ and $\hat{\theta}_s$. Therefore,

$$\underline{\alpha}(k+1) = \underline{\Phi}(k)\underline{\alpha}(k) + \underline{\Delta}(k)u(k) + \underline{\Gamma}(k)w(k) \quad , \tag{42}$$

---

* It should be noted that because of the nonlinearity of Eqs. (A-6) and (A-7), $\hat{\phi}_s$ and $\hat{\theta}_s$ are not optimal estimates in the usual sense.

where

$$\underline{\Phi}(k) = \begin{bmatrix} \Phi_1(k) & 0 \\ 0 & \Phi_r(k) \end{bmatrix}$$

$$\Phi_1(k) = \begin{bmatrix} I & 0 \\ 0 & \Phi_x(k) \end{bmatrix}, \quad \Phi_x(k) = I + \Im[\hat{x}_e(k/k)]\Delta t$$

$$\underline{\Delta}(k) = \begin{bmatrix} 0 \\ \Delta_r(k) \end{bmatrix}$$

$$\underline{\Gamma}(k) = \begin{bmatrix} \bigcirc & \\ \Gamma_x & 0 \\ 0 & \Gamma_r(k) \end{bmatrix}.$$

Substituting Eq. (39) into Eq. (38) and rewriting J according to the standard formulation gives

$$J = E\left[\sum_{k=0}^{M} \{\underline{\alpha}^T(k)A(k)\underline{\alpha}(k) + u^T(k)B(k)u(k)\}\right], \tag{43}$$

where

$$B(k) = B = \begin{bmatrix} \gamma & 0 \\ & \ddots \\ 0 & \gamma \end{bmatrix}$$

$$A(k) = \begin{bmatrix} A_1(k) & A_3(k) \\ A_3^T(k) & A_2 \end{bmatrix},$$

in which $A_1(k)$ is 8×8; A_2 is 18×18; $A_3(k)$ is 8×18; and $A(k)$ is symmetric and positive semidefinite. After comparing Eq. (38) with Eq. (43), it is a straightforward matter to determine $A(k)$:

$$A_1(k) = \left[\begin{array}{cc|c} & & -\underline{a}^T(k) \\ \multicolumn{2}{c|}{I} & \\ & & -\underline{b}^T(k) \\ \hline -\underline{a}(k) & -\underline{b}(k) & \underline{a}(k)\underline{a}^T(k) + \underline{b}(k)\underline{b}^T(k) \end{array}\right]$$

$$A_3(k) = \left[\begin{array}{c|c|c|c|c} \bigcirc & -1 & & 0 & \\ & 0 & \bigcirc & -1 & \bigcirc \\ (8 \times 4) & -a(k) & (8 \times 8) & -b(k) & (8 \times 4) \end{array}\right]$$

$$A_2 = \left[\begin{array}{cc} 0 & \\ \ddots & \\ 0 & \\ 1 & \bigcirc \\ 0 & \\ \ddots & \\ 0 & \\ 1 & \\ 0 & \\ \ddots & \\ & 0 \end{array}\right]$$

(the 5th and 14th elements on the diagonal of A_2 are equal to one).

The design objective is to find the sequence of controls

$$[u(0),\ u(1),\ \ldots,\ u(M)]$$

that minimize J. The control equations will be derived by applying some results obtained by Larson;[8] this work is an extension of results in linear optimal control theory.[3]

The optimal control $u(k)$ is given by

$$u(k) = -K(k)\underline{\hat{\alpha}}(k/k) \quad , \tag{44}$$

where the gain matrix $K(k)$ is denoted by

$$K(k) = [B + \underline{\Delta}^T(k)P_c(k+1)\underline{\Delta}(k)]^{-1}\underline{\Delta}^T(k)P_c(k+1)\underline{\Phi}(k) \quad , \tag{45}$$

and P_c satisfies the discrete Riccati equation

$$P_c(k) = A(k) + \underline{\Phi}^T(k)P_c(k+1)\underline{\Phi}(k)$$

$$-\underline{\Phi}^T(k)P_c(k+1)\underline{\Delta}(k)[B + \underline{\Delta}^T(k)P_c(k+1)\underline{\Delta}(k)]^{-1}\underline{\Delta}^T(k)P_c(k+1)\underline{\Phi}(k) \quad , \tag{46}$$

$$0 \leq k < M$$

$P_c(M) = A(M)$.

For convenience, $P_c(k)$ will be rewritten in a form entirely analogous to $A(k)$:

$$P_c(k) = \begin{bmatrix} P_1(k) & P_3(k) \\ P_3^T(k) & P_2(k) \end{bmatrix} \quad ,$$

where $P_c(k)$ is symmetric and positive semidefinite.

Upon performance of the indicated matrix multiplications, the optimal control in Eq. (44) becomes

$$u(k) = -[B + \Delta_r^T(k)P_2(k+1)\Delta_r(k)]^{-1}\Delta_r^T(k)P_3^T(k+1)\Phi_1(k)\hat{\underline{x}}(k/k)$$

$$-[B + \Delta_r^T(k)P_2(k+1)\Delta_r(k)]^{-1}\Delta_r^T(k)P_2(k+1)\Phi_r(k)\hat{r}(k/k) \quad , \tag{47}$$

where

$$\hat{\underline{x}}(k/k) = \begin{bmatrix} \hat{\phi}_s(k/k) \\ \hat{\theta}_s(k/k) \\ \hat{\tilde{x}}_c(k/k) \end{bmatrix} \quad . \tag{48}$$

The Riccati equation (46) can be partitioned into separate equations for P_1, P_2, and P_3:

$$P_1(k) = A_1(k) + \Phi_1^T(k)P_1(k+1)\Phi_1(k)$$
$$-\Phi_1^T(k)P_3^T(k+1)\Delta_r(k)[B + \Delta_r^T(k)P_2(k+1)\Delta_r(k)]^{-1}\Delta_r^T(k)P_3(k+1)\Phi_1(k)$$
$$0 \le k < M \qquad (49)$$
$$P_1(M) = A_1(M);$$

$$P_2(k) = A_2 + \Phi_r^T(k)P_2(k+1)\Phi_r(k)$$
$$-\Phi_r^T(k)P_2(k+1)\Delta_r(k)[B + \Delta_r^T(k)P_2(k+1)\Delta_r(k)]^{-1}\Delta_r^T(k)P_2(k+1)\Phi_r(k)$$
$$0 \le k < M \qquad (50)$$
$$P_2(M) = A_2$$

$$P_3(k) = A_3(k) + \Phi_1^T(k)P_3(k+1)\Phi_r(k)$$
$$-\Phi_1^T(k)P_3(k+1)\Delta_r(k)[B + \Delta_r^T(k)P_2(k+1)\Delta_r(k)]^{-1}\Delta_r^T(k)P_2(k+1)\Phi_r(k)$$
$$0 \le k < M \qquad (51)$$
$$P_3(M) = A_3(M).$$

Equation (50) can be solved for P_2 independently of Eqs. (49) and (51). Hence, the dimension of the Riccati equation to be solved has been reduced from 26 × 26 to 18 × 18. It should be noted that Eq. (50) is the Ricatti equation for the antenna control system of Eq. (25) with the performance criterion

$$E\left[\sum_{k=0}^{M}\{r^T(k)A_2r(k) + u^T(k)Bu(k)\}\right].$$

Once P_2 has been found, it is substituted into Eq. (51), which is a linear equation in P_3 (of dimmension 8 × 18) and very easy to solve. Since P_1 does not enter into the control equation (47) or the calculation of P_2 and P_3, it is not necessary to solve Eq. (49).

Thus, the computational requirements have been reduced markedly. Instead of solving Eq. (46) for P_c, it will suffice to solve Eq. (50) for P_2 and calculate P_3 from Eq. (51). The optimal control u is then obtained by substituting $\hat{P}_2$ and P_3 into Eq. (47). Equations (47), (50), and (51), together with α, give the solution to the control problem.

A. STEADY-STATE APPROXIMATION

Suppose that the antenna control system of Eq. (25) is stationary (*i.e.*, the matrices Φ_r, Δ_r, and Γ_r are constant), which is equivalent to assuming that F_θ of Eq. (21) is constant. This assumption is fairly reasonable over a substantial time interval, since the rate of change of F_θ is slow with respect to the control system time constants. Additionally, it will be assumed that the summation in the performance criterion J of Eq. (43) is over an infinite time interval (*i.e.*, $M = \infty$). This assumption is quite reasonable, since the interval of time during which the antenna is tracking the satellite will be appreciably larger than the control system time constants. With these two assumptions, computation of the optimal control $u(k)$ is greatly simplified, as will be shown below. Formulation of the control problem in this manner will be referred to as the "steady-state approximation."

The Riccati equation (50) becomes

$$P_2 = A_2 + \Phi_r^T P_2 \Phi_r - \Phi_r^T P_2 \Delta_r [B + \Delta_r^T P_2 \Delta_r]^{-1} \Delta_r^T P_2 \Phi_r \quad . \tag{52}$$

The above is a nonlinear algebraic equation in the steady-state matrix P_2. In general, Eq. (52) is very difficult to solve. The most straightforward way to obtain P_2 is by the iterative solution of Eq. (50). That is, let $P_2(k+1)$ be some positive definite matrix and then solve Eq. (50) iteratively until it converges to a steady-state solution.

Instead of solving Eq. (51) for P_3, consider the following quantity from the first term of Eq. (47):

$$P_3^T(k+1)\Phi_1(k)\hat{\underline{x}}(k/k) \quad . \tag{53}$$

It will be shown that this approach simplifies the computation of the optimal control $u(k)$. From Eq. (40) it can be seen that

$$\hat{\tilde{x}}_e(k/k) = 0 \quad ;$$

hence, Eq. (48) yields

$$\underline{\hat{x}}(k/k) = \begin{bmatrix} \hat{\psi}_s(k/k) \\ \hat{\theta}_s(k/k) \\ 0 \\ \cdot \\ \cdot \\ \cdot \\ 0 \end{bmatrix} \quad . \tag{54}$$

From Eqs. (42) and (54), it follows that

$$\Phi_1(k)\underline{\hat{x}}(k/k) = \underline{\hat{x}}(k/k) \quad . \tag{55}$$

In effect, the linearization in Eqs. (39) and (40) enables the left-hand side of Eq. (55) to be rewritten as

$$\Phi_1(k)\underline{\hat{x}}(k/k) = \underline{\hat{x}}(k+1/k+1) \quad . \tag{56}$$

Transposing Eq. (51) and multiplying by $\underline{\hat{x}}(k/k)$ yields

$$P_3^T(k)\underline{\hat{x}}(k/k) = A_3^T(k)\underline{\hat{x}}(k/k) + \Phi_r^T P_3^T(k+1)\Phi_1(k)\underline{\hat{x}}(k/k)$$

$$-\Phi_r^T P_2 \Delta_r [B + \Delta_r^T P_2 \Delta_r]^{-1} \Delta_r^T P_3^T(k+1)\Phi_1(k)\underline{\hat{x}}(k/k) \quad . \tag{57}$$

For convenience, define

$$\eta(k) \triangleq P_3^T(k)\underline{\hat{x}}(k/k) \quad . \tag{58}$$

Hence, substitution of Eqs. (56) and (58) into Eq. (57) gives

$$\eta(k) = A_3^T \underline{\hat{x}}(k/k) + \Phi_r^T \eta(k+1)$$

$$-\Phi_r^T P_2 \Lambda_r [B + \Delta_r^T P_2 \Lambda_r]^{-1} \Lambda_r^T \eta(k+1) \quad . \tag{59}$$

From Eqs. (43) and (54), it can be shown that

$$A_3^T(k)\underline{\hat{x}}(k/k) = \begin{bmatrix} 0 \\ \cdot \\ \cdot \\ \cdot \\ 0 \\ -\hat{\phi}_s(k/k) \\ 0 \\ \cdot \\ \cdot \\ \cdot \\ 0 \\ -\hat{\theta}_s(k/k) \\ 0 \\ \cdot \\ \cdot \\ \cdot \\ 0 \end{bmatrix} \tag{60}$$

($-\hat{\phi}_s$ and $-\hat{\theta}_s$ are the 5th and 14th elements, respectively).

From Eqs. (55) and (56), it can be seen that the 18-dimensional vector in Eq. (60) is effectively constant. Therefore, the steady-state solution to Eq. (59) is given by

$$\eta = [I - \Psi]^{-1} A_3^T(k)\underline{\hat{x}}(k/k) \quad , \tag{61}$$

where

$$\Psi = \Phi_r^T - \Phi_r^T P_2 \Delta_r [B + \Delta_r^T P_2 \Delta_r]^{-1} \Delta_r^T \quad . \tag{62}$$

If the state $r(k)$ were known exactly, Ψ^T would correspond to the closed-loop transition matrix of the antenna control system. For a control law that is asymptotically stable, $|\lambda_i(\Psi)| < 1$, where the $\lambda_i(\Psi)$ are the eigenvalues of Ψ. With this condition satisfied it can be demonstrated that the inverse of $[I - \Psi]$ exists.

From Eqs. (56) and (58), it can be seen that the expression in Eq. (53) is equivalent to η; therefore, the optimal control is

$$u(k) = -[B + \Delta_r^T P_2 \Delta_r]^{-1} \Delta_r^T \eta$$

$$-[B + \Delta_r^T P_2 \Delta_r]^{-1} \Delta_r^T P_2 \Phi_r \hat{r}(k/k) \quad . \qquad (63)$$

As the succeeding estimates of the satellite state ($\hat{x}_c$) are computed, $\hat{\phi}_s$ and $\hat{\theta}_s$ will actually change. Thus, Eqs. (60) and (61) show that it is necessary to update η at each discrete time and then substitute it into the first term of Eq. (63). Since $\hat{\phi}_s$ and $\hat{\theta}_s$ (the estimates of the elevation and azimuth angles of the satellite) change slowly with respect to the control system time constants, use of the steady-state solution to compute the optimal control is quite reasonable. In addition, as successive estimates of the antenna control system state ($\hat{r}$) are calculated, they are substituted into the second term of Eq. (63). Equations (52), (61), and (63), together with $\hat{\alpha}$, give the solution to the control problem under the steady-state approximation.

As a further refinement to this approximation, the time-varying nature of F_θ can be taken into account as follows: Update F_θ periodically and recalculate Φ_r, Δ_r, and Γ_r of Eq. (25). With these new matrices, P_2 [the solution to Eq. (52)] and η [the solution to Eq. (61)] are recomputed. Finally, u is obtained from Eq. (63) by substituting these updated matrices. Thus, a nonstationary problem is solved as a series of different, stationary problems. It is not necessary to repeat this procedure at every discrete instant $k\Delta t$, since the rate of change of F_θ is slow with respect to the control system time constants.

The solutions to the control problem can be readily implemented on a digital computer. Although these solutions are suboptimal, the approach used seems quite reasonable. The validity of these results remains to be investigated.

V CONCLUSION

The digital computer program for implementation of the operation of the (approximately) optimal estimator and controller in conjunction with the satellite tracking system has been written and is now functioning properly. The program has been organized so that it will be sufficiently general and flexible enough for the proposed applications.

This program is a valuable study tool for the investigation of several important topics. Primarily, it will provide a way of evaluating existing tracking techniques; *i.e.*, it will be a yardstick for comparing system performance.

An important question relates to the linearizations employed in Secs. III and IV in order to obtain solutions to the estimation and control problems. Since the satellite tracking problem is nonlinear, the solutions obtained in this manner are suboptimal. Although this approach is intuitively reasonable, its validity has not been rigorously established. The extent to which these solutions differ from the optimum will be studied by computer simulations in conjunction with analytical investigations.

APPENDIX A

DETERMINATION OF ϕ_s, θ_s, $\dot{\rho}_s$

APPENDIX A

DETERMINATION OF ϕ_s, θ_s, $\dot{\rho}_s$

The equations of motion of the satellite, as given by Eqs. (1) or (3), are expressed in terms of an earth-centered Cartesian coordinate system. However, the actual operation of the antenna control system is in terms of radar coordinates—elevation, azimuth, and range. In fact, the measurement system [Eq. (27)] observes the elevation and azimuth components of the difference between the angle of the antenna's electrical axis and the satellite angle, in addition to the range rate of the satellite.

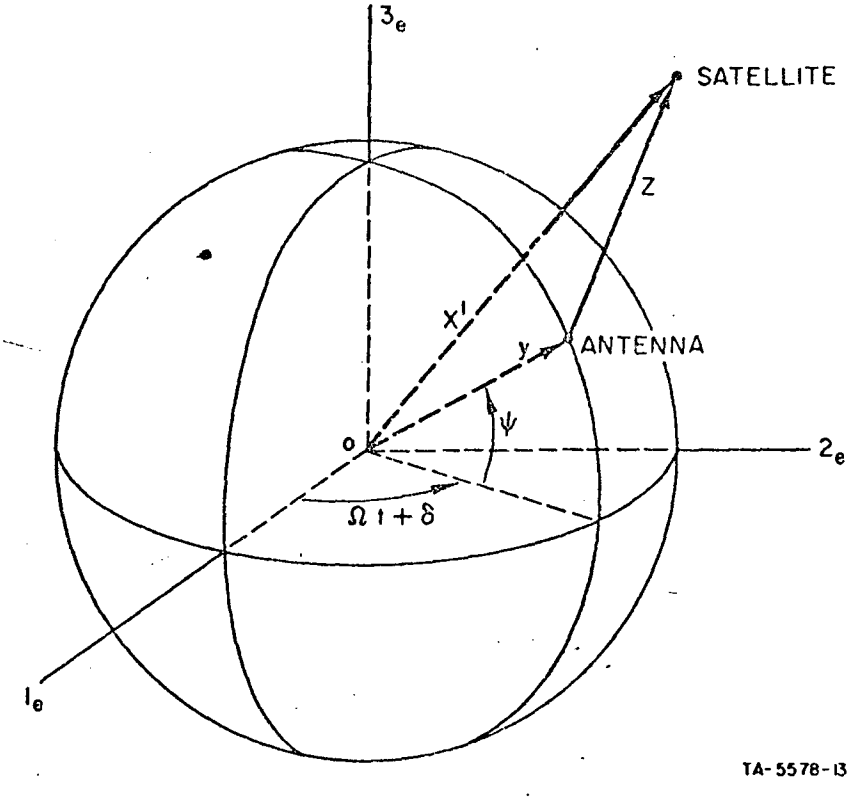

FIG. A-1 GEOMETRY OF THE SATELLITE TRACKING PROBLEM

The geometry of the satellite tracking problem is illustrated in Fig. A-1. The 1_e and 2_e axes, which lie in the equatorial plane of the

earth, and the 3_e axis, which is coincident with the earth's polar axis, comprise an earth-centered Cartesian coordinate system. The position of the antenna is given by the three-dimensional vector

$$y = \begin{bmatrix} y_1 \\ y_2 \\ y_3 \end{bmatrix} .$$

In the 1_e, 2_e, 3_e coordinate system,

$$y_e \begin{cases} y_{1_e} = R_e \cos\psi \cos(\Omega t + \delta) \\ y_{2_e} = R_e \cos\psi \sin(\Omega t + \delta) \\ y_{3_e} = R_e \sin\psi \quad , \end{cases} \tag{A-1}$$

where

R_e = radius of the earth,

Ω = angular rate of rotation of the earth,

δ = an arbitrary angle.

The position of the satellite is given by the three-dimensional vector

$$x' = \begin{bmatrix} x_1 \\ x_2 \\ x_3 \end{bmatrix} .$$

In the 1_e, 2_e, 3_e coordinate system, x_e' consists of the x_{i_e} defined in Eqs. (1). Now, the vector from the antenna to the satellite is denoted by

$$z = x' - y = \begin{bmatrix} z_1 \\ z_2 \\ z_3 \end{bmatrix} . \tag{A 2}$$

Before proceeding any further, it is necessary to define certain terminology that will be used:

* This study considers the relative motion of the antenna with respect to the satellite as the earth rotates on its axis.

Azimuth plane	- plane tangent to the earth at the antenna site; this plane is perpendicular to y
Zero-azimuth line	- perpendicular projection onto the azimuth plane of a great circle passing through the North Pole and the antenna site
Azimuth line	- perpendicular projection of z onto the azimuth plane
Elevation angle ϕ_s	- the angle between the azimuth line and z
Azimuth angle θ_s	- the angle between the zero-azimuth line and the azimuth line.

In the 1_e, 2_e, 3_e coordinate system, Eq. (A-2) yields

$$z_e = x'_e - y_e \quad . \tag{A-3}$$

The expressions for the satellite angles ϕ_s and θ_s can be obtained from Eq. (A-3) by expressing z in terms of the 1_r, 2_r, 3_r coordinate system depicted in Fig. A-2. The 1_r, 2_r, 3_r and the 1_e, 2_e, 3_e coordinate systems are related by the following two rotations (or orthogonal transformations):

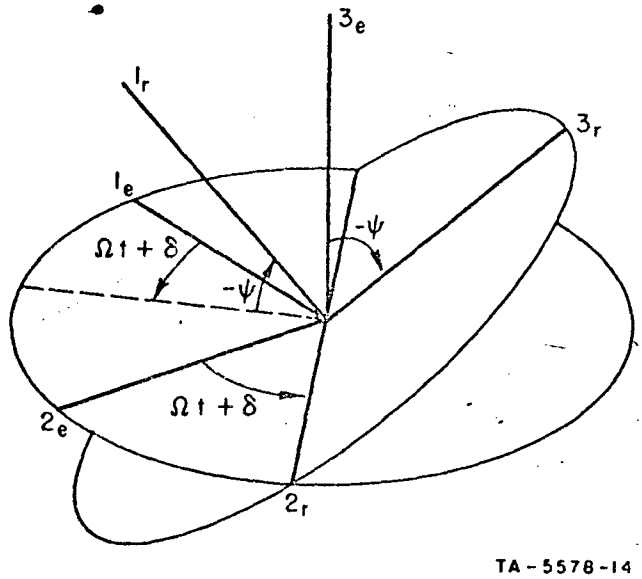

FIG. A-2 RELATION OF THE 1_e, 2_e, 3_e AND 1_r, 2_r, 3_r COORDINATE SYSTEMS VIA THE TRANSFORMATION $R_{r/e}$

(1) rotation about the 3_e axis by the angle $\Omega t + \delta$; (2) rotation about the displaced 2_e axis by the angle $-\psi$. It can be seen that the 1_r axis is perpendicular to the azimuth plane, while the 2_r and 3_r axes lie in the azimuth plane and the 3_r axis is coincident with the zero-azimuth line. The resulting orthogonal transformation can be represented by

$$R_{r/e} = \begin{bmatrix} \cos\psi & 0 & \sin\psi \\ 0 & 1 & 0 \\ -\sin\psi & 0 & \cos\psi \end{bmatrix} \begin{bmatrix} \cos(\Omega t + \delta) & \sin(\Omega t + \delta) & 0 \\ -\sin(\Omega t + \delta) & \cos(\Omega t + \delta) & 0 \\ 0 & 0 & 1 \end{bmatrix}$$

$$= \begin{bmatrix} \cos\psi\cos(\Omega t + \delta) & \cos\psi\sin(\Omega t + \delta) & \sin\psi \\ -\sin(\Omega t + \delta) & \cos(\Omega t + \delta) & 0 \\ -\sin\psi\cos(\Omega t + \delta) & -\sin\psi\sin(\Omega t + \delta) & \cos\psi \end{bmatrix} . \quad (A\text{-}4)$$

Thus, in the 1_r, 2_r, 3_r coordinate system,

$$z_r = R_{r/e} z_e . \quad (A\text{-}5)$$

Inspection of Fig. A-3 enables one to readily determine ϕ_s and θ_s, which are given by

$$\phi_s = \sin^{-1}\left[\frac{z_{1_r}}{|z_r|}\right] , \quad (A\text{-}6)$$

$$\theta_s = \cos^{-1}\left[\frac{z_{3_r}}{\left(z_{2_r}^2 + z_{3_r}^2\right)^{1/2}}\right] , \quad (A\text{-}7)$$

where

$$|z_r| = |z_e| = \left[\sum_{i=1}^{3}\left(x_{i_e} - y_{i_e}\right)^2\right]^{1/2} * .$$

Finally, ϕ_s and θ_s can be expressed in terms of the x_{i_e} and y_{i_e} by substituting from Eqs. (A-5) and (A-3). The x_{i_e} are contained in the state vector α of Eq. (26) [see Eqs. (2)], and the y_{i_e} are known time-varying

* It should be noted that the magnitude of a vector is independent of the coordinate system.

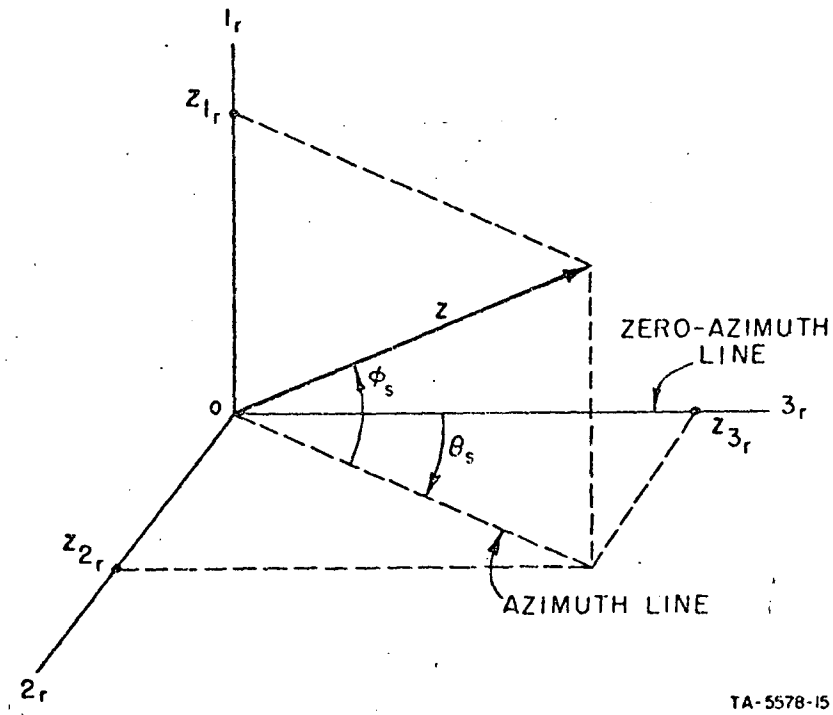

FIG. A-3 DETERMINATION OF ϕ_s AND θ_s

functions [see Eqs. (A-1)]. Hence, the satellite elevation and azimuth angles are time-varying, nonlinear functions—$\phi_s[\alpha(k),k]$ and $\theta_s[\alpha(k),k]$.

The range ρ_s, the distance from the antenna to the satellite, is given by

$$\rho_s = |z_e| \quad . \tag{A-8}$$

From Eqs. (A-8) and (A-3),

$$\dot{\rho}_s = \frac{\sum_{i=1}^{3} \left(x_{i_e} - y_{i_e}\right)\left(\dot{x}_{i_e} - \dot{y}_{i_e}\right)}{\left[\sum_{i=1}^{3} \left(x_{i_e} - y_{i_e}\right)^2\right]^{1/2}} \tag{A-9}$$

The x_{i_e} and $\dot{x}_{i_e}$ are contained in α of Eq. (26) [see Eqs. (2)], and the y_{i_e} and $\dot{y}_{i_e}$ are known time-varying functions [the $\dot{y}_{i_e}$ are readily obtained from Eqs. (A-1)]. Thus, the satellite range rate is a time-varying, nonlinear function—$\dot{\rho}_s[\alpha(k),k]$.

APPENDIX B

CALCULATION OF THE a_i, b_i, c_i, d_i

APPENDIX B

CALCULATION OF THE a_i, b_i, c_i, d_i

The matrices $H(k)$ of Eq. (31) and $\underline{a}(k)$ and $\underline{b}(k)$ of Eqs. (39) contain the partial derivatives of ϕ_s, θ_s, and $\dot{\rho}_s$ with respect to the elements of α [or x_e—see Eqs. (2) and (4)]; *i.e.*,

$$-a_i = \frac{\partial \phi_s}{\partial x_{i_e}} = \frac{\partial \phi_s}{\partial \alpha_i} \tag{B-1}$$

$$-b_i = \frac{\partial \theta_s}{\partial x_{i_e}} = \frac{\partial \theta_s}{\partial \alpha_i} \tag{B-2}$$

$$c_i = \frac{\partial \dot{\rho}_s}{\partial x_{i_e}} = \frac{\partial \dot{\rho}_s}{\partial \alpha_i} \tag{B-3}$$

$$d_i = \frac{\partial \dot{\rho}_s}{\partial \dot{x}_{i_e}} = \frac{\partial \dot{\rho}_s}{\partial \alpha_{3+i}} , \tag{B-4}$$

for $i = 1, 2, 3$.

Applying the chain rule for differentiation to Eqs. (A-5), (A-6), and (A-7), one can express the terms in Eqs. (B-1) and (B-2) in the compact form:

$$\begin{bmatrix} -a_1 \\ -a_2 \\ -a_3 \end{bmatrix} = R_{r/e}^T \begin{bmatrix} \partial \phi_s / \partial z_{1_r} \\ \partial \phi_s / \partial z_{2_r} \\ \partial \phi_s / \partial z_{3_r} \end{bmatrix} , \tag{B-5}$$

where

$$\frac{\partial \phi_s}{\partial z_{1_r}} = \frac{\left(z_{2_r}^2 + z_{3_r}^2\right)^{1/2}}{|z_r|^2}$$

$$\frac{\partial \phi_s}{\partial z_{2_r}} = \frac{-z_{1_r} z_{2_r}}{\left(z_{2_r}^2 + z_{3_r}^2\right)^{1/2} |z_r|^2}$$

$$\frac{\partial \phi_s}{\partial z_{3_r}} = \frac{-z_{1_r} z_{3_r}}{\left(z_{2_r}^2 + z_{3_r}^2\right)^{1/2} |z_r|^2} \quad ;$$

and

$$\begin{bmatrix} -b_1 \\ -b_2 \\ -b_3 \end{bmatrix} = R_{r/e}^T \begin{bmatrix} \partial\theta_s/\partial z_{1_r} \\ \partial\theta_s/\partial z_{2_r} \\ \partial\theta_s/\partial z_{3_r} \end{bmatrix} , \qquad \text{(B-6)}$$

where

$$\frac{\partial \theta_s}{\partial z_{1_r}} = 0$$

$$\frac{\partial \theta_s}{\partial z_{2_r}} = \frac{z_{3_r}}{z_{2_r}^2 + z_{3_r}^2}$$

$$\frac{\partial \theta_s}{\partial z_{3_r}} = \frac{-z_{2_r}}{z_{2_r}^2 + z_{3_r}^2}$$

The above results make use of the fact that

$$\frac{\partial z_{i_e}}{\partial x_{j_e}} = \begin{cases} 1 & , \quad \text{for } i = j \\ 0 & , \quad \text{for } i \neq j \end{cases}$$

and that the element in the i^{th} row and j^{th} column of $R^T_{r/e}$ corresponds to $\partial z_{j_r}/\partial z_{i_e}$. Finally, the $\partial \phi_s/\partial z_{j_r}$ and $\partial \theta_s/\partial z_{j_r}$ can be expressed in terms of the x_{i_e} and y_{i_e} by substitution from Eqs. (A-5) and (A-3).

From Eq. (A-11), it is a straightforward matter to show that the terms in Eqs. (B-3) and (B-4) are given by

$$c_i = \frac{\left(\dot{x}_{i_e} - \dot{y}_{i_e}\right) \sum_{l \neq i} \left(x_{l_e} - y_{l_e}\right)^2}{\left[\sum_{j=1}^{3} \left(x_{j_e} - y_{j_e}\right)^2\right]^{3/2}} \tag{B-7}$$

$$d_i = \frac{x_{i_e} - y_{i_e}}{\left[\sum_{j=1}^{3} \left(x_{j_e} - y_{j_e}\right)^2\right]^{1/2}} \tag{B-8}$$

REFERENCES

1. E. C. Fraser, "Application of Adaptive Filtering to Satellite Tracking and Attitude Control," Memorandum 1, SRI Project 5578, Contract NAS 12-59, Stanford Research Institute, Menlo Park, California (22 October 1965).

2. E. C. Fraser, "Evaluation of Modern Estimation and Control Techniques as Applied to Satellite Tracking and Attitude Stabilization," Memorandum 2, SRI Project 5578, Contract NAS 12-59, Stanford Research Institute, Menlo Park, California (26 November 1965).

3. L. Meier, "Combined Optimum Control and Estimation Theory," Contractor Report, SRI Project 5237, Contract NAS 2-2457, Stanford Research Institute, Menlo Park, California (October 1965).

4. G. C. Newton, L. A. Gould, and J. F. Kaiser, *Analytical Design of Linear Feedback Controls* (John Wiley & Sons, Inc., New York, New York, 1957).

5. R. E. Kalman, "A New Approach to Linear Filtering and Prediction Problems," *Trans. ASME, J. Basic Engineering*, pp. 35-45 (March 1960).

6. L. Meier, "Adaptive Control and the Combined Optimization Problem," Memorandum 6, SRI Project 5578, Contract NAS 12-59, Stanford Research Institute, Menlo Park, California (10 February 1966).

7. J. Peschon and R. E. Larson, "Analysis of an Intercept System," Final Report, Contract DA-01-021-AMC-90006(Y), SRI Project 5188-7, Stanford Research Institute, Menlo Park, California (December 1965).

8. R. E. Larson, R. M. Dressler, and J. Peschon, "Research on Adaptive Control System Design," Quarterly Report 3, SRI Project 5578, Contract NAS 12-59, Stanford Research Institute, Menlo Park, California (to appear April 1966).

APPENDIX A
A SUMMARY OF SOME RESULTS FROM LINEAR OPTIMAL ESTIMATION THEORY

The optimal estimation algorithm has been worked out, in particular, for systems whose dynamics may be expressed by a set of linear difference equations of the following form:[1-5]

$$\underline{x}_k = \Phi(k,k-1)\ \underline{x}_{k-1} + \underline{w}_{k-1} \tag{A-1}$$

where

$\underline{x}_k$ = n-dimensional state vector at the discrete time instant $t = t_k$

$\underline{w}_k$ = n-dimensional random noise vector at $t = t_k$

$\Phi(k,k-1)$ = nxn state transition matrix

Usually, most of the states of the system are not directly measurable. The set of physical entities that are directly measurable, constitute the so called measurement vector $\underline{\beta}$. In some particular cases, several components of $\underline{\beta}$ may be identical with the corresponding state variables.

It will be assumed that the measurement vector may be expressed as a linear function of the state vector:

$$\underline{\beta}_k = H(k)\ \underline{x}_k + \underline{v}_k \tag{A-2}$$

where

$\underline{\beta}_k$ = m-dimensional measurement vector at $t = t_k$

$\underline{v}_k$ = m-dimensional measurement noise vector at $t = t_k$

$H(k)$ = mxn measurement matrix at $t = t_k$

It will be further assumed that both $\underline{w}_k$ and $\underline{v}_k$ are uncorrelated white noise sequences and:

$$\text{The mean } E[\underline{w}_k] = E[\underline{v}_k] = \underline{0} \quad \text{for all } k \tag{A-3}$$

$$\text{The covariance matrices } E[\underline{w}_k \underline{w}_k^T] = Q_k \delta_{kj} \text{ for all } k \tag{A-4}$$

$$E[\underline{v}_k \underline{v}_k^T] = R_k \delta_{kj} \quad \text{for all } k \tag{A-5}$$

where δ_{kj} is the Kronecker delta

Q_k and R_k are non-negative definite (nxn) and (mxm) matrices respectively.

The initial state $\underline{x}(o)$ is assumed to be a random variable with the following statistics:

$$E[\underline{x}(o)] = \underline{0} \tag{A-6}$$

$$E[\underline{x}(o)\ \underline{x}^T(o)] = P_o \tag{A-6}$$

where

P_o is an nxn matrix.

Further, it is assumed that $\underline{x}(o)$ and $\underline{w}_k$ and $\underline{v}_k$ are uncorrelated for all k.

The optimal estimation problem consists of establishing an estimate of $\underline{x}_k$ at $\underline{t} = t_k$, denoted by $\hat{\underline{x}}_k$, based on the previous estimate $\underline{x}_{k-1}$ and on the present measurement $\underline{\beta}_k$, so that the error is minimized, i.e.,

$$\text{Minimize } J = E[(\hat{\underline{x}}_k - \underline{x}_k)^T(\hat{\underline{x}}_k - \underline{x}_k)] \qquad \text{(A-8)}$$

The optimal solution to this problem is the following:[2-5]

The optimal state estimate at $t = t_k$ is given by:

$$\hat{\underline{x}}_k = \Phi(k,k-1)\ \hat{\underline{x}}_{k-1} + K_k\ [\underline{\beta}_k - H(k)\ \Phi(k,k-1)\hat{\underline{x}}_{k-1}] \qquad \text{(A-9)}$$

where K_k is the so called weighting or gain matrix (of dimension nxm in this case), and is given by the relation:

$$K_k = P_k'\ H^T(k)\ [H(k)\ P_k'\ H^T(k) + R_k]^{-1} \qquad \text{(A-10)}$$

where P_k is the covariance matrix (nxn) at time $t = t_k$:

$$P_k = E[(\hat{\underline{x}}_k - \underline{x}_k)\ (\hat{\underline{x}}_k - \underline{x}_k)^T] \tag{A-11}$$

and

$$P'_k = \Phi(k,k-1)\ P_{k-1}\ \Phi^T(k,k-1) + Q_{k-1} \tag{A-12}$$

The covariance matrix, P_k satisfies the matrix Riccati equation:

$$P_k = P'_k - K_k\ H(k)\ P'_k - P'_k\ H^T(k)\ K_k^T$$

$$+K_k[H(k)P'_kH^T(k) + R_k]K_k^T \tag{A-13}$$

It can be shown[4], that P_k reduces to:

$$P_k = P'_k - K_k\ H(k)\ P'_k \tag{A-14}$$

Equations (A-9), (A-10), (A-12) and (A-14) constitute the Kalman filter for the system described by the mathematical model of Eqs. (A-1) and (A-2).

L. Meier proposed an extension of Kalman's method to nonlinear system, using a linearization procedure[1,6]. This so-called "Extended Kalman Filter" will be described next. The system under consideration is described now, by the following set of nonlinear difference equations:

$$\underline{x}_{k+1} = \underline{f}(\underline{x}_k, \underline{u}_k, k) + \underline{w}_k \qquad \text{(A-14)}$$

$\underline{u}_k$ is a r-dimensional control vector. Other variables are the same as in Eq. (A-1). The measurement equation is also described by the following nonlinear set of equations:

$$\underline{\beta}_{k+1} = \underline{h}(\underline{x}_{k+1}, k+1) + \underline{v}_{k+1} \qquad \text{(A-15)}$$

Equations (A-14) and (A-15) are linearized using a first order approximation around $\hat{\underline{x}}_k$ and $\hat{\underline{x}}_{k+1}$ respectively.

$$\underline{x}_{k+1} = \underline{f}(\hat{\underline{x}}_k, \underline{u}_k, k) + f_x(\hat{\underline{x}}_k \underline{u}_k, k)\ (\underline{x}_k - \hat{\underline{x}}_k) + \underline{w}_k \qquad \text{(A-16)}$$

$$\underline{\beta}_{k+1} = \underline{h}(\hat{\underline{x}}_{k+1}, k+1) + h_x(\hat{\underline{x}}_{k+1}, k+1)\ (\underline{x}_{k+1} - \hat{x}_{k+1}) + \underline{v}_{k+1} \qquad \text{(A-17)}$$

where:

$$f_x^{ij} \equiv \frac{\partial f_i}{\partial x_j} \quad \text{a (nxn) matrix} \qquad \text{(A-18)}$$

$$h_x^{ij} \equiv \frac{\partial h_i}{\partial x_j} \quad \text{a (mxn) matrix} \qquad \text{(a-19)}$$

Introducing

$$\tilde{\underline{x}}_{k+1} = \underline{x}_{k+1} - \underline{f}(\hat{\underline{x}}_k, \underline{u}_k, k) = \underline{x}_{k+1} - \hat{\underline{x}}_{k+1} \tag{A-20}$$

$$\tilde{\underline{x}}_k = \underline{x}_k - \hat{\underline{x}}_k \tag{A-21}$$

Equation (A-16) now becomes:

$$\tilde{\underline{x}}_{k+1} = f_x(\hat{\underline{x}}_k, \underline{u}_k, k)\ \tilde{x}_k + \underline{w}_k \tag{A-22}$$

As one may see, Eq. (A-22) is of the same form as Eq. (A-1), where the matrix f_x has replaced the state transition matrix $\Phi(k+1, k)$, and $\tilde{\underline{x}}_{k+1}$, $\tilde{\underline{x}}_k$ have replaced $\underline{x}_{k+1}$, $\underline{x}_k$ respectively.

In a similar manner one may introduce:

$$\tilde{\underline{\beta}}_{k+1} = \underline{\beta}_{k+1} - \underline{h}(\hat{\underline{x}}_{k+1}, k+1) \tag{A-33}$$

and the measurement equation (A-17) will take the form:

$$\tilde{\underline{\beta}}_{k+1} = h_x(\hat{\underline{x}}_{k+1}, k+1)\ \tilde{\underline{x}}_{k+1} + \underline{v}_{k+1} \tag{A-24}$$

This is a linear set of equations completely analogous to Eq. (A-2), where the matrix h_x replaces matrix $H(k+1)$, and the vectors $\tilde{\beta}_{k+1}$, $\tilde{\underline{x}}_{k+1}$ replace $\underline{\beta}_{k+1}$ and $\underline{x}_{k+1}$ respectively.

The Extended Kalman Filter may now be formulated as follows, based on Eqs. (A-9), (A-10), (A-12), (A-14), (A-22), (A-24):

$$\hat{\underline{x}}_k = \underline{f}(\hat{\underline{x}}_{k-1}, \underline{u}_{k-1}, k-1) + K_k[\tilde{\underline{\beta}}_k - h\ (\hat{\underline{x}}_k,\ k)] \tag{A-25}$$

$$K_k = P'_k\ h_x^T(\hat{\underline{x}}_k,\ k)\ [h_x(\hat{\underline{x}}_k, k)\ P'_k\ h_x^T\ (\hat{\underline{x}}_k,\ k) + R_k]^{-1} \tag{A-26}$$

$$P'_k = f_x(\hat{\underline{x}}_{k-1}, \underline{u}_{k-1},\ k-1)\ P_{k-1}\ f_x^T(\hat{\underline{x}}_{k-1}, \underline{u}_{k-1},\ k-1) + Q_{k-1} \tag{A-27}$$

$$P_k = P'_k - K_k\ h_x(\hat{\underline{x}}_k, k)\ P'_k \tag{A-28}$$

REFERENCES

1. J. Peschon, R.M. Dressler, L. Meier, R.E. Larson, E.C. Fraser, O.J. Tveit, "Research on the Design of Adaptive Control Systems," Final Report, Vol. 2, Stanford Research Institute, Menlo Park, California, September 1966.

2. R.E. Kalman, "A New Approach to Linear Filtering and Prediction Problems," J. Basic Eng., 82D, pp. 35-45, 1960.

3. R.E. Kalman, R.S. Bucy, "New Results in Linear Filtering and Prediction Theory," J. Basic Eng., 83D, pp. 95-108, 1961.

4. H.W. Sorenson, "Kalman Filtering Techniques," Advances in Control Systems, edited by C.T. Leondes, Vol. 3, pp. 219-292, Academic Press, New York, 1966.

5. R.S. Bucy, P.D. Joseph, "Filtering for Stochastic Processes with Applications to Guidance," Interscience, New York, 1968.

6. L. Meier, "Combined Optimum Control and Estimation Theory," Stanford Research Institute Report, Menlo Park, California, October 1965.

APPENDIX B
A SUMMARY OF PERTINENT RESULTS FROM LINEAR OPTIMAL CONTROL THEORY

The optimal control techniques applied in the programs ORBRAC, ATRK30 and RATS are described in detail in previous publications[1,2].

The performance criterion adopted in these programs is the minimization of the pointing error, or rather the sum of squares of the pointing errors at the sampling times. In addition, a weighted energy term (square of the control signal) is added to the performance index at each sampling time. Basically one has a Minimum-Error, Minimum-Energy optimal control problem. The performance index is expressed as:

$$\text{Minimize} \quad J = \sum_{i=1}^{N} \Big\{ [X(i) - X_t(i)]^2 + [Y(i) - Y_t(i)]^2 + w_X u_X^2(i) + w_Y u_Y^2(i) \Big\} \qquad \text{(B-1)}$$

where

$X(i)$ = antenna X angle at the sampling time $t = t_i$.

$X_t(i)$ = the true, or predicted X angle

$Y(i)$ = antenna Y angle

$Y_t(i)$ = the true, or predicted Y angle

w_X = weighting factor for the X-channel

w_Y = weighting factor for the Y-channel

u_X = control signal on the X-channel

u_Y = control signal on the Y-channel

The state equations are linearized, so one has the classical problem of optimal control of a linear system with a quadratic performance criterion. The solution to this type of problem is well known and was documented in numerous publications. A good tutorial exposition on the subject may be found in References [3,4], to mention only a few.

After applying the basic Maximum Principle techniques, the optimal control vector is given by:

$$\underset{\sim}{u}(i) = -K(i)\ \hat{\underset{\sim}{x}}\ (i/i) \qquad \text{(B-2)}$$

where

$\hat{\underset{\sim}{x}}(i/i)$ = estimated state vector at $t = t_i$ based on previous estimates up to $t = t_i$ (of Appendix A);

$K(i)$ = gain matrix at $t = t_i$.

The gain matrix is a function of the P_c matrix which is a solution of a matrix Riccati equation. The details concerning the solution of the Riccati equation in these programs are found in References [1,2].

REFERENCES

1. J. Peschon, et. al., "Research on the Design of Adaptive Control Systems," Final Report, Vol. 2, Stanford Research Institute, Menlo Park, California, September 1966.

2. R.M. Dressler, E.C. Fraser, "Optical Communication and Tracking Systems," Final Report, Stanford Research Institute, Menlo Park, California, October 1967.

3. M. Athans, P.L. Falb, "Optimal Control," McGraw Hill, New York, 1966.

4. A.P. Sage, "Optimum Systems Control," Prentice Hall, Englewood Cliffs, New Jersey, 1968.

APPENDIX C
RATS Program Documentation

INPUT (Program RATS)

Input to program RATS is supplied by six NAMELIST data statements in the following sequence:

/PLOTS/	NOPTS
/TYMSTA/	DTC, DT, PSI, DELTA, ST
/STATE1/	XO, AE, RP
/NOISCV/	R, QV
/STCOV/	PK
/SCALE/	VM, EM
/DYNMIC/	FP, DPHI

A full description of the NAMELISTs follows.

NAMELIST	ITEM	DESCRIPTION
/PLOTS/	NOTPS	Number of time points to be
/TYMSTA/	DTC	Time-interval in seconds fo gration of satellite motion tions occurring at times be two successive values of DTC are obtained by straight lin polation.
	DT	Data sampling interval in se
	PSI	Latitude of tracking antenna degrees.
	DELTA	Right ascension of antenna at start of tracking interval in degrees.
	ST	End time of tracking interval seconds.
/STATE1/	XO(1)	X-Coordinate of Satellite*
	XO(2)	Y-Coordinate of Satellite
	XO(3)	Z-Coordinate of Satellite
	XO(4)	$\dot{X}$-Coordinate of Satellite
	XO(5)	$\dot{Y}$-Coordinate of Satellite
	XO(6)	$\dot{Z}$-Coordinate of Satellite
	AE(1-6)	Estimated initial values of XO(1-6)
	AE(7-12)	Estimated initial values of ~~elevation~~ Yaxis n channel state.
	AE(13-18)	Estimated initial values of ~~azimuth~~ X-axis channel state.
	RP(1-6)	True values of initial ~~elevation~~ Y-axis channel state.
	RP(7-12)	True values of initial ~~azimuth~~ X-axis channel state.

*Values at start of tracking interval, t=0.

NAMELIST	ITEM	DESCRIPTION
/NOISCV/	R (11,11)	Covariance matrix of system measurement noise, $E[v,v^T]$.
	QV (5,5)	Covariance of system disturbance vector, $E[w,w^T]$.
/STCOV/	PK (18,18)	Covariance of initial system estimate $E[\alpha,\alpha^t]$ ie $E[AE,AE^t]$.
/SCALE/	VM (11)	Weighting vector for measurement noise.
	EM	Scaling factor for R, QV, VM Nominal value=1.
/DYNAMIC/	FP (12,12)	Matrix representation of system dynamic function.
	DPHI (12)	Coefficients of control input.

RATS PROGRAM
SUBROUTINES DESCRIPTION

Name	Function
RATS	Read plot control.
BLOCKDATA	Preset common block variables.
TRAK1	Read items from namelists: TYMSTA, STATE1, NOISCV, STCOV, and SCALE. Write initial conditions and system constants.
FPHI	Read items from namelist DYNMIC. Compute ϕ_o, Δ_θ, Γ_θ, Eq. (24)* , Γ, Eq. (33)
TRAK2	Calculate control as in Eq.*(63). Form plot if all points finished. Calculate $\hat{\alpha}(k/k-1)$ as in Eq.*(32).
TRAK3	Calculate the coefficient of $\hat{\gamma}(k/k)$ in Eq.(63); and write as feedback coefficients.
TZERO	Calculate $\hat{\phi}_s$, $\hat{\theta}_s$ Eq.(41)
AGBT	Calculate $\beta(k)$ Eq.(27)
PFEEH	Calculate ϕ_s, θ_s (Eq.(41)

* The equation numbers correspond to these of reference [3], referred to in chapter 3.

SUBROUTINES DESCRIPTION (cont.)

Name	Function
PXAGBH	Calculate predicted satellite data, using Eq.(32). Find ϕ_s, θ_s and calculate $\hat{\beta}(k/k-1)$ Eq.(34).
PKKM	Calculate $P(k/k-1)$ Eq.(33)
HMAT	Calculate H(k) Eq.(31). (Note: For system in actual program the form of H used may differ from Eq. (31).)
WATE	Calculate W(k), Eq.(36).
POSITN	Integrate equations of motion to update satellite position-velocity.
PCNTRL	Find steady state solution of the Riccati equation in Eq.(52).
ECNTRL	Calculate coefficient of $\hat{x}(k/k)$ in Eq.(61).
BARN	Random number function.
DNVERT	Matrix inversion routine.
ITRVRS	Iterative matrix invertion.

RATS PROGRAM
Program Variables

Variable		Units	Description
Program	Report		
A2	$\phi^T P_2 \Delta$		
	$[B+\Delta^T PA]\Delta^T$		See #59, #62
AS	$[B+\Delta^T P_2 \Delta]^{-1}$		See #52
AE	$\hat{\alpha}(k/k)$		Estimated system state #35
ANGOUT		Deg.	Output arrary for angles and t... errors
AP	$\hat{x}(k/k-1)$		Predicted satellite state #32
BETA	$\beta(R)$		Measurement vector #27
BETAH	$\hat{\beta}(k/k-1)$		Predicted measurement vector #3...
CNT			Horizontal counter for plot rou...
CP	$\cos\psi$		cos of station latitude (App...
C2	$\cos(\Omega t+\delta)$		cos of station right asce... (Appendix A)
DELTA	δ	Radians	Initial value of rig... a... station

Variable		Units	Description
Program	Report		
DLC	$-\Delta[\Delta P_2 \Delta^T + B]^{-1}\Delta$		See #62, 63
DLP	$\Delta_r(k-1)$		Antenna system control variable constraints #24, #32
DPHI	D_ϕ		Control constraints for continuous case #17
DT	Δt	SEC	Sampling interval
DTC		SEC	Time interval over which satellite position-velocity is to be found by linear interpolation
ETA	Col. 1 of $[I-\psi]^{-1}A_3^T(k)$		Corresponds to constant portion, for Y-channel, of η #61, multiplication by $\hat{\phi}$ occurs in TRAK2
ETA1	Col. 1 of $[I-\psi]^{-1}A_3^T(R)$		Corresponds to constant portion, for X-channel, of η #61.
ETN			In routine TRAK2; $P_2\Phi_Y\hat{Y}-\eta_Y$ #63, for Y angle channel.
ETN1			In routine TRAK2; $P_2\Phi_X\hat{X}-\eta_X$, #63, for X angle channel.
FP	F_ϕ		State transition matrix for continuous antenna system, #17 assumed identical for each channel.

Variable		Units	Description
Program	Report		
G	$\Gamma(k-1)$		Complete constraint matrix for system, #33
GAMP	$\Gamma_r(k-1)$		Antenna system noise constraints #19, #25
GAMSUB	$\Gamma(k-1)Q(k-1)\Gamma^T(k-1)$		Contribution to $\Gamma(k/k-1)$ from system noise covariance, Q, #33
GS	$\Gamma.Q$		Dot product $\Gamma.Q$ #33
H	$H(k)$		Matrix of partials of β with respect to $\hat{X}$ #31, #34
HE		SEC	Integration step size for orbital motion
KPASS			Program branch control must be presc to 0 for first pass
LI			Unit number for input normally = 5
LO			Unit number for output normally = 6
Omega	Ω	Rad/Sec	Rotational velocity of the earth
P2			Temporary storage in calculations Φ_r from F_r #19
PC	P_2		Steady state solution to Riccati equation #52.

Variable		Units	Description
rogram	Report		
N	P_2		Temporary storage for P_2
HI	$\phi_s(k)$	Rad	True elevation angle (in this system Y angle) #27
HERR		Deg.	Error in Φ(Y) for plot routine
HH	$\phi_s(k)$	Rad	Estimated elevation angle (Y)
HP	$\hat{\phi}_s(k/k-1)$	Rad	Predicted elevation angle (Y) #34
	$P(k,k)$		Covariance matrix of error in estimate #37
M	$P(k/k-1)$		Covariance matrix of error in prediction
	$\Phi_r(k-1)$		Antenna system state discrete transition matrix. Assumed constant and identical for both channels, #19
	ψ	Radians	Latitude of station
	u		Control variable for Y-angle channel
			Control variable for X-angle channel
	Φ (k-1)		Linearized state transition matrix, #33
			Temporary storage no longer used

Variable		Units	Description
Program	Report		
QV	Q(k)		Covariance of system noise. See page 16 and #33.
R	R(k)		Covariance of measurement noise See page 14 and #35, 37.
RCP		Meters	re*cosψ
RE	re	Meters	Radius of the earth
RP	r(k-1)		True antenna system state #25
RP1	r(k)		True antenna system state #25
SA	b_1, b_2, b_3		$-\frac{\partial Y}{\partial \alpha_i}$ #31
SB	a_1, a_2, a_3		$-\frac{\partial X}{\partial \alpha_i}$ #31
SL	SIN ($\Omega t+\delta$)		SIN of station right ascension (Appendix A)
SP	SINψ		SIN of station latitude Appendix A)
ST		SEC	Time after epoch of last desired data point
T			Temporary variable used in calculation X,Y angles
THE	$\Phi_S(R)$		True azimuth angle (X angle) #27

Variable		Units	Description
Program	Report		
THEERP		Deg.	Error in θ (X) for plot routine
THEH	$\hat{\phi}_s(k)$		Estimated azimuth angle (X-angle)
THEP	$\hat{\phi}_s(k-1)$		Predicted azimuth angle (X angle)#34
TIME		SEC	Current sample time
TYME		SEC	Interpolation time
UC	Γ		Variance of control variable page 22, #43
UCN	$P_2\Phi_Y$		Y angle channel #63
UCN1	$P_2\Phi_X$		X angle channel #63
UE	ue	km^3/sec^2	Gravitational constant
V	V(k)		Measurement noise, #27
VM	W(k)		Scale factor for measurement noise before use V(k) = V(k)*VM
WTK	W(k)		Weight matrix #36
X	x	Meters	Actual position vector of satellite (Appendix A)
XN		Meters	Satellite state at end of interpolation period

Variable		Units	Description
Program	Report		
XO		Meters	Satellite state at beginning of interpolation period
Y	y	Meters	Position vector of station (Appendix A)
Z	z	Meters	x-y
ZA	$\|Z_r\|$	Meters	True range of satellite
ZAP		Meters	Predicted range of satellite
ZE		Meters	Difference between estimated satellite position and station position vector
ZP		Meters	Topocentric coordinates of true position of satellite
ZR	Z_Y	Meters	Topocentric coordinates of true position of satellite
ZRP		Meters	Topocentric coordinates of predicted position of satellite

APPENDIX D

DIRECTION ANGLES

The direction angles used in this study will be defined with respect to the coordinates system in figure D.1. The Elevation (EL) and Azimuth (AZ) angles as well as the X, Y angles for a 30 ft. antenna, are defined in figure D.1. (a). The same X, Y convention is also used in the 40 ft. antenna.

If the satellite coordinates are (x', y', z'), the angles are:

$$AZ = tg^{-1}\left(\frac{x'}{y'}\right) \tag{D.1}$$

$$EL = tg^{-1}\left(\frac{z'}{\sqrt{\rho^2 - z'^2}}\right) = tg^{-1}\left(\frac{z'}{\sqrt{x'^2+y'^2}}\right) \tag{D.2}$$

where

$$\rho^2 = x'^2+y'^2+z'^2$$

$$X_{30} = tg^{-1}\left(\frac{x'}{z'}\right). \tag{D.3}$$

$$Y_{30} = tg^{-1}\left(\frac{y'}{\sqrt{\rho^2 - y'^2}}\right) = tg^{-1}\left(\frac{y'}{\sqrt{x'^2 + z'^2}}\right) \qquad (D.4)$$

The relationships between them are, [1]:

$$\sin Y_{30} = \cos EL \cos AZ \qquad (D.5)$$

$$tg\ X_{30} = \cot EL \sin AZ \qquad (D.6)$$

$$\sin EL = \cos Y_{30} \cos X_{30} \qquad (D.7)$$

$$tgAZ = \cot Y_{30} \sin X_{30} \qquad (D.8)$$

The X, Y angles for the 85 ft. antenna are defined in figure D.1 (b). The corresponding relationships are:

$$X_{85} = tg^{-1}\left(-\frac{y'}{z'}\right) \qquad (D.9)$$

$$Y_{85} = tg^{-1}\left(\frac{x'}{\sqrt{\rho^2 - x'^2}}\right)$$

$$= tg^{-1}\left(\frac{x'}{\sqrt{y'^2 + z'^2}}\right) \qquad (D.10)$$

$$\sin Y_{85} = \cos EL \sin AZ \tag{D.11}$$

$$\text{tg } X_{85} = -\cot EL \cos AZ \tag{D.12}$$

$$\sin EL = \cos Y_{85} \cos X_{85} \tag{D.13}$$

$$\text{tg } AZ = -\text{tg } Y_{85} / \sin X_{85} \tag{D.14}$$

REFERENCES

1. I.M. Salzberg, "Mathematical Relationships of the MFOD Antenna Axes," NASA Report, X-553-67-213, GSFC, May 1967.

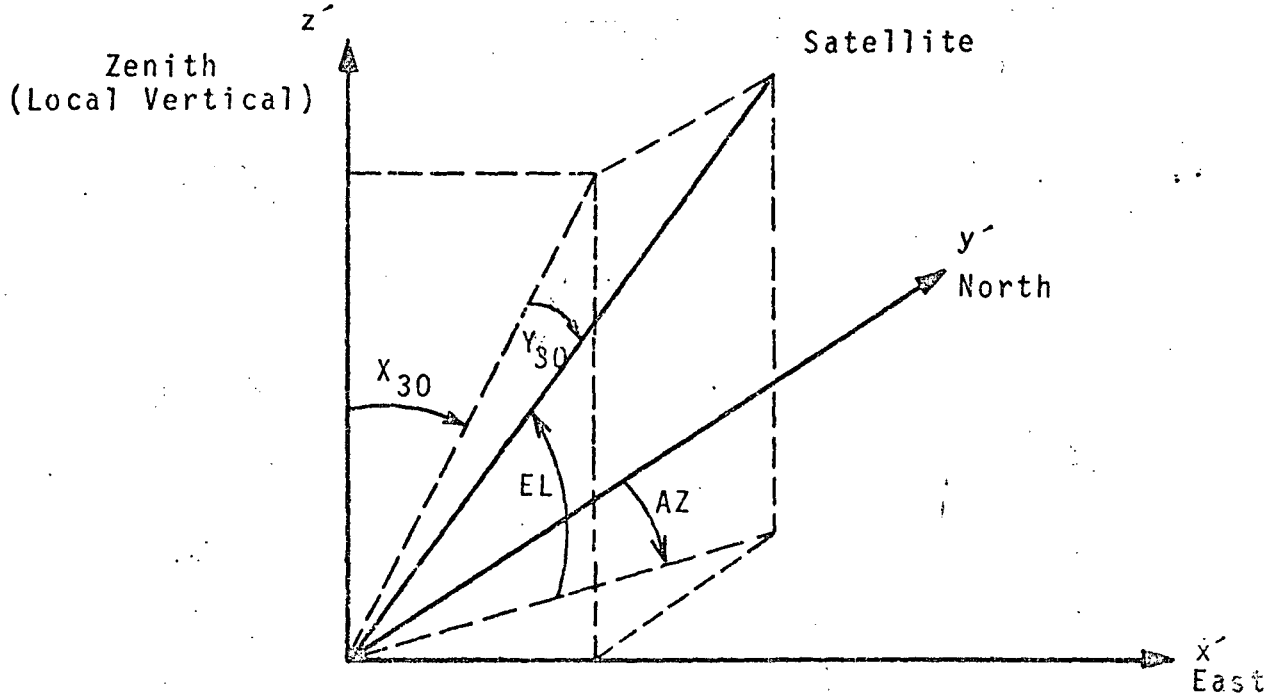

(a) AZ-EL; X_{30}-Y_{30} angles

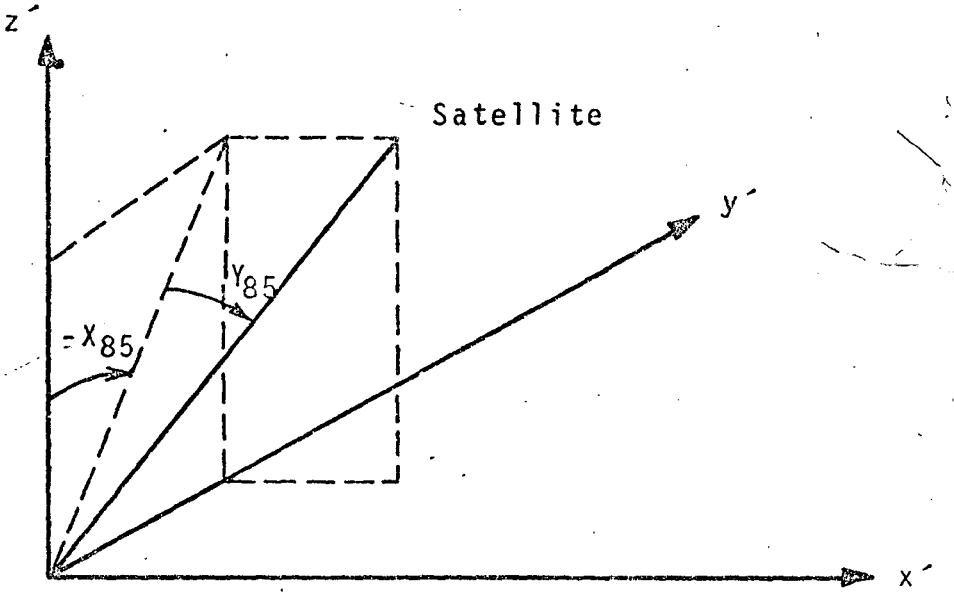

(b) X_{85}-Y_{85} angles

Figure D.1
Coordinate System